PhD thesis

Doctorado en Biología Molecular y Biomedicina

Dimerización de ERK como determinante de de factores de progresión tumoral

---

ERK dimerization as a determinant of tumour progression factors

Dalia de la Fuente Vivas

Directores: Dr. Piero Crespo y Dra. Berta Casar

Santander, 2021

Escuela de doctorado de la Universidad de Cantabria

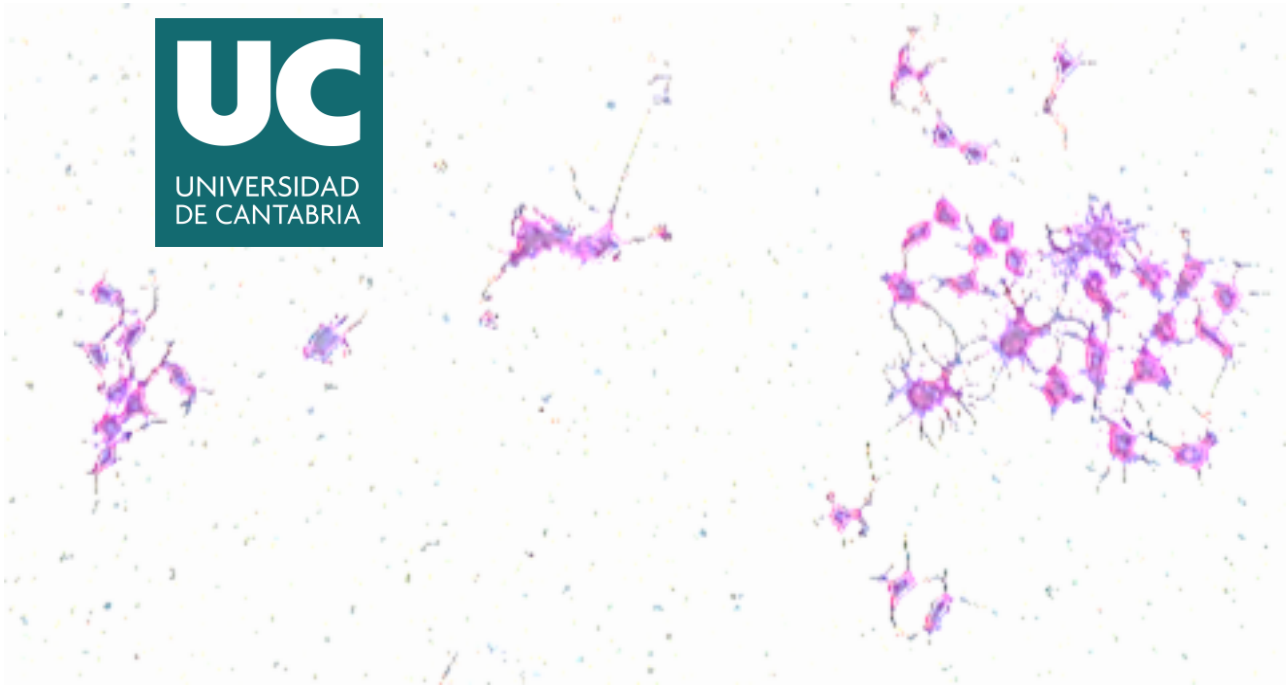

UNIVERSIDAD DE CANTABRIA

TESIS DOCTORAL

Dimerización de ERK como determinante de factores de progresión tumoral

---

PhD THESIS

ERK dimerization as a determinant of tumour progression factors

Autor: Dalia de la Fuente Vivas

Directores: Piero Crespo Baraja y Berta Casar Martínez

Escuela de Doctorado de la Universidad de Cantabria

Santander, 2021

El Dr. PIERO CRESPO BARAJA, profesor de investigación del Consejo Superior de Investigaciones Científicas (CSIC) en el laboratorio de Regulación espacial de las señales RAS-ERK en cáncer en el departamento "Señalización celular y molecular" ubicado en el Instituto de Biomedicina y Biotecnología de Cantabria (IBBTEC), como tutor/director de esta tesis y la Dra. BERTA CASAR MARTÍNEZ, Investigadora del Consejo Superior de Investigaciones Científicas (CISC) en el mismo instituto, como codirectora de esta tesis CERTIFICAN: Que DALIA DE LA FUENTE VIVAS ha realizado bajo su dirección el presente trabajo de Tesis Doctoral en el Instituto de Biomedicina y Biotecnología de Cantabria (IBBTEC) titulado "Dimerización de ERK como determinante de factores de progresión tumoral" consideran que dicho trabajo se encuentra terminado y reúne los requisitos necesarios para su presentación como Memoria de Doctorado al objeto de poder optar al grado de Doctor en Biología Molecular y Biomedicina por la Universidad de Cantabria. Y para que conste y surta los efectos oportunos, expiden el presente certificado.

Santander a 13 de octubre de 2021.

CRESPO BARAJA PEDRO - DNI 00402259N

Firmado digitalmente por CRESPO BARAJA PEDRO - DNI 00402259N
Fecha: 2021.10.13 11:50:39 +02'00'

Fdo. Piero Crespo Baraja

Berta Casar Martinez

Firmado digitalmente por Berta Casar Martinez
Fecha: 2021.10.13 11:44:50 +02'00'

Fdo. Berta Casar Martínez

La presente Tesis Doctoral titulada “Dimerización de ERK como determinante de factores de progresión tumoral”, en inglés: “*ERK dimerization as a determinant of tumour progression factors”*, ha sido realizada en el Instituto de Biomedicina y Biotecnología de Cantabria (IBBTEC) en el laboratorio “Regulación espacial de las señales RAS-ERK en cáncer” gracias al contrato predoctoral de la Ley y de la Ciencia del CIBERONC y a los proyectos financiados por:

Durante el presente trabajo Dalia de la Fuente Vivas ha realizado una estancia predoctoral de 3 meses y medio en el laboratorio del Dr. Michael Grusch en el Institute of Cancer Research - Medical University of Viennaa, Austria, gracias a Ayudas de movilidad CIBERONC 2021.

A mi familia.

“Somewhere, something incredible is waiting to be known”

Carl Sagan

Agradecimientos (Acknowledgements)

Resilencia, vocación, constancia, resolución son algunas de las actitudes que sin duda se requieren en ciencia, pero no es suficiente sin una oportunidad y un apoyo anímico. Cuatro intensos años han pasado y como dice A. Einstein “en medio de la dificultad reside la oportunidad”.

Después de distintos intentos en conseguir el propósito de hacer la tesis, quiero agradecer a Piero Crespo por ofrecerme la oportunidad de realizar este trabajo en su laboratorio y enseñarme a sintetizar ideas. Mi gratitud sincera por estos cuatro años que han sido tan enriquecedores laboral y personalmente.

Gracias Berta Casar por tu apoyo, esfuerzo y optimismo hacia este trabajo. Eres el símbolo de la perseverancia, sin duda los muros nunca son los suficientemente altos para poder perder la esperanza. Tu cercanía me ha ayudado a recordar por qué quise hacer la tesis y por qué he llegado a escribir estas palabras.

Querría agradecer a Michael Grusch y a los miembros de su laboratorio por acogerme como parte del equipo y permitirme trabajar en un ambiente tan acogedor, “ich danke Ihnen vielmals”. La estancia en Viena ha sido un suspiro para ver con otra perspectiva la carrera investigadora, una experiencia increíble.

La formación durante este tiempo: asistencia a congresos, cursos y la estancia internacional ha sido posible por la aceptación de mis directores y la financiación concedida, principalmente del CIBERONC, pero también por parte de la Universidad de Cantabria, y por los proyectos concedidos al grupo. Beneficiarme de ello, ha enriquecido mi pensamiento y supuesto una gran oportunidad de ver nuevas fronteras.

Sin duda, la tesis no ha significado la simplicidad de seguir unos protocolos, ha sido una carrera de fondo con desafíos y resultados gratificantes. Sin embargo, recibir apoyo anímico ha sido esencial.

Nunca hay palabras suficientes para dar las gracias a mis padres y mi hermana, siempre me empujan a llegar más alto, me ponen una colchoneta para tener la oportunidad de volver a saltar y alcanzar mis metas. Gracias por marcar vuestra huella de amor y apoyo incondicional. Víctor, nunca tendré las suficientes palabras para expresar lo que ha significado tu cariño y respeto a mis decisiones. La espera no es eterna. Me habéis dado la energía de cada día.

No olvido a los que me rodean, los que me llaman desde otras tierras en cualquier época de año, a los que quieren que te despejes el pelo de la cara, te relajes a la luz de una vela, pintes en tus cuadernos y abras tus alas. Vuestras conversaciones al teléfono y charlas desenfadadas no tienen precio.

Querría agradecer a los compañeros de laboratorio por tantos momentos compartidos. Ha sido un placer trabajar con un árbol navideño, música italiana o una copla de feria. Por otro lado, valoro el trabajo y disponibilidad del personal del centro: administradores, técnicos y especialistas que han facilitado el trabajo diario.

No me olvido de A. Berrocal, A.M. Vivas, C. de la Fuente, M. Caño, M.A. García y R. Álvarez. Vuestro dolor y el de millones de personas dais fuerza y sentido a las siguientes páginas. Nunca podré entender vuestro sufrimiento sin que esté dentro de mí, pero sí confío en que “sin ciencia no hay futuro”. Sois el impulso de que investigadores quieran dar un paso más allá.

Gracias a todos los que me habéis abrazado y empujado a sentirme como en mi hogar. Esta etapa no se olvida.

Resumen

Resumen en español (Spanish summary)

LA DIMERIZACIÓN DE ERK COMO DETERMINANTE

DE FACTORES DE PROGRESIÓN TUMORAL

Introducción

Un conjunto de datos vincula la ruta de señalización de ERK a la tumorogénesis y progresión tumoral. En general, aproximadamente el 30 % de los tumores malignos humanos albergan mutaciones activadoras en los componentes de la vía RAS-ERK; particularmente en miembros de la familia RAS (22 %) y B-RAF (7 %), en menor medida, en las quinasas de doble especificidad, MEK (Yaeger & Corcoran, 2019), que dan como resultado una señalización aberrante de ERK. Así, la inhibición de la señalización a través de dicha ruta resulta una estrategia válida como terapia antineoplásica en estos tumores. La búsqueda de nuevas dianas moleculares sobre las que dirigir dichas terapias es imperativa, una vez que los abordajes clásicos, centrados en la inhibición de la actividad catalítica de las distintas quinasas no han dado los resultados esperados (García-Gómez et al., 2018).

La señalización de la vía RAS-ERK se activa por diferentes factores externos (factores de crecimiento, citoquinas, hormonas) que regulan la amplitud, intensidad y duración de la señal de forma distinta, promoviendo diferentes respuestas biológicas (Lambert et al., 2012; Pearson et al., 2001)Publicaciones previas revelan que distintos factores externos pueden regular procesos biológicos de manera distinta a través de la activación de ERK (Ma et al., 2012).

Resultados previos de nuestro laboratorio han demostrado que la dimerización de ERK juega un papel importante en tumorogénesis y metástasis (Herrero et al., 2015). En células estimuladas con factor de crecimiento epidérmico (EGF), ERK fosforilada en forma de dímeros, libres o unidos a proteínas scaffold, se localiza en el citoplasma, mientras que ERK fosforilado en forma de monómero fundamentalmente se transloca al núcleo (Casar et al., 2008). Esto sugiere que la dimerización de ERK podría ser crucial

en la regulación de las diferentes respuestas celulares mediadas por la activación de la ruta RAS-ERK.

Además, otros estudios publicados por nuestro laboratorio demuestran que las proteínas de andamiaje o *scaffold* intervienen modulando la intensidad, la amplitud y la localización de la señal de ERK mediante la formación de complejos con los distintos componentes de la ruta ERK (RAF-MEK-ERK) (Casar et al., 2009). Además, hemos demostrado que las proteínas *scaffold* sirven como plataformas de dimerización de ERK en el citoplasma (Casar et al., 2008). Por ello, estas proteínas se han considerado susceptibles de ser utilizadas como dianas terapéuticas en cáncer.

Por otro lado, estudios previos describen que la señalización de ERK también está regulada por factores dinámicos del citoesqueleto que controlan la regulación de la morfología, adhesión y migración celular, procesos íntimamente involucrados en la metástasis celular (Deakin et al., 2012; Fife et al., 2014). Por tanto, la relación del citoesqueleto con la regulación de la señalización mediada por ERK es un factor para tener en cuenta como posible determinante de los acontecimientos biológicos inducidos por la activación ERK.

Hipótesis y objetivos

Basándonos en estos datos previos nuestra **hipótesis principal** es:

La dimerización de ERK es determinante en la regulación de procesos biológicos específicos, asociados a tumorogénesis, desencadenados en respuesta a diferentes estímulos.

Nuestro objetivo principal es estudiar el papel de la dimerización de ERK en respuesta a diferentes estímulos involucrados en la tumorogénesis y la progresión tumoral.

Se han propuesto los siguientes objetivos para desarrollar en este estudio:

Objetivo 1.- Análisis de la dimerización de ERK en respuesta a diferentes estímulos.

1.1. Estudiar la dimerización de ERK en respuesta a estimulación diferencial en líneas tumorales.

1.2. Determinar el interactoma de ERK en líneas celulares estimuladas con diferentes agonistas.

1.3. Estudiar la función de KSR en quimiotaxis y degradación de la matriz celular.

Objetivo 2.- Estudiar la función de los dímeros de ERK en la morfología celular a través de la remodelación del citoesqueleto de actina.

Objetivo 3.- Determinar el papel de los dímeros de ERK en migración y transición epitelio mesénquima (EMT) y metástasis

3.1. Estudiar el efecto de DEL-22379 sobre la morfología celular en un modelo de migración 2D.

3.2. Estudiar la expresión de genes relacionados con EMT en función del estímulo y el inhibidor de dímeros de ERK.

3.3. Determinar el papel de la dimerización de ERK en modelos de invasión 3D y de embrión de pollo.

Materiales y métodos

Para determinar el papel de la dimerización de ERK en quimiotaxis e invasión celular, se ha empleado el ensayo *transwell*. Para ello, se estudió la migración y la invasión celular tras el tratamiento del inhibidor de dimerización de ERK, DEL-22379, y el inhibidor de la actividad catalítica de MEK, U0126. También se ha analizado la capacidad quimiotáctica usando los mutantes de ERK2: ERK2 H176E: mutante incapaz de dimerizar que actúa como dominante inhibitoria impidiendo la dimerización de ERK endógeno (Khokhlatchev et al., 1998); y ERK2 R65S, ERK2 constitutivamente activo (Levin-Salomon et al., 2008) y en forma dimérica.

Para determinar los interactores específicos de ERK en función de su estado monomérico/dimérico realizamos espectrometría de masas utilizando los factores de

crecimiento EGF (factor de crecimiento epidérmico) e IGF-1 (factor de crecimiento insulínico).

Distintos estímulos externos median distintas respuestas celulares que requieren cambios en la morfología celular (Pandya et al., 2017; Saw et al., 2014). Por ello, se ha prestado interés en observar mediante inmunofluorescencia la morfología celular y su relación con la expresión de KSR1, como potenciador de la dimerización de ERK.

Se ha evaluado la morfología celular y el comportamiento de distintas líneas celulares mediante video microscopía durante 48 h, teniendo en cuenta la distancia migratoria, velocidad, direccionalidad y proporción celular.

Se han empleado líneas tumorales de cáncer M38K (línea celular de mesotelioma) y A549 (células de pulmón), en los que se ha caracterizado previamente la transición epitelio-mesénquima (EMT) en un modelo 2D de migración celular. En estas células, se ha analizado la expresión génica en función del estado de oligomerización de ERK utilizando el inhibidor de dimerización DEL-22379, mediante qPCR. Se han utilizado los modelos celulares de cáncer de mama: MCF-7 y MDA-MB-231 para estudiar su capacidad de EMT.

Para determinar la relación entre el citoesqueleto de actina y la dimerización de ERK en un modelo de invasión 3D (formación de organoides). Se ha investigado el papel de los dímeros de ERK en la formación de esferoides de mama, MDA-MB-231, utilizando los inhibidores de ERK, DEL-22379 y U0126. Además, se ha investigado la relación entre el estado de ERK y el citoesqueleto de actina durante la invasión celular colectiva.

Para determinar el papel de la dimerización de ERK en el proceso de metastásico se ha utilizado el modelo de metástasis espontánea de embrión de pollo. Se ha utilizado el modelo celular MDA-MB-231 bajo el tratamiento de inhibidores de ERK, DEL-22379 y U0126.

Resultados y discusión

1. La dimerización de ERK es estímulo dependiente

En este trabajo se ha utilizado como modelo celular la línea celular de cáncer de mama MCF-7 que responde a los estímulos externos EGF e IGF-1. Nuestros resultados indican que mientras que ambos estímulos inducen la fosforilación /activación de ERK, sólo EGF induce dimerización, no siendo el caso en células estimuladas con IGF-1.

2. La dimerización de ERK promueve distintas respuestas celulares

Hemos determinado que el estímulo EGF incrementa la respuesta quimiotáctica de las células. Por el contrario, IGF1 estimula la degradación de la matriz celular. De lo que podría deducirse que son los dímeros de ERK quienes median en la respuesta quimiotáctica, mientras que serán los monómeros de ERK quienes induzcan la degradación de la matriz.

Además, la expresión de ERK H176E, que evita la dimerización de ERK, evita la quimiotaxis e incrementa la degradación inducida por IGF-1. Mientras que la expresión de ERK R65S, constitutivamente activo, potencia la quimiotaxis celular pero no la degradación en cualquiera de las condiciones: basales, estimulas con EGF o estimuladas con IGF-1.

3. Identificación de KSR1 como interactor específico de ERK2

La espectrometría de masas se llevó a cabo con el propósito de identificar interactores de ERK2 y relacionar estas proteínas con la dimerización de ERK cuando se estimula con EGF.

Se obtiene de este ensayo que KSR1 es una proteína específica del estímulo EGF, que como ya se había descrito previamente, facilita la dimerización de ERK en el citoplasma (Casar et al., 2008). De acuerdo con el análisis de enriquecimiento de genes, KSR1 está involucrada en respuestas celulares bajo un estímulo externo.

4. KSR1 regula la habilidad quimiotáctica de las células a través de la dimerización de ERK

Los resultados revelan que la sobreexpresión de KSR1 promueve la quimiotaxis celular mientras que la ausencia de KSR (siKSR1) potencia la degradación de la matriz. Se interpreta que altos niveles de KSR1 incrementan la proporción de ERK en estado dimérico, mientras que la disminución de la expresión de KSR1 tiene el efecto contrario al incrementar la concentración de ERK monomérico.

5. Efecto de la dimerización de ERK, mediado por KSR1 y el citoesqueleto de actina, en la morfología celular.

Se han observado efectos similares en la morfología celular mediados por a la disminución de la expresión de KSR1 y la disrupción del citoesqueleto de la actina inducido por la citocalasina D. Se observa una morfología ameboide.

La inhibición de la polimerización de actina promueve la localización perinuclear de la actina y un incremento en la degradación de la matriz celular, efecto visto cuando se disminuye la expresión de KSR1 (siKSR1). La morfología redondeada-ameboide adquirida por las células cuando se disminuye la expresión de KSR1 favorece la invasión celular (Pandya et al., 2017).

6. El inhibidor de dímeros de ERK, DEL-22379, aumenta la expresión de genes relacionados con la transición epitelio-mesénquima (EMT)

Se ha estudiado la EMT en dos modelos celulares control (M38K y A549) y en las líneas celulares de mama (MCF-7 y MDA-MB-231) añadiendo el estímulo correspondiente (EGF, IGF-1, TGFβ) y tratando con DEL-22379. Estudios previos han corroborado que la estimulación TGFβ (factor de crecimiento transformante β) incrementa la EMT en células A549 (Schelch et al., 2021). Además, TGFβ es considerado el estímulo desencadenante de la principal vía de señalización involucrada en la EMT (Hao et al., 2019). El inhibidor de los dímeros de ERK (DEL-22379) es utilizado a una concentración inferior a la IC50 (2 μM) para evitar la apoptosis celular, pero suponiendo el aumento de los niveles de ERK en forma de monómero.

Los resultados indican que la ruta RAS-ERK está implicada en la EMT tras la estimulación con EGF, como vemos en células M38K, pero esta ruta de señalización no es única y necesaria para promover la EMT. En células A549 la EMT es dependiente de la estimulación TGFβ e independiente de ERK según se ha descrito previamente (Schelch et al., 2021). Nuestros resultados indican que el inhibidor DEL-22379 activa la expresión de genes relacionados con la EMT. Esto podría sugerir que el incremento de monómeros de ERK en el núcleo median la expresión de genes relacionados con EMT/invasión. Sin embargo, DEL-22379 parece tener un efecto inhibitorio en la migración individual de las células tumorales (distancia recorrida y desplazamiento cuadrático medio).

En los modelos celulares de cáncer de mama, MCF-7 y MDA-MB-231, se observa una baja respuesta de experimentar EMT. Sin embargo, de nuevo se observa un aumento de la expresión de los genes relacionados con esta transición cuando se trata con DEL-22379, por ejemplo: Twist.

7. Los dímeros de ERK están implicados en la quimiotaxis y la capacidad de invasión junto con el citoesqueleto de actina en esferoides de mama.

Para el estudio del papel de dímeros de ERK en cultivos 3D hemos utilizado la línea celular MDA-MB-231, que presenta dímeros en estado basal y podemos estudiar efectos biológicos al tratar con inhibidores de ERK, DEL-22379 y U0126.

Nuevamente observamos que la dimerización de ERK promueve la habilidad quimiotáctica celular y la invasión a través de la matriz extracelular compuesta por colágeno I.

Observamos por inmunofluorescencia, que en las células tumorales que componen el organoide experimentan invasión colectiva. ERK y el citoesqueleto de actina co-localizan en la membrana celular cuando analizamos una célula invasiva individual. Esto sugiere que dímeros de ERK junto al citoesqueleto de actina intervienen en la unión célula-matriz extracelular.

8. Dímeros de ERK están relacionados con la metástasis celular en el modelo de embrión de pollo

En el modelo de metástasis espontánea de embrión de pollo hemos observado que la línea celular MDA-MB-231, en la que ERK se mantiene en estado dimérico, los inhibidores de ERK, DEL-22379 y U0126, disminuyen la intravasación y la colonización de órganos secundarios como el hígado y el cerebro. Estos datos sugieren que los dímeros de ERK se relacionan con el progresión tumoral y la metástasis como anteriormente se ha publicado en líneas celulares de melanoma (Herrero et al., 2015).

Conclusiones

1. La regulación de la señal de ERK depende de su dimerización en respuesta a estímulos externos. El factor de crecimiento EGF desencadena la dimerización de ERK pero IGF-1 no.
2. La dimerización de ERK promueve distintas respuestas celulares. ERK dimérica aumenta la quimiotaxis celular y ERK monomérica la degradación de la matriz extracelular.
3. La proteína *scaffold* KSR1, específica del estímulo EGF, incrementa la quimiotaxis celular mientras que la inhibición de su expresión aumenta la degradación de la matriz extracelular. Estos efectos celulares se relacionan con un cambio en la morfología celular.
4. El tratamiento con DEL-22379 inhibe la dimerización de ERK. Bajo su efecto, se activa la expresión de genes relacionados con la EMT al tiempo que detiene la migración celular.
5. ERK dimérica junto a la actina en la membrana plasmática se relacionan con la invasión colectiva de células.
6. Dímeros de ERK se relacionan con el desarrollo tumoral y la metástasis espontánea en el modelo animal de embrión de pollo.

INDEX

LIST OF FIGURES

INTRODUCTION

MATERIALS Y METHODS

RESULTS

DISCUSSION

LIST OF TABLES

INTRODUCTION

MATERIALS AND METHODS

RESULTS

ABREVIATIONS

ABBREVIATIONS

APS	Ammonium persulfate
BSA	Bovine serum albumin
CAM	Chorioallantois membrane
Ct	Cycle threshold
D	Dimensional (2D/3D)
DAPI	4’,6-diamidino-2-phenylindole
Ddw	Distilled deionized water
DMEM	Eagle's minimal essential medium
DNA	Deoxyribonucleic acid
DTT	1,4-ditiotreitol
DUSP	Dual specificity phosphatases
ECL	Immunoblotting substrate
ECM	Extracellular matrix
EGFR	Epidermal growth factor receptor
EGF	*Epidermal growth factor*
EMT	Epithelial–mesenchymal transition
ERK1/2	Extracellular signal regulated kinases 1 and 2
FBS	Fetal bovine serum
For	Forward primer
GAP	GTPase activating protein

GEF	Guanine nucleotide exchange factors
GPCR	Heterotrimeric G protein-coupled receptors
IB	Immunoblotting analysis
IC50	Half maximal inhibitory concentration
IF	Immunofluorescence
IGF	Insulin-like growth factor
IP	Immunoprecipitation
KDa	Kilodalton
LQF	Label-Free Quantification
KSR 1/2	Kinase suppressor of RAS 1 and 2
LFQ	Label-free quantitative proteomics
MAP	Mitogen-activated protein
MG	Matrix gel
MEK 1/2	MAPK/ERK kinase 1 and 2
Min	minutes
MMP	Matrix metalloproteinase
MS/MS	Tandem mass spectrometry
MSD	Mean square displacement
MW	Molecular weight
PAGE	Polyacrylamide gel electrophoresis
PBS	Phosphate buffered saline

PCR	Polymerase chain reaction
PEA15	Phosphoprotein-enriched in astrocytes 15
PEI	Polyethyleneimine
PI3K	Phosphatidylinositol-3-kinase
PM	Plasma membrane
O/N	Overnight
Rev	Reverse primer
RT	Room temperature
SEM	Standard error of the mean
SDS	Sodium dodecyl sulfate
TBS-T	Tris buffered saline-Tween
TEMED	Tetramethyl ethylenediamine
TGFβ	Transforming growth factor-β
RAF	Rapidly accelerated fibrosarcoma
RNA	Ribonucleic acid
RSK	Ribosomal Protein S6 Kinase
RTK	Tyrosine kinase receptor
SAPK	Stress-activated protein kinase
SF	Serum free media
siRNA	Small interfering RNA
st	Starved
TAE	Tris, acetate and EDTA

WB	Western blot
w/o	DMEM without phenol red
w/v	Weight by volume

INTRODUCTION

1. INTRODUCTION

The integrated function of cells in an organism requires a repertoire of signal transducers and interactions implicated in the switch-on of genetic programmes whereby cellular functions are regulated. Protein kinases cascades involving mitogen-activated protein (MAP) kinases are pivotal elements responsible for controlling a vast spectrum of biological responses, including proliferation, differentiation, migration, invasion, survival, apoptosis, and stress (Pearson et al., 2001).

1.2. MAP KINASES: a general overview

MAPKs are activated by a three-tier kinase cascade in response to multiple external stimuli. The activation of this route is also affected by inputs from other signalling pathways, impinging on the signal intensity and its amplification and target specificity (Pearson et al., 2001).

Four MAPK pathways have been identified in eukaryotic cells: ERK (Extracellular Signal-Regulated Kinase), p38, JNK/SAPK (Stress-Activated Protein Kinase), and ERK5. Each one consists of three kinase tiers, specifically: MAP3K, MAPKK and MAPK (Figure 1). None of the MAPKs can be specifically associated to one single cellular function and all of them play important roles in most cellular events. However, the activation of JNK and p38 cascades is mostly related to processes involved in cellular stress and apoptosis, whereas the ERK cascade is preferentially related to cell proliferation and differentiation (Guo et al., 2020).

ERK (Extracellular Sgnal-Regulated Kinases) 1 and 2 constitute the MAPK/ERK pathway. Their molecular weights are 44 and 42 KDa, respectively. They share nearly 85 % homology (Boulton et al., 1991). Three splice variants have been described: ERK1b, ERK1c and ERK2b. Both kinases contain two phospho-acceptor sites which must be phosphorylated for activation. These two amino acids are separated by a glutamate

residue to form the motif TEY in the activation loop (Pearson et al., 2001). They are stimulated by a vast number of ligands and cellular perturbations, for example, growth factors (PDGF, EGF, NGF, and insulin) ligands for heterotrimeric G Protein-Coupled Receptors (GPCRs), cytokines, osmotic stress, and cytoskeleton disorganization (Raman et al., 2007). These kinases are ubiquitously expressed (Cargnello & Roux, 2011).

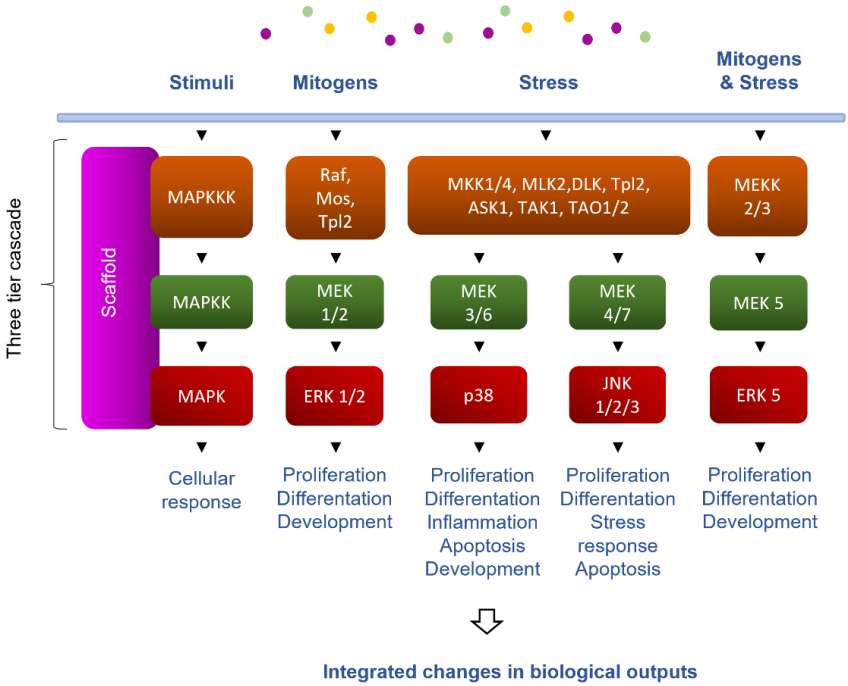

Figure 1. ***The four classical MAPK are three-tiered signalling pathways.*** *The first tier illustrates the biological outcomes of each pathway. The following tiers represent the specific pathways: ERK1/2, JNK, p38 and ERK5.*

p38 MAPKs. Four isoforms have been identified (α, β, γ and δ). p38α is also known as CSBP, mHOG1, RK, or SAPK2; p38γ as ERK6 or SAPK3, and p38δ as SAPK4 (Pearson et al., 2001). The most abundant isoform is p38α. Both p38α and p38β are ubiquitously expressed whereas the rest of isoforms have more restricted expression. It is worth noting that p38α has 50 % homology to ERK2, this suggests they might share functional characteristics. p38 MAPKs display a TGY motif in their activation loop. p38 isoforms are strongly activated by various environmental stresses and inflammatory cytokines such as Tumour Necrosis Factor-alpha (TNFα) (Cuadrado & Nebreda, 2010).

SAPK/JNK Jun amino-terminal kinases/Stress-Activated Protein Kinases. There are three JNK/SAPK isoforms JNK1, 2 and 3 that share 85 % identity. They display multiple splice isoforms that range between 46 and 54 kDa (Cargnello & Roux, 2011). JNK protein kinases are distantly related to ERKs and exhibit the motif TPY in the activation loop (Sluss et al., 1994). JNK isoforms are strongly activated in response to cellular stresses, growth factor deprivation, and to a lesser extent by growth factors, some GPCR ligands, and serum (Bogoyevitch et al., 2010). JNK isoforms play a relevant role in the apoptotic response to cellular stresses. Even though, JNK1 and JNK2 have also been shown to play an important role in cell proliferation (Pearson et al., 2001).

ERK5 is also known as BMK1 for big MAP kinase 1. ERK5 is twice the size of other MAPKs (100 kDa). Its N-terminal half kinase domain resembles ERK1/2 displaying 51 % identity and harbours a TEY motif in the activation loop. In its C-terminus, ERK contains a Nuclear Localization Signal (NLS). ERK5 is mainly activated by growth factors, oxidative stress and hyperosmolarity (Wang & Tournier, 2006), and it is expressed in all tissues and involved in early development (Zhou et al., 1995).

1.2.1. The RAS-ERK signalling pathway

RAS-ERK signalling has been intensely studied for over three decades, due to its pivotal role in cell physiology but also in human pathologies, including cancer. This pathway is probably the best studied signalling pathway, particularly in its response to the activation of membrane Receptors of the Tyrosine Knase type (TKRs) (Pearson et al., 2001), which include multiple stimuli such as the growth factors EGF (Epidermal Growth Factor) and IGF-1 (Insulin like Growth Factor 1) (Figure 2).

Aberrant autocrine and/or paracrine signalling through RTKs has long been known to promote malignancy (Walsh, 1991). Moreover, RTKs can behave as oncogenes as a

consequence of transcriptional overexpression, mutational activation and loss of negative regulators (Du & Lovly, 2018).

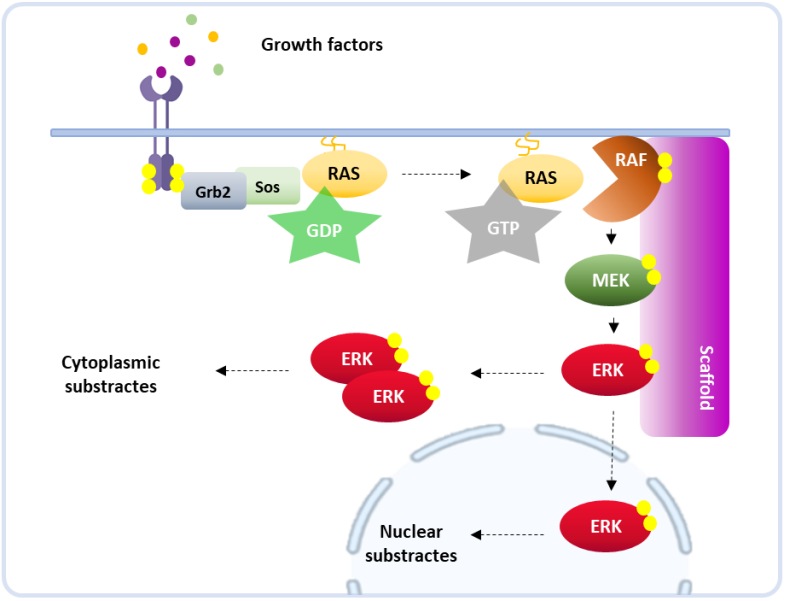

Figure 2. **The RAS-ERK signalling**. *Upon activation by ligand binding, receptor tyrosine kinase is phosphorylated at multiple tyrosine residues. That promotes RAS binds to GTP (active state) responsible for recruiting RAF to the membrane that triggers MEK1/2 and ERK1/2 activation. Active ERK can phosphorylate a vast number of substrates at the cytoplasm as ERK dimers or into the nucleus where it activates transcription factors as ERK monomers mainly.*

RAS is a small GTPase (21 kDa). In mammalians, three isoforms have been described: H-RAS (Harvey Rat sarcoma), K-RAS (Kirsten Rat sarcoma), and N-RAS (Neuroblastoma oncogene). K-RAS has two splicing forms: K-RAS4A and K-RAS4B. Overall, RAS proteins display 90 % sequence identity, their sequence markedly diverges in the C-terminal hypervariable region where RAS proteins exhibit a CAAX motif (in which C is cysteine, A is an aliphatic amino acid and X is any amino acid). This sequence serves as a recognition motif for post-translational modifications, namely farnesylation and palmytoilation, required for RAS membrane association, an essential requisite for RAS activity. Isoform-specific differences in posttranscriptional modifications give rise to distinct and dynamic partitioning of the RAS isoforms between various endomembranes and the plasma

membrane. This, in turn, contributes to isoform-specific localization and signalling (Ahearn et al., 2018; Prior & Hancock, 2012) (Figure 3 B).

Upon stimulation, RAS is activated by guanine nucleotide exchange factors (GEFs) which promote the exchange of GDP for GTP leading tom its activation. On the other hand, GTPase activating proteins (GAPs) enhance RAS GTPase activity, promoting the hydrolysis of GTP to GDP and consequently RAS inactivation (Dohlman & Campbell, 2019) (Figure). 30 % of human tumours harbour mutations on RAS genes which diminish RAS GTPase activity, leading to constitutive activation and aberrant signalling (Fernández-Medarde & Santos, 2011) (Figure 3 A).

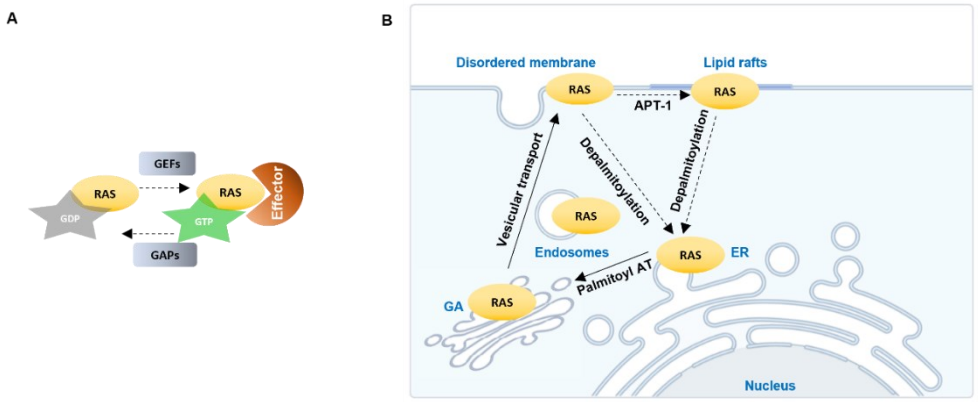

Figure 3. ***RAS-GTP activity and RAS post-translational modifications****. A. RAS-GTP activity: GEFs and GAPs work to regulate the small GTPase activity. Activated RAS-GTP can phosphorylate an effector. B. RAS post-translational modifications and palmitoylation cycle. In the cellular cytoplasm, RAS is gets synthesized, farnesylated the, and directed to endoplasmic reticulum (ER) membrane where it encounters the subsequent CAAX-processing enzymes. Following CAAX first modification, RAS proceed to the cytosolic face of the Golgi apparatus (GA), where is allowing it to traffic via vesicular transport to the plasma membrane, locating at the disordered membrane (DM). The duo-palmitoylated RAS can be partially depalmytoilated by APT-1 causing RAS segregation to lipids rafts. Also, depalmitoylation is possible by retrograde Golgi transport with the purpose of starting another round of palmitoylation again. APT1: Acyl-protein thioesterase AT: Acyltransferase, RCE1: RAS-converting enzyme 1, ICMT: isoprenyl cysteine carboxymethyl transferase.*

RAF. RAS activation triggers the activation of RAF family serine/threonine protein kinases. RAF-1 (Rapidly Accelerated Fibrosarcoma) that was described in the eighties as a retroviral gene (Rapp et al., 1983; Sutrave et al., 1984) which encoded the first oncogene with serine/threonine activity (Moelling et al., 1984).

Three different RAF isoforms have been found in mammals, RAF-1/c-RAF, B-RAF and A-RAF (Bonner et al., 1983). All RAF proteins share MEK1/2 as an effector and RAS as an activator (Dhillon et al., 2002; Leicht et al., 2007; Wellbrock et al., 2004). Under resting conditions RAF N-terminal region contacts and represses its catalytic domain. Its activation is dependent on its recruitment to the plasma membrane, which is accomplished by GTP-loaded RAS (Nussinov et al., 2019).

MEK 1/2 (Mitogen-Activated Protein Kinase 1 and 2) are dual-specificity protein kinases of 46 and 45 kDa, respectively, with the ability of phosphorylating substrates both in threonine and tyrosine (Crews et al., 1990; Nakielny et al., 1992; Seger et al., 1992). These proteins are located downstream of RAF proteins phosphorylate them in two serine residues at the activation loop (Takekawa et al., 2005). To date, MEK substrate repertoire is limited to ERK1/2 (Seger et al., 1992),

ERK 1/2 (Extracellular signal-regulated kinase 1/2) are two isoforms of 44 and 42 kDa respectively. Before of their molecular cloning of ERKs by Cobb's group (Boulton et al., 1990), ERK1 and ERK2 were known as p44 and p42 MAPK (Kohno & Pouyssegur, 1986; Strurgill. et al., 1988). Human ERK1 and ERK2 are 87 % identical in their primary structure.

The conversion from inactive to an active form involves ERKs being dually phosphorylated by MEK1 and MEK2 on their TEY motif (Ahn et al., 1991), first at Tyr204/187 and then Thr202/185. (Roskoski R, 2012). Inactivation of ERKs requires the removal of phosphate from either one or both sites of the TEY motif by phosphatases (Li et al., 2007; Maillet et al., 2008).

Active ERK phosphorylate numerous substrates. The identification of ERK1/2 substrates have increased significantly in the past three decades. Ünal and colleagues

have compiled 2507 ERK target sites with corresponding human Uniport IDs and phospho-site information (Ünal et al., 2017). The huge number of ERK targets can explain the wide spectrum ERK1/2 functions.

ERK dimerization. ERK activity can be controlled by multiple mechanisms, such as dimerization. This was initially described by Cobb's laboratory which determined that upon being phosphorylated ERK1 and 2 form homodimers, whereas heterodimers are unstable (Khokhlatchev et al., 1998). Philipova and Whitaker elucidated that ERK dimerization could be associated with higher catalytic activity, suggesting that ERK dimers could be more active than ERK monomers (Philipova & Whitaker, 2005). More recently, our lab has demonstrated that ERK dimerization is specific of mammalian ERK (Herrero et al., 2015). Furthermore, our lab has also published that ERK dimers are formed at the cytoplasm using scaffold proteins as dimerization platforms (Casar et al., 2008). This entails that ERK cytoplasmic substrates are mainly activated by ERK dimers. In this respect, the cellular localization of the scaffold proteins determines the specificity of ERK substrate activation (Casar et al., 2009). By contrast, ERK is translocated to the nucleus as a monomer and as such, ERK nuclear substrates are activated by ERK in monomeric form. Importantly, ERK dimerization is an essential process in tumorigenesis; its prevention precludes cellular transformation and tumour progression. As evidence by the effects of DEL-22379, a small molecule inhibitor that blocks ERK dimerization but not ERK phosphorylation. This ERK dimerization inhibitor blocks the activation of cytoplasmic ERK substrates and impedes tumorigenesis and metastatic dissemination (Casar et al., 2008; Herrero et al., 2015).

1.2.3. Alterations and inhibitors in the RAS-ERK pathway

Dysregulation of RAS signalling causes RASopathies that include developmental syndromes, congenital heart disease, psoriasis, or cancer. The relevance of the RAS-ERK pathway in cancer is the reason to keep the attention and interest of finding therapeutic targets and optimal drugs to restrict the signalling. The frequency of genomic alterations in the MAPK pathway decreases the incidence as one moves further downstream signalling across human tumours: RAS mutations occur in 22 %, B-RAF in 7 %, and MEK in <1 % of cases, and ERK mutations are weird (Yaeger & Corcoran, 2019). These mutations causing an increment of the signalling.

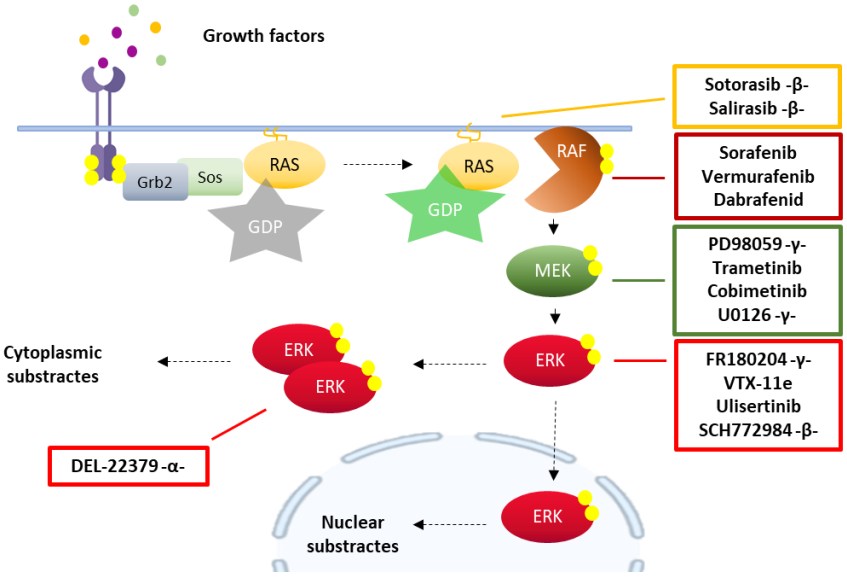

Figure 4. ***Targets of classical inhibitors in the RAS-ERK pathway****. Pharmacological evaluation of the classical inhibitors: -α- in vitro assays, -β- clinical evaluation in progress, -γ- not successful clinical evaluation but useful in laboratory uses.*

In 1982 it was found RAS as the guilt of human cancer, and several strategies were aimed at this small molecule as a potential antitumoral target (Cox & Der, 2010). The first steps were towards reverting oncogenic RAS GTP-bound without successful results. Thus, RAS was considered for a long time as a difficult druggable target (A. D. Cox et al., 2014;

Mörchen et al., 2019). It was decided to focus on RAS sublocalizations in the plasma membrane, essential for RAS signalling (Arozarena et al., 2011). Recently, the attention has been focused on RAS-GDP activity, which is under clinical evaluation (Ostrem & Shokat, 2016; Stephen et al., 2014). However, RAS inhibitor farnesylthiosalicylic acid, salirasib, has had modest success in the first clinical trials (Rotblat et al., 2008). Rising inhibitors are aimed at RAS allele-specific sites, despite not being still used ruled out the use of classical alternatives in a cocktail of treatments. Successfully sotorasib has been newly accepted by FDA as a RAS GTPase family inhibitor for adult patients with K-RAS G12C -mutated locally advanced or metastatic non-small cell lung cancer (NSCLC) (Hong et al., 2020).

Similar strategies have focused on the kinases downstream from RAS. The high percentage of mutations in RAF had been an incentive to invest in new drugs. Sorafenib was the first B-RAF inhibitor approved (Wilhelm et al., 2004). Inhibitors based on RAF V600E mutant structure are vemurafenib (PLX4032) (Bollag et al., 2012), to be followed by dabrafenib (GSK2118436) (Rheault et al., 2013). These ATP-competitive inhibitors are highly selective for B-RAF-mutant form and have been approved for use against B-RAF-mutant melanoma. Unfortunately, these drugs could present resistance after about one year, leading to a fatal end (Samatar & Poulikakos, 2014).

In the early 90s, PD098059 was synthesised as the first MEK1/2 inhibitor (Dudley et al., 1995) based on a non-ATP competitive allosteric inhibitor. However, pharmacological limitations are not sufficiently soluble and bioavailable. PD098059 was followed by new generations of derivatives, which are being evaluated to the final stages of clinical trials (Wang et al., 2007). On the other hand, U0126 was the first MEK inhibitor that acts on ERK activation without affecting the JNK and p38 pathways. Despite its high specificity towards MEK, U0126 showed poor pharmacological properties, and its use has been limited to the laboratory scope (Frémin & Meloche, 2010).

In the last few years, compounds targeting ERK have made their appearance. The first one is FR180204 (Ohori et al., 2005) and did not progress as a consequence of

pharmacological shortcomings but served as a guide for structure-based studies that have led to the development of VTX11E (Aronov et al., 2009) and its derivative ulixertinib (BVD523) (Germann et al., 2017). These compounds are reversible ATP-competitive inhibitors. Another king of ERK inhibitor, SCH772984 (Wong et al., 2014) and its derivative MK8353 (Boga et al., 2018) have been shown to inhibit phosphorylation. All of them are now undergoing phase I clinical trials.

An alternative strategy targeting ERK dimers is DEL-22379. This compound inhibits ERK dimerization. DEL-22379 has shown a remarkable efficiency with mild toxicity in pre-clinical models, B-RAF and RAS-mutant tumours (Herrero et al., 2015) (Figure 4).

Besides the classical inhibitors targeting MAPK members, there have been developed other strategies adopting cell therapies, cancer vaccines, and combination therapies in clinical development including siRNA therapies. It is worth saying that promising inhibitors, like RAS allele-specific sites, are not still ruled out the use of classical alternatives in a cocktail of treatments.

1.2.4. Scaffold proteins

Scaffold proteins play an essential role in the ERK signalling cascade regulation by increasing the effective local concentration of its components and enhancing their interactions (Levchenko et al., 2000). The intensity and duration of ERK signals depend on the expression level and binding affinity of scaffold proteins. Whether the concentration of the scaffold exceeds that of its substrates, incomplete complexes will form, and the signal will diminish. Likewise, if there are too few scaffold proteins, the number of optimal complexes will drop. This bell shape effect indicates that scaffolds must be at an optimal concentration for effectively conveying ERK signals (Morrison & Davis, 2003). A scaffold can bind three clients: RAF, MEK and ERK (Kolch et al., 2005) (Figure 5 A). Thus, it could be hypothesized that scaffold proteins act in conjunction, influencing the activity of each other. In this respect, it is quite evident how up-or down-regulation on the expression

levels of any scaffold could affect others since they compete for the same pool of kinases (Casar & Crespo, 2016) (Figure 5 B).

Another scaffold protein function is based on shielding the components of the cascade from phosphatases` dephosphorylation (Levchenko et al., 2000). The controversial notion in this scaffold`s regulation is the idea of this protection promotes or impedes the signal amplification. Conceptually, free kinases can phosphorylate multiple substrates, it is believed that the signal is amplified exponentially along the pathway. However, when

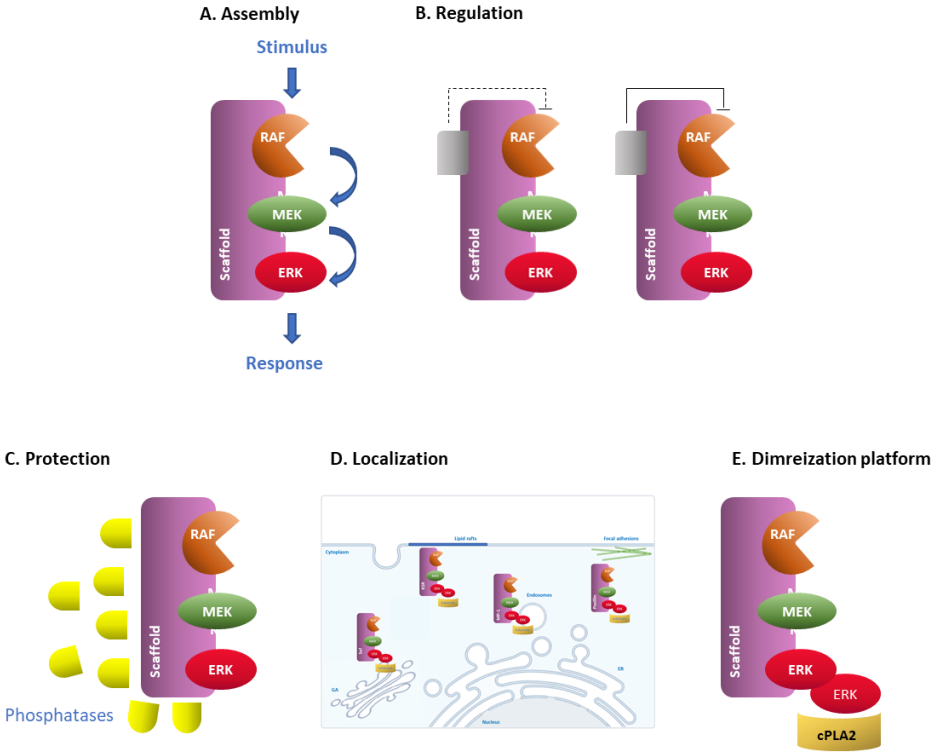

Figure 5. ***Scaffold regulations****. A. Scaffold proteins serve as an assembly platform for the kinases orienting them and facilitating phospho-transfer reactions. B. They have a regulatory function when a small molecule binds to them that can induce or inhibit signal transduction. C. Scaffolds protect kinases from dephosphorylation like soluble phosphatases. D. Scaffolds confer spatial regulation for ERK signals due to the specific subcellular localization. E. Scaffold proteins serve as dimerization platforms for ERK dimers, where they can activate specific cytoplasmic substrates.*

proteins are locked onto a scaffold, each kinase can only phosphorylate its accompanying substrate, preventing signal amplification. On the contrary, in an environment with a high concentration of phosphatases, in which signalling is based on freely diffusing kinases this will be strongly inhibited, scaffolding will achieve a local concentration effect and signal amplification despite the surrounding high levels of deactivating phosphatases (Locasale et al., 2007) (Figure 5 C).

Another important function of scaffolds is to organise the spatial arrangement of the signalling pathway architecture and direct ERK to different substrates in different subcellular compartments. For example, KSR scaffolded complex forms mainly at the cell membrane, specifically in lipid rafts (Matheny et al., 2004), MP-1 in endosomes (Teis et al., 2002), Sef in the Golgi apparatus (Torii et al., 2004) and paxillin in focal adhesions (Ishibe et al., 2003) (Figure Figure 5D, Figure 6).

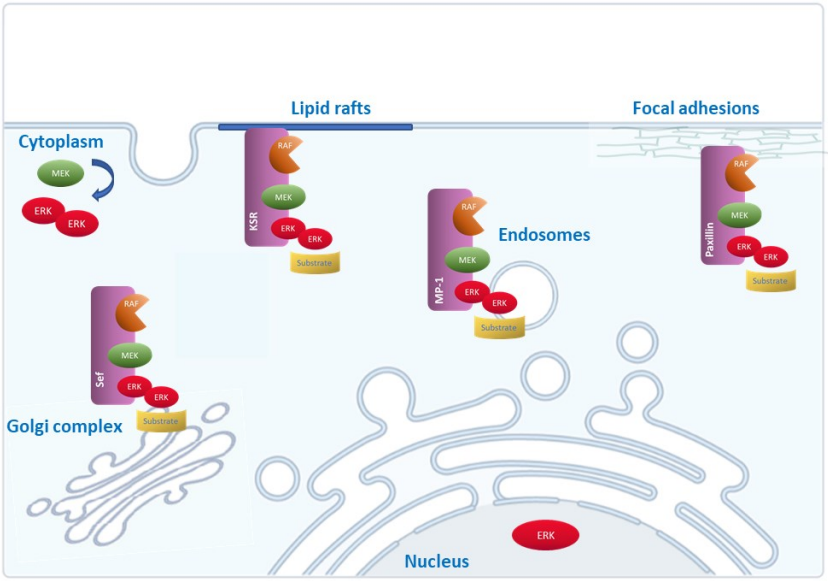

Figure 6. ***Scaffold proteins as spatial regulators of ERK signalling****. In response to stimulation, phosphorylated ERK dimerize in the cytoplasm. Specific scaffolds act as dimerization platforms in a sublocalization-specific fashion (KSR1 in lipid rafts, paxillin in focal adhesions, MP-1 in endosomes and Sef in Golgi apparatus), where ERK dimers are assembled, and the new complexes can interact with different cytoplasmic pools of substrates.*

Our lab has shown that spatial selectivity provided by scaffold proteins are essential for defining ERKs substrate specificity. In this respect, it has been shown that the different membrane sublocalizations of RAS regulate which specific substrates are amenable for ERK phosphorylation and activation. This is achieved by the intervention of defined scaffolds proteins (Casar et al., 2009) (Figure 5 E). Up to now, sixteen bona fide mammalian scaffolds have been identified (Table 1). Adapted from (Casar & Crespo, 2016).

Table 1. ***ERK MAPK scaffolds in mammalian cells***

Scaffold name	**References**
Sef	(Fürthauer et al., 2002; Tsang et al., 2003)
Paxillin	(Glenney & Zokas, 1989; Turner et al., 1990)
β-Arrestin 1/2	(DeFea, Zalevsky, Thoma, Déry, et al., 2000; Luttrell & Lefkowitz, 2002)
βDystroglycan	(Weir & Muschler, 2003)
MORG1	(Vomastek et al., 2004)
MP-1	(Schaeffer et al., 1998)
KSR1/2	(Kornfeld et al., 1995; Sundaram & Han, 1995; Therrien et al., 1995)
IQGAP1/2/3	(Weissbach et al., 1994) (Roy et al., 2005) (Kunimoto et al., 2009; Nojima et al., 2008)
RKIP	(Sungdae Park et al., 2005)
OSBP	Oxysterol-binding protein (P.-Y. Wang et al., 2005)
RGS12	(Willard et al., 2007)
PEA15	(Mace et al., 2013; Zaballos, Acuña-Ruiz, et al., 2019)
archvillin	(Gangopadhyay et al., 209)
grb10	(Charalambous et al., 2003; Deng et al., 2008; Khojasteh Poor et al., 2021; Langlais et al., 2004)
dyrk1a	(Ritterhoff et al., 2010)
GIT1	(Yin et al., 2004, 2005)

- **KSR 1/2 (Kinase Suppressor of RAS)**

The KSR family of scaffold proteins includes two members, KSR1 (Roy & Therrien, 2002) and KSR2 (Channavajhala et al., 2003), both with a MW of 105 kDa. Their structure consists of five conserved regions, CA1-CA5 (Therrien et al., 1995). Which include a pseudokinase region, a constitute regulatory domain, and a sequence implicated in KSR subcellular localization (Clapéron & Therrien, 2007; Driedger & Blumberg, 1980; Michaud et al., 1997; Zhou et al., 2002). KSR has been classified as a pseudokinase (Boudeau et al., 2006; Eyers & Murphy, 2013; Hu et al., 2011; H. Zhang et al., 2013). However, this has been a point of controversy since KSR discovery. Indeed, while some studies have reported a residual kinase activity (Brennan et al., 2011; Goettel et al., 2011; Hu et al., 2011; Y. Zhang et al., 1997), others have failed to detect it (Michaud et al., 1997; F. Roy & Therrien, 2002; Stewart et al., 1999).

Upon RAS activation, KSR is translocated with MEK1/2 to the plasma membrane (PM) and coordinates the assembly of a multiprotein complex containing RAF, MEK, and ERK (Lavoie & Therrien, 2015; Raman et al., 2007b; F. Roy & Therrien, 2002). KSR1 acts preferentially on ERK1/2 signals emanating from the plasma membrane (PM) cholesterol-rich domains (Matheny et al., 2004).

In vivo KSR1 is highly phosphorylated. It is known that ERK can phosphorylate KSR at T260, T274, S320 and S443 in response to growth factor stimulation or RAS activation (Cacace et al., 1999; McKay et al., 2009; Volle et al., 1999). Even though the functional significance of these phosphorylations is still unclear, some studies suggest that the phosphorylation of these sites by ERK contribute to B-RAF - KSR1 dissociation and relocates KSR1 from the plasma membrane to the cytoplasm (McKay and Morrison, 2007). Phosphorylation of KSR1 on S297 and S392 by the kinase C-TAK1 creates 14-3-3 binding sites, whose dephosphorylation by PPA2 is required to localize KSR to triton resistant microdomains (lipid rafts) (Cacace et al., 1999; Müller et al., 2001) (Figure 7). In this respect, results from our group have shown that KSR selectively couples RAS signals from

lipid rafts to the activation of cPLA2 by ERK (Casar et al., 2009). Also, KSR phosphorylation has been associated with its nucleus-cytoplasmic shuttling (Brennan et al., 2002). However, KSR nuclear localization is controversial.

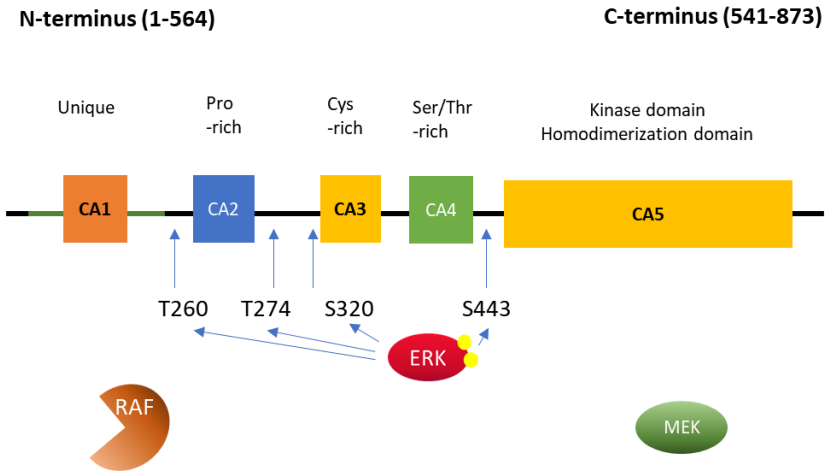

Figure 7. ***Schematic depiction of KSR1****.* The KSR family proteins are structurally formed by five conserved domains: a domain unique to the KSR proteins (CA1), a proline-rich region (CA2), a cysteine-rich domain (CA3), a serine/threonine-rich region (CA4), and a putative kinase domain (CA5). The main interacting proteins are shown below their corresponding interaction domain. Arrows originating in the proteins that, in addition, to interact, phosphorylate KSR1 indicate phosphorylation sites by ERK, T260, T274, S320 and S443.

KSR proteins exhibit a high homology with RAF family kinases (Manning et al., 2002), both in amino acid sequence as in the domain distribution and as in its tertiary structure (Clapéron & Therrien, 2007; Therrien et al., 1995). Furthermore, it is described that KSR and RAF share an identical dimerization interface (Rajakulendran et al., 2009; Verlande et al., 2018). In a similar fashion to what occurs with RAF proteins, KSR1 and KSR2 can also homodimerize (Matheny & White, 2009; Rajakulendran et al., 2009). Mutations at the dimerization site block RAS activity, suggesting that KSR dimerization may play an influential role in RAS signals. However, how dimerization affects KSR function is unknown up to date.

Regarding the physiological role of KSR, KSR1 knock-out mice are viable and fertile and resemble EGF receptor -/- mice in defective hair follicles. That suggests that KSR1 may participate downstream from EGF signals. Probably, the most significant biological consequence of KSR1 loss in mice is their resistance to RAS-dependent tumour formation. In this respect, carcinogens, which induce mammary and skin tumours by promoting H-RAS, mutations are markedly reduced in KSR1 -/- mice (Hansen et al., 1997; Lozano et al., 2003; Nguyen et al., 2002). On the other hand, KSR2 -/- mice have reduced fertility and become spontaneously obese; adaptive thermogenesis, metabolic rate and leptin sensitivity are compromised in these mice. In agreement, humans harbouring KSR2 mutations present early-onset obesity (Henry et al., 2014; Pearce et al., 2013; Revelli et al., 2011). Interestingly, whereas KSR1 is ubiquitously expressed (Giblett et al., 2002; Nguyen et al., 2002), KSR2 is almost exclusively found in the brain and the pituitary. Brain-specific disruption of KSR2 is enough to cause obesity in mice (Li et al., 2017).

PEA15 (Phosphoprotein-Enriched in Astrocytes 15)

PEA15 binds to active cytoplasmic ERK1/2, blocking their cytoplasmic activity and promoting nuclear translocation. PEA15-ERK complex reduces ERK dephosphorylation, by that means providing a store of active ERK (Mace et al., 2013; Zaballos, Acuña-ruiz, et al., 2019). PEA15-ERK dissociation is mediated by the phosphorylation of PKC and AKT (Mace et al., 2013). Additionally, alterations in PEA15 expression have been associated with resistance in tumour cells (Zaballos, Acuña-ruiz, et al., 2019).

IQGAP1

IQGAP1 binds B-RAF, MEK, and ERK facilitating ERK activation by EGF stimulation (Roy et al., 2005). IQGAP1 regulates the phosphorylation of EGFR by ERK (Casar et al., 2009). Other proteins that bind IQGAP1 include E-cadherin, β-catenin and calmodulin (White et al., 2009). Over-expressed IQGAP1 in some cancers is related to poor prognosis (Brown & Sacks, 2006; Jadeski et al., 2008). It is demonstrated that blocking the interaction between IQGAP1 and ERK inhibits skin carcinogenesis driven by RAS-ERK pathway oncogenes (Jameson et al., 2013).

Paxillin

Paxillin regulates ERK signalling at focal adhesions (Ishibe et al., 2004). The Paxillin-MEK-ERK complex regulates tumour cell invasion, plasticity and metastasis (Deakin et al., 2012). Mutations in this scaffold have been associated with enhancing tumour growth and invasion in lung cancer (Deakin et al., 2012). Paxillin is overexpressed in lung-adenocarcinoma high-risk patients (Mackinnon et al., 2011).

β-Arrestin

β-Arrestin mediates ERK activation in clathrin-coated pits (DeFea, Zalevsky, Thoma, Dery, et al., 2000). β-Arrestin triggers ERK activation and direct signalling to the cytosol, preventing ERK translocation to the nucleus (Dewire et al., 2007; Shenoy & Lefkowitz, 2011). Dysregulation of β-arrestin is associated with more aggressive cancer phenotypes and poorer prognosis in several tumours (Sobolesky & Moussa, 2013).

Sef

Sef resides at the Golgi apparatus and binds active MEK/ERK complexes preventing ERK translocation to the nucleus retaining it in the cytoplasm (Torii et al., 2004). As result, Sef allows phosphorylation to cytosolic substrates but not nuclear targets (Philips, 2004).

MP-1

MP-1 specifically binds to MEK1 and ERK1, but not MEK2 or EKR2 (Schaeffer et al., 2016), and it is showed an evident correlation between MP-1 and phosphorylated ERK expression. (Teis et al., 2002). MP-1 interacts with p14 and ERK in late endosomes (Teis et al., 2006). What is more, the MP1-p14 scaffold enhances MEK activation by binding PAK1 to regulate cell adhesion and spreading on fibronectin (Pullikuth et al., 2005).

Intracellular signals such as RAS-ERK tiers, scaffold proteins and therapeutic drugs have been used to take control of tumour progression. But also, external factors that trigger the RAS-ERK signalling pathway must also be taken into account to control malignancy signalling.

1.3. Extracellular cues in tumour progression

The final ERK activation is triggered by RAS in response to external microenvironmental factors. Over the past few decades, different omics approaches defined the tumour microenvironment as crucial to tumour progression and dissemination. This microenvironment consisted of non-cancerous cells (fibroblasts, immune and inflammatory cells, and cells forming the tumour vasculature), macromolecular components, mechanical signals, and interacting with tumour cells (Masi et al., 2020).

The term growth factor is generally used to describe a chemical signal, protein or peptide, whose function is predominantly related to the regulation of target tissue growth and potential proliferation. Growth factors are produced and released into the vasculature by a variety of different cell types. These external signals interact with and bind specific receptors on the cell surface, like tyrosine kinases receptors, eliciting responses within the target tissue. Multiple extracellular signals mediated by growth factors, cytokines and hormones regulate biological processes through RAS-ERK signalling. External stimuli can work in an additive, synergistic, antagonistic, or independent fashion as modifiers of cell behaviour. As an example, in lung cancer, EGF (Epidermal Growth Factor) and TGFβ (Transforming Growth Factor-beta) promote ERK-dependent cell migration, but only TGFβ enhances ERK-dependent EMT (Epithelial-Mesenchymal Transition) degradation via proteins like matrix metalloproteinase 1 (MMP1) (Schelch et al., 2021). Apart from the type of the external factor, the duration and the intensity of the stimulus are essential in cell tumoral behaviour regulation (Celià-Terrassa et al., 2018).

Growth factors play pivotal roles in critical aspects of cellular migration and metastatic dissemination. For instance, the constitutive activation of EGFR signalling caused by gene mutations and gene amplification has a narrow connection with tumour initiation, progression (Morgillo et al., 2016), and transformation (Walsh, 1991). It is worth adding that autocrine stimulation of the EGF receptor can contribute to sustained mitogenic activity and proliferation in some types of cancer cells (Murphy et al., 2001). As well as an abroad variety of cellular responses, such as proliferation, differentiation, migration, and

survival, can result from activation of the IGF system. It has been published that both EGF and IGF-1 have effects on ERK activation. The selective blockade of the EGF receptor in cancer cells does not only inhibit the action of EGF but also IGF-1 -induced activation of the MAPK pathway in prostate cancer cells (Putz et al., 1999).

The wide range of cellular responses to a variety of stimuli through ERK signalling is still misunderstood. Early notions might indicate that growth factors modulate the autocrine and paracrine loops of MAPK signalling activation (Putz et al., 1999). And also, growth factor context might determine the MAPK signalling network in different cell spacial locations and that the resulting dynamics govern cell response (Santos et al., 2007).

1.4. Tumour dissemination: key features

The ability of transformed cells to directionally respond to chemoattractants is known as chemotaxis (Pijuan et al., 2019). This chemotaxis implies that inputs from growth factor receptors and integrins, like the family of tyrosine kinase receptors (included EGFR), are involved in the creation of extensions of the cell plasma membrane (Bredin et al., 1999; Masi et al., 2020). These lamellipodia formations are flattened actin-rich protrusions at the leading edge of a cell that has transformed into a migrating cell (Horwitz & Parsons, 1999; Olson & Nechiporuk, 2021; Petrie et al., 2009). The molecular mechanisms by which extracellular cues control motility mechanics through the actomyosin cytoskeleton, the central hub coordinating cell migration responses, are still poorly understood (Pandya, Orgaz, & Sanz-Moreno, 2017). There are first pieces of evidence that ERK signal can amplify protrusive and contractile forces for cell motility through ERK specific targets like RSK (Ribosomal Protein Kinase) (Samson et al., 2019).

The mechano-transduction and sensing cellular responses alter the cell migration properties due to a chemoattractive substance. Cells do not migrate preferably in the direction of that substance (Bredin et al., 1999), even though it is the basal surface, a

specialized form of the ECM, that provides structural support and polarization signals to epithelial cells (Bissel & Radisky, 2001). These signalling networks modulate the efficiency of cell migration which depends on two essential parameters: directionality and speed. The directionality ratio is referred to the cell trajectory between the start and the end, the curves for individual cell trajectories, and the changes of the speed index over time.

Tumour dissemination entails cellular movement. Such movement can involve the migration of i) individual cells ii) groups of cells or iii) the movement of large sheets of conjoined cells. Irrespective of its mode, cell migration requires a fine spatial-temporal integration of the hundreds of proteins that comprise or regulate the fundamental processes that drive cell migration; these proteins include membrane receptors, signalling kinases, phosphatases, adapters, and cytoskeletal and adhesion components (Orgaz et al., 2020; Pandya, Orgaz, & Sanz-moreno, 2017; Vicente-Manzanares & Horwitz, 2011).

Adherent cells migrating in groups are more directed than a single-cell persistent random walk. Adherent cells migrating require cell-cell adhesion apart from lamellipodia extension, cell body contraction and focal adhesions, all of them characterized in single-cell migration (Saw et al., 2014). Focal adhesions are called a large protein complex that mediates the attachment of the extracellular matrix to the actin cytoskeleton through integrins. On the other hand, compact groups or clusters of cells and strands of connected tumour cells migrating in groups migrate more directed than the single ones. The collective migration has an additional constraint of cell-cell adhesion during migration, transmitting forces between cells (Saw et al., 2014). When cell-cell junctions are maintained, cells can move collectively as multicellular streams, budding or larger clusters (Figure 8). The principal individual and collective modes of tumour invasion together with plasticity allow interconversion between modes. It means invading individually cells can use protrusion based on Mesenchymal-Amoeboid Transition (MAT) and Amoeboid-Mesenchymal Transition (AMT), the reverse process. The case of collective-individual transition plasticity modes includes epithelial-mesenchymal transition and integrin-mediated ECM (extracellular matrix) adhesion strategies (Pandya, Orgaz, & Sanz-moreno,

2017; Wu et al., 2021). The cell plasticity in motility patterns enables cancer cells to disseminate further and thus limit the efficiency of anti-neoplastic therapies.

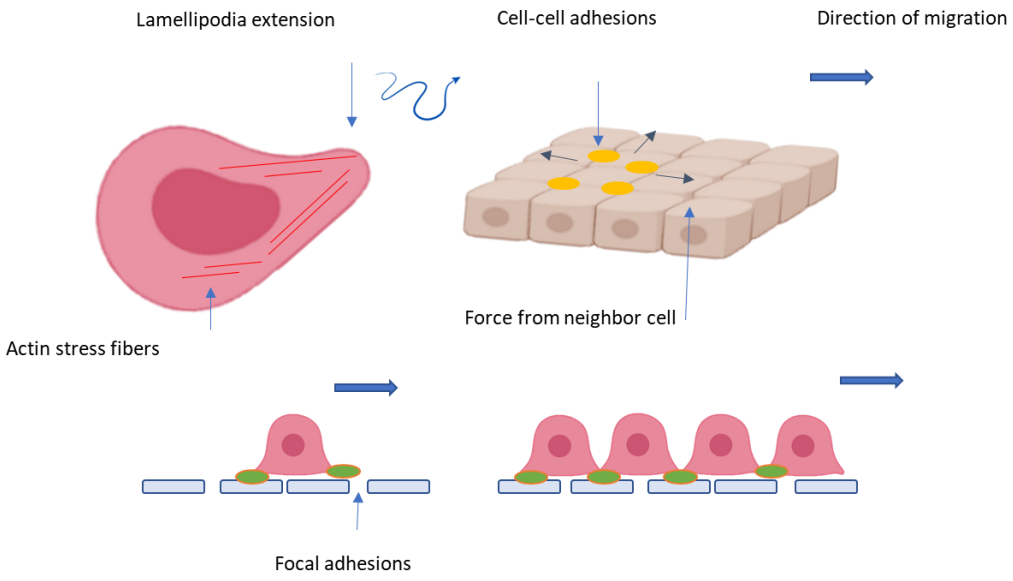

Figure 8. ***Cells migrating singly and collectively present different modes of cell scattering****. On the left, single cell migration involves lamellipodia extension, actin contraction and adhesion to substrate through focal adhesions. On the right, adherent cells migrating in groups are more directed. There is additional constraint of cell–cell adhesion during migration, transmitting forces between cells.*

Despite interconversion morphologies, ECM degradation is also required for tumour cells to migrate and invade. Proteolysis-mediated matrix degradation is indispensable for the collective invasion of cancer cells. Differently, amoeboid-roundish cells can squeeze through narrow spaces and smaller pores of the ECM without proteolysis-dependent ECM remodelling. During this type of movement, the cells maintain weak and dynamic cell adhesion to ECM, resulting in high-speed migration (Pandya, Orgaz, & Sanz-moreno, 2017; Wu et al., 2021). Several studies reveal that matrix metalloproteases (proteolytic ECM enzymes) are induced by ERK signals, for instance, MMP9 (Kim et al., 2009) or MMP1, an

EGF specific collagenase for EMT (Sarah Park et al., 2011) (Figure 9). According to this data, ERK molecular signal takes part in tumour invasion, but how is not still understood.

During tumour progression (chemotaxis, migration and invasion), cytoskeleton components are highly integrated. Actin cytoskeleton functions are well orchestrated in normal cells, maintaining cell shape and structure by phosphorylation of actin-binding proteins (Fife et al., 2014). The actin cytoskeleton components form a dynamic network

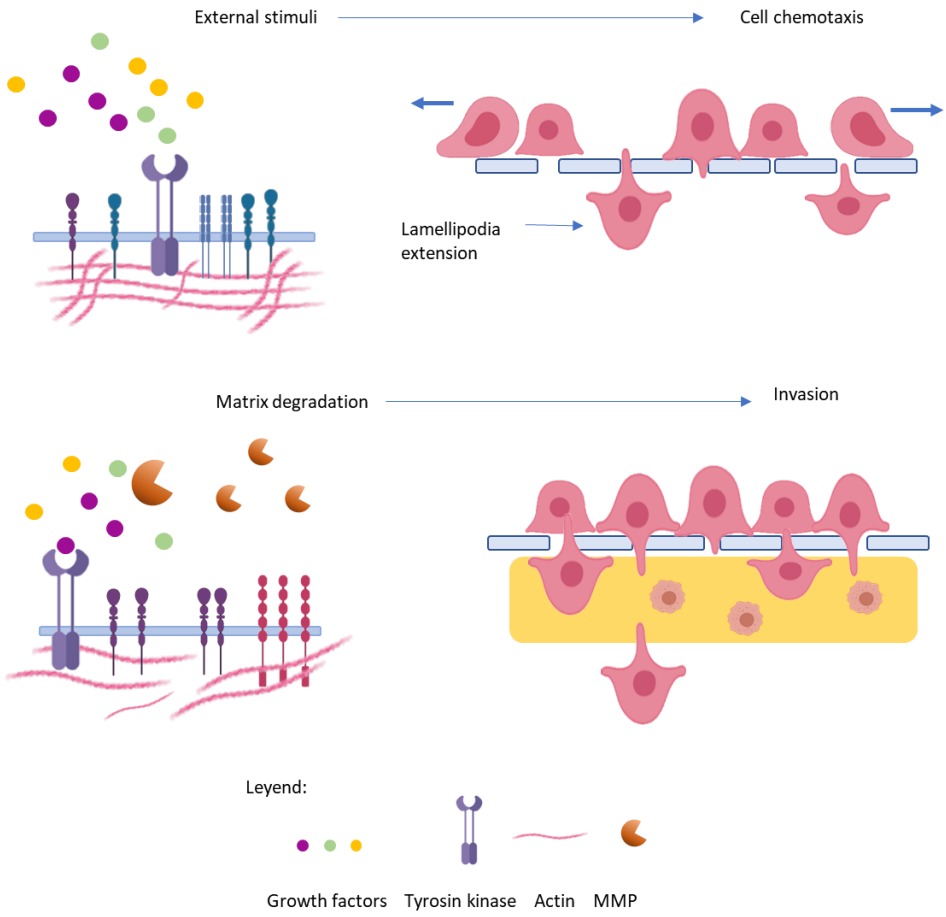

Figure 9. ***Stimulus cell migration response.*** *Normal epithelial cells respond to stimuli (chemotaxis). As a result, actin signalling networking originates lamellipodia. The actin filament contractions allow the cell to change a suitable morphology to migrate on the surface, creating focal adhesions (on the top), or invade the ECM thanks to matrix metalloproteases (on the bottom). MMP: matrix metalloproteases.*

interacting with signalling molecules as an adaptive response to alterations. Participate in morphological changes like cell protrusion formation and cell adhesions (cell-cell or cell-ECM). Furthermore, actin is involved in matrix topology migration and invasion (Nassef et al., 2019).

1.5. Epithelial-mesenchymal transition

Epithelial-Mesenchymal Transition (EMT) is a reversible cellular programme that transiently places epithelial cells into mesenchymal cell states. The contrary process is known as a Mesenchymal-Epithelial Transition (MET). During the EMT process, epithelial cells adopt a spindle-shaped and mesenchymal morphology. Besides, EMT is orchestrated by EMT- inducing transcriptions factors (EMT- TFs) to induce the expression of genes that promote the mesenchymal cell state and repress the expression of genes that maintain the epithelial state (Ye et al., 2015). In the course of tumour progression, EMT confers on individual cancer cells multiple traits associated with high-grade malignancy (Morel et al., 2008). That causes the ability of mesenchymal carcinoma cells to mount resistance to several treatments (Dongre & Weinberg, 2019).

EMT-invasion programme is activated by external signals like TGFβ, Wnt, NOTCH, and mitogen growth factors. TGFβ is considered the main inductor of EMT in different cell types, switches on EMT-TFs through SMAD proteins. It is evident cross-communication between ERK, p38 MAPK, PI3K-AKT and RHO-GTPases, which collaborate in various ways to the EMT programme expression (Lamouille et al., 2014). Otherwise, mitogenic growth factors that in turn enables the activation of the PI3K-AKT, ERK-MAPK, p38 MAPK and JNK pathways. For instance, EGF and IGF-1 activate EMT through PI3K-AKT and MEK-ERK (Liao et al., 2014). Furthermore, the tumour microenvironment serves as a reservoir for various cytokines and chemokines secreted by stromal cells. Some of these paracrine signals, acting in combination, induce an EMT programme in carcinoma cells, promoting tumour progression (Dongre & Weinberg, 2019).

Activation of EMT results in the loss of cell polarity, disruption of cell-cell junctions, degradation of the underlying basement membrane and reorganization of the extracellular matrix (ECM). This reaffirming that actin stress fibres play important roles in morphogenesis, cell adhesion and migration (Pandya, Orgaz, & Sanz-moreno, 2017). Together with morphological changes, the expression of Zeb1, Snail or Twist genes is well-characterized in epithelial-mesenchymal transition (Figure 10). However, the triggering signals associated with signal transduction pathways of EMT are not well understood. Tumour cells can gain access to signalling programs that allow epithelial cells to migrate and invade. Though it is not clear how long and concentration of growth factors influence over worse prognosis, neither is understood the intracellular signalling pathway behaviour under-stimulation. Nevertheless, the previous studies support that EMT might arise dependent on ERK and EGF stimulation (Schelch et al., 2021).

Newly, Rao and colleagues have published that KSR1- ERK promotes EMT phenotype in colon cancer (Rao et al., 2021). In the same way, the inhibition of IQGAP2-ERK (Kumar et al., 2021), and Paxillin-ERK suppresses EMT and metastasis (Wen et al., 2020).

Therapeutical development to block EMT is focused on inducing the MET, the revert process of EMT, due to the transiency associated with each phase and function depending on the state of metastatic progression (Pasquier et al., 2015). There are approaches to specific targeting of RTKs oncogenic signalling (Imai & Takaoka, 2006). But targeting EMT receptors is not easy due to the redundant nature of several EMT pathways and focusing on EMT-TFs as a target could be more effective (Singh et al., 2018). However, some representative therapeutics controlling EMT has been approved by FDA, like an ERBB2 (Erb-B2 Receptor Tyrosine Kinase 2) target in breast cancer or EGFR target, in NSCLC tumours (Imai & Takaoka, 2006).

Although the causal roles of EMT programmes in metastasis formation are scarce, there is initial proof that expression at least transiently of an EMT process is crucial for the metastatic dissemination of diverse types of cancer (Dongre & Weinberg, 2019). The expression of E- cadherin in the cells that form these clusters would seem to contradict

the notion that the EMT programme promotes invasiveness, like E- Cadherin typically repressed during EMT. In this way, the transformation of mesenchymal stem cells and tumorigenic characters driven by EMT induction (Morel et al., 2008) is a point of interest in the search for new therapeutical targets that reverse the mesenchymal stem cells towards epithelial cells (Figure 10).

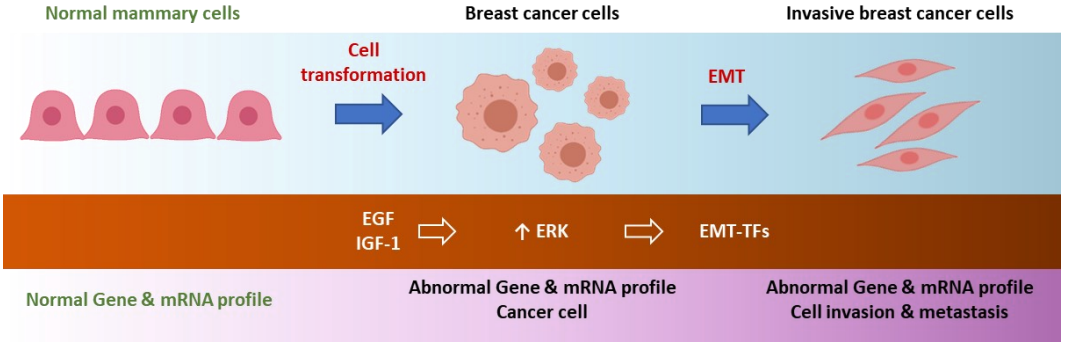

Figure 10. ***Epithelial-mesenchymal transition diagram****. EMT is described by cell shape and mRNA profile. Proliferative stimuli increase aberrant signalling which is able to enhance transcript factors involved in EMT.*

1.6. Metastasis

As the biology of metastasis, it becomes increasingly clear that disseminated cancer cells must contrive various kinds of adaptive programmes to thrive in their new locations and succeed in colonizing the newly encountered microenvironments of different tissues away from the original tumour. The metastatic cascade involves multiple steps, including invasion, entry into the circulation from the primary tumour, systemic dissemination, arrest and extravasation in secondary organs, settlement into latency, reactivation, outgrowth, and potential seeding of tertiary metastasis (Obenauf & Massagué, 2015; Pijuan et al., 2019). The plasticity of cellular phenotypes and possible therapeutic interventions are focus on scattering cells.

In cancer development and progression, the ERK signal and its hyperactivation are critical. The role of the MAPK signalling pathway in tumour extracellular matrix degradation and tumour angiogenesis is emphasised. The cellular processes triggering by

signalling pathways requires further analysis to clarify the role of the MAPK pathway in tumorigenesis and development (Guo et al., 2020). So, the ERK specific targets that regulate cell morphology, RNA profiles and cytoskeleton signalling are not well-known.

OBJECTIVES

2. Objectives

As mentioned in the introduction, ERK dimerization is determinant in the shaping of ERK signals. Thus, it could play pivotal roles in the regulation of specific biological processes associated with tumorigenesis, triggered in response to different stimuli.

In this respect, our main objective is to investigate whether ERK dimerization is differentially involved in defined cellular responses to different ERK-activating stimuli involved in tumorigenesis and tumour progression. This will propel us in our understanding of the fundamentals of ERK signal variability and will help us to identify specific cellular processes regulated by ERK dimerization, making them subject to modulation by ERK dimerization-aimed therapies.

Objective 1.- Analysis of ERK dimerization in response to different stimuli.

1.1. To study the dimerization of ERK in response to differential agonist stimulation.

1.2. To analyze the ERK interactome resulting from stimulation with different agonists, in order to identify ERK dimerization-dependent partners.

Objective 2.- To study the role of ERK dimerization in cell morphology through the remodelling of the actin cytoskeleton.

Objective 3.- To determine the role of ERK dimerization in Epithelial-Mesenchymal Transition (EMT), 3D-invasion and metastasis.

3.1. To study the effect of DEL-22379 on cell morphology in a 2D migration model.

3.2. To investigate the expression of EMT-related genes as a function of the stimulus and DEL-22379 treatment

3.3. To determine the role of ERK dimerization in a 3D invasion model and chicken embryo.

MATERIALS AND METHODS

3. MATERIALS AND METHODS

3.1. Plasmid DNA purification

Plasmid purification is a technique used to isolate and purify plasmid DNA. This technique was carried out in bacterial cultures derived from bacterial competent cells, DH5α (Invitrogen), an *Escherichia coli* strain modified to maximize transformation efficiency. Transformed bacteria were inoculated in Luria-Bertani Broth (LB) culture medium with specific antibiotics according to the resistance provided by the plasmid, usually ampicillin or kanamycin at a concentration of 50 µg/mL. For maxiprep, the Qiagen Plasmid Maxi Kit was used. After being incubated overnight (O/N), bacteria were centrifuged at 6,000 rpm for 10 min. Pellet was resuspended in 10 mL of resuspension buffer (50 mM Tris/HCl pH 8, 10 Mm EDTA, 10 µg/mL RNAase A). Then, cells were lysed with 10 mL of lysis buffer (200 mM NaOH, 1 % SDS), mixed by inverting 6 times and incubated for 5 min at room temperature. A neutralization solution (3 M CH3COOH pH 5.5) was added and incubated for 5 min. After, the mix was centrifuged at 12,000 rpm for 5 min to eliminate the precipitated material containing genomic DNA, proteins, and cellular debris. The supernatant, containing the plasmid DNA, was filtrated in a properly equilibrated anion-exchange Qiagen column by gravity flow. After two washes, the DNA was eluted with 5 mL of elution buffer and 10 mL of cold isopropanol were added to precipitate the DNA. After 5 min, this mix was centrifuged at 10,000 rpm 30 min at 4 °C, and then washed with 1 mL of 70 % ethanol. Once dried, DNA was resuspended in 300 µL of distilled deionized water (ddw).

In the case of bacterial cultures of a lower scale (5 mL of volume), the bacterial culture was processed by GeneJET Plasmid Miniprep Kit (Thermo Fisher) according to the manufacturer's instructions. The purified DNA was eluted in 40 µL of Elution Buffer (10 mM Tris, 1 mM EDTA).

The plasmid DNA was quantified using Nanodrop (Thermo Scientific), 1 µL of DNA was needed for the quantification. To further analyse the quality and any possible RNA contamination, 2 µL of DNA was loaded in a 0.8 % agarose gel electrophoresis, run at 80 V in TAE buffer (0.09 M Tris-acetate, 2 mM EDTA) and stained with SYBER Safe (Invitrogen). A loading buffer with bromophenol blue to monitor the progress of the electrophoresis was added to the DNA sample.

All the plasmid (Table 2), as well as siRNA (Table 3), utilized in the experiments of this thesis are described in the following tables:

Table 2. Description of the plasmids used in this thesis

Plasmid	**Description**
pCEFL	Mammal expression vector. EF-1α Promoter/ bGH poly-A. The empty vector used as a control to normalize the amount of DNA to transfect.
pCMV FLAG KSR1 wt	Mammal expression vector. CMV promoter/ bGH poly-A. Encodes the scaffold protein KSR1 fused to N-Terminal FLAG epitope. Source: Dr J. Lozano
pCEFL HA ERK2 wt	Mammal expression vector. EF-1α Promoter/ bGH poly-A. Encodes the isoform ERK2 fused to HA epitope. Source: Dr Engelberg
pCEFL HA ERK2 H174EL4A	Mammal expression vector. ERK2 mutant unable to dimerize, which acts as an inhibitory dominant preventing the dimerization of endogenous ERK. Encodes the isoform ERK2 fused to HA epitope. Source: Dr M. Cobb

pCEFL HA ERK2 R65S	Mammal expression vector. EF-1α Promoter/ bGH poly-A. Encodes the isoform ERK2 fused to HA epitope. Source: Dr Engelberg

Table 3. siRNAs used to knock down ERK interactors

siRNA	Company
siKSR1	siRNA against KSR1 (human) (Santa Cruz Biotechnology)
siPEA15	siRNA against PEA15 (human) (Santa Cruz Biotechnology)

3.2. Cell culture

The cell lines utilized during this thesis are listed in the following table (Table 4):

Table 4. Cell lines used in this thesis

Cell line	Description
HEK 293T	Epithelial cells derived from the human embryo kidney. Immortalized with SV40 T-antigen.
MCF-7	Epithelial cells derived from the human mammary gland, breast. PI3KCA mutant.
MDA-MB-231	Epithelial cells derived from the human mammary gland, breast. B-RAF mutant.
A549	Human non-small cell lung carcinoma Source: Dr M. Grusch

M38K	Human biphasic mesothelioma (MPM)-derived cell line. Source: Dr M. Grusch
DF-1	Fibroblast spontaneously transformed cells derived from embryo *Gallus gallus.* Source: ATCC company cat #CVCL_0570

All cell lines were grown on DMEM (Dulbecco`s Modified Eagle Medium, Sigma), 10 % FBS (fetal bovine serum, Gibco) and 1 % penicillin-streptomycin (10,000 U/mL) (Sigma). Except for M38K and A549 cell lines that were grown on RPMI (Roswell Park Memorial Institute, Sigma), 10 % FBS and 1 % penicillin-streptomycin (10,000 U/mL) (Sigma).

3.2.1. Cellular transfections

- Polyethylenimine (PEI)

HEK 293T were transfected using polyethylenimine (PEI, Polysciences). PEI condenses purified plasmid DNA into positively charged particles that bind to anionic cell surfaces. In this way, the DNA-PEI complex is endocytosed by the cells through the cytoplasmic membrane (Longo et al., 2014).

Cells were split into P60 (60 mm) plates to reach a final confluence of around 60-70 % at the time of the transfection. In this way, all cell surfaces are completely exposed, and it makes DNA entrance easier into the cell and subsequently into the nucleus. PEI (1 mg/mL) was used in a ratio of 1:3 w/v (DNA: PEI) diluted in Opti-MEM medium (Gibco). This dilution is incubated for 5 min, vortexed and incubated again for 20 min at room temperature. Finally, the mix was added to the cells, reaching a final volume of 2.5 mL in the P60 plate.

- Lipofectamine 3000

MCF-7, MDA-MB-231 and M38K were transfected in P60 with Lipofectamine 3000 (Invitrogen), a lipid nanoparticle technology. Following the protocol, 5 µg of DNA plus 5 µL of P3000 reagent were diluted in 125 µL of Opti-MEM medium and 3 µL of Lipofectamine 3000 reagent were added to another tube with 150 µL of Opti-MEM medium. They were incubated separately for 5 min at room temperature and then, the content of the DNA tube was added to the one with Lipofectamine. They were incubated for 10 min and finally added to the cells.

- Lipofectamine RNAiMAX

The small interfering RNA (siRNA) were transfected in MCF-7 cell using Lipofectamine RNAiMAX (Invitrogen), a chemical method of transfection. Following the manufacturer's protocol, 2.5 µL of siRNA (final concentration of 25 pM) were diluted in 150 µL of Opti-MEM medium. In another tube, 1.5 µL of Lipofectamine RNAiMAX were diluted in 150 µL of Opti-MEM medium. After 5 min at room temperature, the 2 tubes were mixed, vortexed and incubated for 10 min. Finally, the mix was added to the cells laid in P60 plates.

For optimal plasmid expression, the cells were harvested at least 48 h post-transfection.

3.2.2. Stable cell lines generation

Stable cell line generation is made possible using positive selection markers such as a G418/Geneticin antibiotic resistance. Selection markers can be delivered using the same plasmid that contains the gene of interest (cis), or on a separate plasmid (trans) that needs to be co-transfected with the plasmid containing the gene of interest. Before starting to obtain stable cells, cells were seeded with different concentrations of antibiotics to determine their sensitivity to the antibiotics before obtaining stable cell lines. The optimal concentration of G418/geneticin (Sigma) in our stable cells is 75 mg/mL.

3.3. 2D-Proliferation assay

To evaluate cell proliferation, we performed 2D-proliferation assay. For that, cells were cultured in T6 (60 mm) plates for 2 days. Medium was removed, and the plates were rinsed carefully with 1x PBS. Cells were fixed with paraformaldehyde 4 % and stained with crystal violet-1 % methanol, then the cells were rinsed with tap water.

The number of cells in each condition was normalized to control (not transfected) samples and expressed as a percentage of the confluence of dyed cells. Cell proliferation was determined by measuring the area covered by cells with ImageJ.

The following growth factors (Table 5) and treatments (Table 6) were used.

Table 5. Growth proliferative stimuli

Growth factor	Company name	Concentration
EGF	Sigma-Aldrich	100 ng/mL for 3 min 50 ng/mL for 48 h
IGF-1	Peprotech	50 ng/mL for 3 min 25 ng/mL for 48 h
TGFB	Peprotech	100 ng/mL for 3 min 5 ng/mL for 48 h

Table 6. List of inhibitors

Drug name	Drug activity	Company name	Concentration
DEL-22379	ERK dimer inhibitor	Vichem Chemie	10 µM, 1h 2 µM, 48h
U0126	MEK inhibitor	Promega	10 µM, 1h
Cytochalasin D	Microfilament inhibitor	Merck	10 µM, 18h

3.4. Cell chemotaxis and invasiveness assays: Transwell assays

These assays were used to analyze cellular chemotaxis and invasiveness. Cell chemotaxis evaluates to the ability of cells to migrate towards a chemoattract. Cell invasiveness is defined as passing the basement membrane and infiltration into the underlying interstitial tissues.

We performed 2D cell chemotaxis by using transwell chambers (Corning) which contain 24 well inserts with 8 μm pores. In this way, non-adherent migrated cells dropped into the media in the lower chamber. By contrast, invasive cells can degrade the matrix through the ECM layer.

To analyse these cell abilities, cells were seeded in gel-based 3D structures to mimic ECM components, for example, collagen I. For that, the protocol continued diluting matrix-gel (Corning) in basal media (1:50) and adding 100 μL to the top of the transwell and incubating for 1 h at 37 degrees. This step was skipped if chemotaxis through the porous membrane was the target for our analysis.

Then, $0.1*10^6$ cells/mL were added in 200 μL of serum-free to the bottom of transwell and added 1 mL FBS media to the bottom. The stimuli were added to the bottom of the transwell (Figure 11).

After 16 hours to study cell chemotaxis and invasion, cells were fixed with 4 % paraformaldehyde and stained with crystal violet-1 % methanol to be visualized by optical microscopy (10 magnification). Quantification of migration was expressed as relative migration and normalized to starved control samples. Migration was determined by measuring the area covered by cells (0.47 μm^2) for each section with the ImageJ tool.

Chemotaxis assay was determined by measuring the covered area by cells in response to stimuli that migrate towards the porous membrane.

Invasion assay was determined by measuring the covered area by cells in response to stimuli that migrate through the matrix gel across the porous membrane.

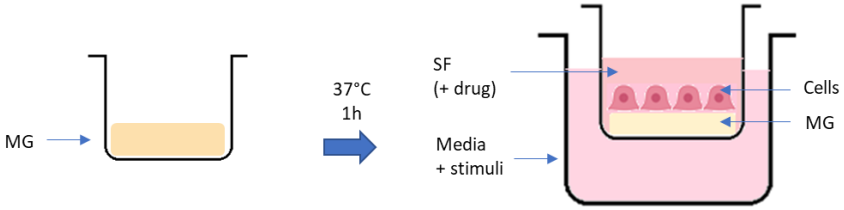

Figure 11. ***Transwell assay method.*** *Firstly, it was added matrix gel, after its solidification that put the cells in the top of the Transwell. The assay starts when the Transwell is put in the plate with the media. MG: Matrigel, SF: Serum-free media.*

3.5. 2D-Cell migration

To measure cell migration in 2D *in vitro* cultures, 100,000 cells were seeded in a T6 plate (60 mm) and treated with drugs and/or stimuli in growing conditions, except for evaluating the indispensable role of ERK signalling in EMT. In this case, the migration assay was performed in basal conditions.

The morphology changes were measured by qualitative and quantitative analysis over time. The qualitative ones were visual, photos were taken in Microspy Ti Eclipse FL invert new #246. The video microscopy was generated using a Nikon Visitron Live Cell System (Visitron Systems GmbH) with images taken every 30 min for 48 h. Migration and cell cycle analyses single cells were manually tracked using ImageJ to obtain coordinates for each cell and time point. For further analysis of migratory behaviour including speed, mean squared displacement (MSD), directionality ratio (DR), and origin plots, the DiPer migration tool was used. The algorithms used by this program have been described in detail by Gorelik & Gautreau, 2014.

3.6. 3D-Tumour spheroids: invasive growth assay

3D spheroids are micro-sized cellular aggregates that have been widely used as models of different cancer types in vitro. Our method allows the production of many spheroids under reproducible conditions with a series of benefits. First, this assay offers cellular heterogeneity. Second, the assay simulates a characteristic gradient of oxygen, nutrients, pH, and cellular density is similar to that observed in solid tumours in humans. Third, as under physiological settings, physical barriers are established, due to ECM-cell and cell-cell interactions, because of ECM deposition. Fourth, the method shows a solid tumour growth similarity, an initial exponential growth (the avascular growth phase), and the dormant phase (a plateau state). And finally, gene expression spheroid patterns are closer to in vivo solid tumours than monolayer cell cultures (Costa et al., 2016) (Figure 12).

$4*10^4$ cells/mL adherent cells were resuspended in a low viscosity medium made of 800 µL -10 % FBS medium and 200 µL of low viscosity methylcellulose solution previously prepared as follows.

-Methylcellulose (Sigma) preparation requires 3 g of methylcellulose in a 500 mL bottle, plus a magnetic stir bar, autoclaved. 125 mL of DMEM were added to the sterile methylcellulose and incubated for 15 min at 60 °C (shake the bottle to destroy the clump of methylcellulose). Stir on a magnetic stirrer for 20 min, then add another 120 mL of DMEM and stir on for ~ 4 hours at room temperature. Keep the bottle overnight at 4 °C. Add 5 mL of penicillin/streptomycin (10,000 U/mL) and stir thoroughly.

Aliquot the Methylcellulose solution in 50 mL Falcon tubes, centrifuge for 20 min; 4,000 rpm at 4 °C and pour the supernatant into 50 mL Falcons.

25 µL droplets of the cell-methylcellulose suspension were suspended on the lid of a P100 tissue culture dish and cultured for 48 hours at 37 °C - 5 % CO2. During this time,

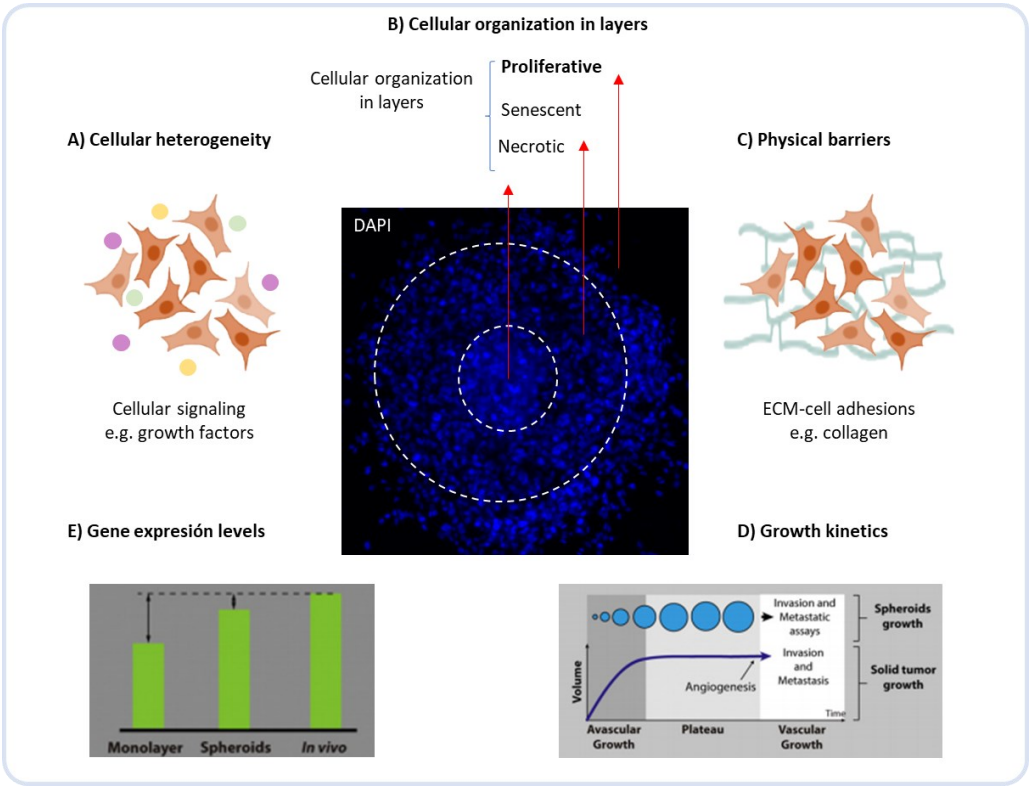

*Figure 12.- **The main characteristics of 3D spheroids**. A. Cellular heterogeneity reproduces the cellular distribution found in tumours in vivo. B. 3D structure is organized in three main layers (proliferative, senescent, and necrotic layers), with a characteristic gradient of oxygen, nutrients, pH and cellular density that is similar to that observed in solid tumours in humans. C. Physical barriers established due to the existence of ECM -cell and cell-cell interactions, because of ECM deposition. D. Correlation between the growth kinetics of spheroids versus solid tumours: initial exponential growth (avascular growth phase) and plateau state. E. Representation of gene expression patterns obtained from monolayer cell cultures, spheroids, and in vivo solid tumours. ECM: extracellular matrix. Image adapted from Costa et al., 2016. The microscopy photo shows the nucleus stained with DAPI. Image taken from MCF-7 spheroids.*

cells clustered into compact sphere-like formations. It is recommendable to add 5 mL of 1x PBS to the P100 plate to avoid droplet evaporation. After that, the spheroids were collected into a 15 mL tube, resuspending them gently in 5 mL of 1x PBS and centrifuged at 300 rpm for 15 seconds. Carefully, the supernatant was removed, and the spheroids were resuspended gently in collagen I solution (1.7 mg/mL in 5 x DMEM, Sigma).

-Collagen I preparation per mL: collagen 555.6 µL (Sigma), 200 µL 5x DMEM, 213 µL dH20 (ultrapure and filtered water), and 30 µL 0.1 M NaOH.

-5 x DMEM preparation: Add the following components of the media in a 1 L bottle, then filtered it. DMEM Powder batch W/O phenol red (Sigma), 44 mM NaHCO3, 1 mM sodium pyruvate (NaH2PO4), 0.2 mM L-methionine (Sigma), 0.2 mM L-cystine (Sigma), 1 mM NaH2PO4*2H2O (Sigma), 3.75 mM L-glutamine (Sigma), adjust pH with NaOH to 6.6.

Reagents were added in the following order: collagen> 5x DMEM> dH20> NaOH. Mix with the pipette, without bubbles.

The spheroids were suspended in 2,200 µL of the collagen I solution. It was obtained around 5 droplets per well. 300 µL of this suspension were seeded in a 24-well plate and left in the incubator at 37 °C – 10 % CO2 for 4 hours until the matrix polymerized. Finally, 1 mL of 10 % FBS medium was added onto the collagen and took phase-contrast pictures every 24 hours for 4 days.

To quantify the spheroid proliferation and invasion, it was calculated the size ratio between day 1 and day 4. For that, the ImageJ tool was used.

3.6.1. 3D-spheroid immunofluorescence assay

Organoids were fixed for 10 min at room temperature in 20 % PFA (paraformaldehyde)/PBS. The excess paraformaldehyde was removed, and the spheroids were washed with 1x PBS 3 times for 5 minutes. Next, the cellular membranes were permeabilized and blocked with 0.3 % Triton in 4 % BSA/PBS for 20 min at room temperature. Again, the organoids were washed 3 times with 1x PBS. The primary

antibody was diluted in 4 % BSA/PBS. Next, the organoids were washed five times with 1x PBS and kept the primary antibody O/N at 4 °C. The next day, the organoids were washed 3 times with 1x PBS, and the secondary antibody was added and incubated for 2 h at RT. Finally, the organoids were washed 5 times with 1x PBS, in the second wash DAPI was added.

Images were acquired using the Leica TCS SP8 laser-scanning confocal microscope with a white light laser source for excitations at 488 nm and 540/565 nm (green and red colour, respectively). Confocal images (512x512 pixels; 0.15mm pixel size) were acquired sequentially on a SP5 laser-scan microscope (Leica) with a 10x objective using LAS AF acquisition software. Images were presented after digital adjustment of curve levels (gamma) to maximize signal with ImageJ software. In all cases, exposure time, sensor gain, and digital manipulation were the same for control and experimental samples. Fluorochromes and colours were as indicated in the figure legends.

3.7. Cytotoxicity assay

To calculate the concentration at which a drug can inhibit 50 % (IC50), we have used Syber Green nucleic acid stain (Thermo Fischer).

First, we seeded 3,000 cells per well in T96 wells. The following day, we added the drug at different concentrations. After 48 h, we discarded the medium and washed the cells with 1x PBS. The plate was frozen at -80 °C O/N or longer. For analyse, plates were defrosted 45 min at room temperature, and 1x lysis Syber buffer with 1:8000 Sybr Green dye was added. Plates were incubated in darkness for 3h at room temperature, and the fluoresce at 485 nm excitation and 535 nm wavelength emission was read.

- Cytotoxicity assay lysis buffer: TrisHCl pH 8 10 mM, EDTA 2.5 mM, TritonX-100

0.1 %.

The results were represented in a dose-response graph using GraphPad Prism 7.

3.8. Epithelial-mesenchymal transition analysis

3.8.1. RNA isolation from cell culture

Before starting the protocol provided by Analytik Jena, cells were centrifugated at 5,000 rpm for 5 min. Then, lysis solution was added at room temperature, avoiding clumps to maximize the final yield of total RNA. The sample was incubated for 3 min at room temperature and centrifuged at 11,000 rpm for 2 min. The elution was added into the spin filter type A. An equal volume of the elution was added (400 µL) of 70 % propanol to the eluted RNA solution. The mix was placed into a new spin filter type B and centrifuged at the same conditions. The spin filter B was placed in a new tube, and 500 µL of washing solution was added. The mix was centrifuged at 11,000 rpm for 1 min. The spin filter B was placed in a new tube and was centrifuged at 11,0000 rpm for 3 min to remove all traces of propanol. The spin filter B was placed into an elution tube. 30-80 µL RNase-free water was added and incubated at room temperature for 1 min. Finally, the elution was centrifuged at 11,000 g for 1 min.

The quality and the quantity of the RNA was measured using the NanoDropTM 2000c (Thermo Fisher).

2 µg of isolated RNA isolated were enough for the retro-transcription into cDNA.

3.8.2. Reverse transcription

For retro-transcription, 2 µg of RNA (final volume 13 µL) were incubated at 70 °C after adding 10 µL ultrapure H_2O. The mix can be stored at -20 °C or placed on ice immediately before retro-transcription. The reverse transcription mix was prepared according to Table 7. The mix was incubated for 1 h at 42 °C (step 1) followed by 10 min at 7 °C (step 2). Finally, 20 µL ultrapure H_2O was added to obtain 40.5 µL of cDNA dilution.

Table 7. ***Mix for retro-transcription***

Reactive	Volume
5x RT Buffer	4 µL
dNTPs	1 µL
RT	1 µL
Ribolock (40U/µL), individual RNAses	0.5 µL
Random hexamer primers (0.2 µg/ µL)	1 µL

3.8.3. Real Time-PCR

Primers for the genes under study were designed using the Clone Manager tool from mRNA and genomic sequences obtained at National Center for Biotechnology Information - Gene/Nucleotide databases (https://www.ncbi.nlm.nih.gov/) (Table 8). qPCR preparation consisted of five steps. Firstly, the PCR mix was prepared according to Table 9. The conditions were calculated for duplicates of a cDNA sample. Secondly, the primers of interest were added to the PCR mix (Table 8). Thirdly, 11 µL of the RT-PCR mix was added to each P96 well. Fourthly, 1 µL of each sample of cDNA was added to each well. Fifthly, the samples were analysed under the PCR conditions according to Table 10Table .

Table 8. ***RT-PCR primers for EMT analysis***

Primer name	Direction	Sequence
ZEB1	for	CCA GTG GTC ATG ATG AAA ATG GAA CAC C
ZEB1	rev	CAG ACT GCG TCA CAT GTC TTT GAT CTC
SNAIL	for	ATG TGC ATC TTG AGG GCA CCC
SNAIL	rev	TAT GCT GCC TTC CCA GGC TTG
TWIST1	for	CGA CGA GCT GGA CTC CAA GAT G
TWIST1	rev	AGA CCG AGA AGG CGT AGC TG

CDH2	for	TTC TCC TCC ACC TTC TTC ATC
CDH2	rev	GCA TCA TCA TCC TGC TTA TCC
CDH1	for	GGC ATT GTA GGT GTT CAC ATC ATC GTC
CDH1	rev	CAG AGC CTC TGG ATA GAG AAC GCA
VIM	for	CTG AAT CTC ATC CTG CAG GC
VIM	rev	GGC TCA GAT TCA GGA ACA GC
GAPDH	for	ACG CCT GCT TCA CCA CCT TC
GAPDH	rev	AGC TCA CTG GCA TGG CCT TC

Table 9. RT-PCR mix for EMT analysis

Reactive	**Volume**
SYBR Green master mix (Biorad)	12.5 µL
5' primer (20 µM)	1 µL
3' primer (20 µM)	1 µL
H_2O	8.5 µL

Table 10. - RT-PCR protocol for EMT analysis

Step	**1**	**2**	**3**	**4**	**5**	**6**	**7**
Temperature	50 °C	95 °C	95 °C	60 °C	95 °C	65 °C	95 °C
Time	10 s	10 min	15 min	1 h	10 min	5 s	5s
Cycles			x 39 cycles				

Gene expression was quantified by the Ct (cycle threshold) of each gene. Ct levels are inversely proportional to the amount of target nucleic acid in the sample. Duplicates of each condition sample were relativized and the log2 fold expression was calculated. The housekeeping gene used as a control was GAPDH.

3.9. Immunoblotting analyses (IB)

This method is commonly named western blotting (WB). This technique analyses protein expression (immunoblotting analysis or Native-electrophoresis), protein-protein interaction (immunoprecipitation) and cell localization of the protein (nuclear-cytoplasmatic fractionation).

- SDS-PAGE gel electrophoresis

For protein extraction, cultured plates were laid on ice, rinsed with cold 1x PBS and harvested using lysis buffer.

The lysates were centrifuged at 13,000 rpm for 10 minutes at 4 °C. The supernatant was collected into a new tube. Proteins contents were quantified by colourimetry evaluating absorbance at 620 nm wavelength using the Bradford Method (Biorad), bovine serum albumin (BSA) standard curve was used. Finally, 4 x Laemmli loading buffer was added to 30 µg of protein. The mix was boiled at 95 °C for 5 minutes to denaturalise the proteins before resolving proteins in sodium dodecyl sulfate (SDS)-polyacrylamide gel electrophoresis (PAGE).

SDS-gels are composed of a stacking gel and a resolving gel. Vertical electrophoresis was performed in a Mini-Protean Bio-Rad device with the running buffer. Then, proteins were electrophoretically transferred to nitrocellulose membranes (Thermo Fisher) at 400 mA constant amperage (1 minute for each 1 kDa of the protein approximately) at 4 °C in transfer solution. Then, membranes were blocked in Tris Buffered Saline-Tween (TBS-T) containing 4 % BSA (blocking solution) for 1 hour shaking at room temperature. Blots were incubated from 1 hour at room temperature to O/N at 4 °C (depending on the antibody affinity) with the different antibodies (Table 11).

- Chemiluminescence method: the membrane was incubated with HRP-conjugated secondary antibodies and revealed with an enhanced chemiluminescent system (ECL). Autoradiography with Konica films was performed to develop the blots.

- The fluorescence method requires the Licor Odyssey technology. This protocol demands Alexa secondary antibodies to visualise the blots.

Buffers required:

- Lysis buffer: 20 mM HEPES pH 7.5, 10 mM EGTA, 40 mM β-Glycerophosphate, 1% NP-40, 2.5 mM $MgCl_2$, 1 mM $NaVO_4$, 1 mM DTT and protease inhibitors (10 µg/mL of aprotinin and 10 µg/mL of leupeptin).
- 4x Laemmli loading buffer**:** 100 mM Tris pH 6.8; 4 % SDS; 20 % glycerol; 20 mM DTT and 0.005 % bromophenol blue.
- Polyacrylamide gels:

  Stacking gel: 4 % acrylamide; 125 mM Tris-HCl pH 6.8; 0.4 % SDS; 0.1 % Ammonium Persulfate (APS); and 0.1 % Tetramethyl ethylenediamine (TEMED) in H_2O.

  Resolving gel: acrylamide (percentage depends on the molecular weight of the protein); 375 mM Tris-HCl pH 8.8; 0.4 % SDS; 0.1 % APS; and 0.1 % TEMED in H_2O.
- Running buffer: 25 mM Trizma base; 192 mM Glycine; 0.1 % SDS.
- Transfer buffer: 25 mM Trizma base and 192 mM Glycine.
- Tris Buffered Saline-Tween (TBS-T): 20 mM Tris; pH 7.4; 137 mM NaCl; and 0.05 % tween.
- Enhanced chemiluminescent system (ECL):

  Solution 1: 1M TRIS HCl pH 8.5; 90 mM Coumaric Acid; and 250 mM Luminol.

  Solution 2: 1M TRIS HCl pH 8.5; and 30 % H_2O_2 (Hydrogen Peroxide).

Antibodies utilized in this work:

Table 11. Immunoblotting antibodies

Antibody	**Specificity**	**Dilution**	**Source**
Activated MAP Kinase	Mouse monoclonal	1:1000 (IB) 1:100 (IF)	Sigma
p-ERK1/2 (Tyr 204)	Mouse monoclonal	1:1000 (IB)	Santa Cruz

ERK2	Mouse monoclonal	1:1000 (IB)	Santa Cruz
FLAG	Mouse monoclonal	1:5000 (IB) 0.5 µg (IP) 1:150 (IF)	Sigma
FLAG	Rabbit polyclonal	2 mg (IP)	Sigma
KSR1	Rabbit policlonal	1:500 (IB)	Abcam
Rho GDI	*Mouse monoclonal*	1:1000 (IB)	Santa Cruz
Lamina A/C	Mouse monoclonal	1:1000 (IB)	CIND

Conjugated secondary antibody

Anti-Mouse-HRP Mouse IgG	Goat	1:10000	Bio-Rad
Anti-Rabbit-HRP Rabbit IgG	Goat	1:10000	Bio-Rad
Alexa Fluor 488 Mouse IgG	Goat	1:10000	ThermoFisher
Alexa Fluor 594 Rabbit IgG	Goat	1:10000	ThermoFisher

- Native gel electrophoresis (Native-PAGE)

The purpose of this kind of electrophoresis is to analyse ERKs' dimerization (Pinto & Crespo, 2010).

In this method, 30 µg of protein were mixed in a 1:1 volume ratio with 2x loading dimer buffer. Samples were run in an 8 % acrylamide gel without SDS (neither in stacking nor in the resolving part of the gel) at 80 V, constant voltage, for 2 h with SDS-free running buffer. The following steps were those of the SDS-PAGE protocol described above. In this case, proteins must be transferred into a nitrocellulose membrane at 400 mA constant amperage for 80 min.

- 10x Running and transfer buffer: 144 g glycine (USB) and 30.3 g tris (USB) per 1 L of H2O
- 2x loading buffer: 0.126 M Tris HCl pH 6.8; 20 % Glycerol: 0.1% (w/v) Bromophenol blue.

3.10. Co-immunoprecipitation assay

Co-immunoprecipitation (in short Co-IP) is a technique to identify protein complexes and determine protein-protein interactions. By targeting a known protein with a specific antibody, it may be possible to pull the entire protein complex out of the total lysate, thereby identifying unknown members of the complex.

Around 30 µg of protein were separated from the total lysate, and 4x Laemmli loading buffer was added to be run as a control for the protein content of the total lysate. For immunoprecipitation, 0.5-1 µg of the specific antibody was added to the rest of the lysate (about 300 µg of protein), and it was incubated rocking at 4 °C from 3 hours to O/N. After this, 15 µL of protein G-Sepharose 4B (GE Healthcare), which binds to the immunoglobulins allowing the precipitation of the immunocomplexes (protein-antibody), were added to the lysates and it was incubated for 20 minutes at 4 °C shaking. The next step was washing the beads twice with lysis buffer. Finally, the beads were resuspended in 20 µL of 2x Laemmly loading buffer and boiled for 5 minutes at 95 °C. The protein interaction was analysed by SDS-PAGE as previously has been described.

3.11. Nuclear-cytoplasmic fractionation

Nuclear-cytoplasmic fractionation was performed to study protein distribution between the nuclear and cytoplasmic cell compartments, either in basal conditions or upon stimulation.

Cells were washed with 1x PBS, and after adding 200 µL of buffer A per P60, cells were scraped carefully. After centrifugation at 1,200 rpm for 5 min, the supernatant was removed, and 200 µL of buffer B were added. The cytoplasmatic fraction was collected and stored at -80 °C after centrifugation at 1,200 rpm for 5 min.

To avoid nuclear contamination, the pellet was washed again with 1x PBS.

Then, 100 µL of buffer C were added to the pellet, pipetting vigorously to facilitate the nuclear disintegration, and centrifuged for 2 min at maximum speed.

Protein localization was analysed by SDS-PAGE as previously described. RhoGDI antibody was used as a cytoplasm marker whereas Lamina A/C was a nuclear marker (Table 11).

- Buffer A: 50 mM β-glycerophosphate pH 7.3; 1.5 mM EGTA; 1 mM EDTA; 1 mM DTT; proteases and phosphatases inhibitors.
- Buffer B: 40 mM HEPES pH 7.5; 1 % NP-40; 5 mM EGTA 400; 5 mM $MgCl_2$; 1 mM DTT, 1 mM Benzamidin; 1 mM orthovanadate; proteases and phosphatases inhibitors.
- Buffer C: 50 mM β-glycerophosphate pH 7.3; 420 mM NaCl; 1.5 mM $MgCl_2$; 0.2 mM EDTA; 1 mM DTT; 25 % glycerol.

The western blot analyses were processed and analysed using Fiji-Image-J Software to quantify protein expression.

3.12. Immunofluorescence assay

Cells were washed twice with cold 1x PBS for 5 min, followed by 4% paraformaldehyde fixation. To analyse cytoplasmic proteins, cells were fixed with 4 % paraformaldehyde for 10 minutes.

Once fixed, cells were washed twice 1x PBS, one wash with 0.1 M glycine and the other two washes with 1x PBS. Subsequently, cells were permeabilized for 5 min with 0.5 % Triton X-100 in 1x PBS and washed again with 1x PBS for 5 min.

Then, cells were incubated with 0.05 % TweenTM20 (Thermofisher) for 5 minutes to reduce surface tension. Primary antibody in PBS was added as a drop (8 µL) over the glass and incubated for 1 hour in a humidity chamber to prevent drying. After incubation with the primary antibody, cells were washed twice for 5 min with 1x PBS. Subsequently, glasses were washed with 0.05 % TweenTM20 to reduce surface tension.

The secondary antibody (conjugated with a fluorophore), specific for the primary antibody (Table 12), was added and incubated for 1 hour in the humidity chamber and then removed washing twice with 1x PBS. Finally, the glasses were set over a slide in mounting media with Prolong-DAPI (Invitrogen) and sealed with clear nail polish. The cells were examined by fluorescence microscopy (photomicroscope Axiophot, Carl Zeiss) or confocal microscopy (Leica TCS SP8). The images were processed using Image J software.

Table 12. ***Secondary antibodies conjugated with a fluorophore***

Antibody	Host	Target species	Dilution	Source
Alexa 594	Goat	Mouse	1:300	Invitrogen
Alexa 488	Goat	Rabbit	1:300	Invitrogen
Alexa 594	Goat	Rabbit	1:300	Invitrogen
Alexa 488	Goat	Mouse	1:300	Invitrogen
Alexa 647	Donkey	Goat	1:300	Invitrogen

3.13. Label Free Quantification proteomics

To identify proteins that interact with our target of interest, it was performed a mass spectrometry analysis.

Cells were transiently transfected with a FLAG-tagged construct. After 48 hours post-transfection, they were either starved O/N and stimulated with growth factors for 3 min. Cells were lysed using a lysis buffer, and proteins were immuno-precipitated using 6 µL of FLAG-M2 agarose beads (Sigma-Aldrich) for 2 hours at 4 °C. The FLAG-tagged construct immunoprecipitated were washed 4 times using a proteomic washing buffer (20 mM HEPES pH 7.5, 150 mM NaCl) to remove detergent contamination. Then,

immunoprecipitants were digested with trypsin, reduced, and alkylated as described by Turriziani and colleagues (Turriziani et al., 2014). Tryptic peptides were analysed on a Thermo Scientific Q-Exactive Mass Spectrometer connected to an Ultimate Ultra 3000 chromatography system incorporating an autosampler. Data were acquired with the mass spectrometry (MS) operating in automatic data-dependent switching mode, selecting the 12 most intense ions before tandem MS analysis. MS raw data were analysed by the MaxQuant software (Cox & Mann, 2008). Specifically, tandem MS spectra were searched against the human Uniprot database with a mass accuracy of 4.5 ppm and 20 ppm (for MS and MS/MS -tandem mass spectrometry-). Carbamylation was selected as a fixed modification. Variable modifications were N-terminal acetylation (protein) and oxidation. LFQ and peak matching was selected and was limited to within a 30 s elution window with a mass accuracy of 4.5 ppm. The results were based on three independent biological replicates.

3.13.1. Mass spectrometry results analysis: Bioinformatic analysis

A gene list was obtained after mass spectrometry, it was matched each gene with cancer datasets. It was used Cancertool (Cortazar et al., 2018), which integrates gene expression data from various publicly available studies. This database includes Gene Ontology (GO) enrichment, among others. GO gives information about the biological process, molecular function, and cellular component.

3.14. Chick embryo invasion model

This assay is a unique *in vivo* model that overcomes many limitations for studying metastasis due to the accessibility of the chorioallantois membrane (CAM), a well-vascularized extra-embryonic tissue located under the eggshell, which is receptive to the xenografting of mammalian tumour cells, including human (Figure 13).

Fertilized chicken eggs were incubated on their side in a rotating incubator at 37 °C and 65 % humidity for 10 days, rotating three times per hour. Then, eggs were placed on their side on an egg rack and using a 30-gauge syringe needle a hole was made in the air sack, which is located at the blunt end of the egg. Another hole was made near the allantoid vein, which was localized using a light source contacting the eggshell. The hole was made using a Dremel rotary tool kit without injuring the CAM. To drop the CAM from the shell, a mild vacuum was applied to the air sack hole working with an automatic pipette with a Tygon tube. Then, a square window around 1 cm^2 was made with a cut off wheel (Dremel) close to the bifurcation of the allantoid vein. After that, 25 µL of the cell suspension were grafted nearby the allantoid vein bifurcation with a laboratory pipette without touching the CAM. The number of the cells depend on the cell type, we were used $2*10^5$ MDA-MB-231 cell in this work. The egg´s window was then sealed with tape and was left incubating for 5-7 days. Then, tumours were located and excised and weighed and portions of distal CAM, liver and brain were harvested and analysed by qPCR to determine the presence of human cells that entered the circulation and invaded the internal organs (Crespo & Casar, 2016; Subauste et al., 2009)

To extract genomic DNA from the different organs, we used the Gentra Puregene Tissue Kit from QIAGEN. Following the manufacture instructions, lysis buffer containing 1 µg/mL Proteinase K was added to every organ harvested, 600 µL for CAM or 400 µL for liver or brain. The mix was homogenized using a Polytron and was incubated overnight at 65 °C. The following day, 200 µL of protein precipitation buffer was added and mixed. Then, samples were centrifuged at 13,000 rpm for 5 minutes. The supernatant was collected and transferred to a tube containing 1 volume of cold isopropanol and allowed to settle for 5 minutes to allow DNA precipitation. Afterwards, 13,000 rpm for 5 min of centrifugation was performed, and the pellet was washed twice with 200 µL of 70 % ethanol, the samples were centrifuged again at the same conditions. The pellet was then dried for 5 minutes and resuspended with 200 µL of hydration buffer.

To quantify the amount of DNA contained in each sample was used NanoDropTM 2000c (Thermo Fisher). To analyse the quality of the DNA, 2 µL of DNA was loaded in a 0.8 % agarose gel electrophoresis, run at 80 V in TAE buffer (0.09 M Tris-acetate; 2 mM EDTA) and stained with SYBER Safe (Invitrogen).

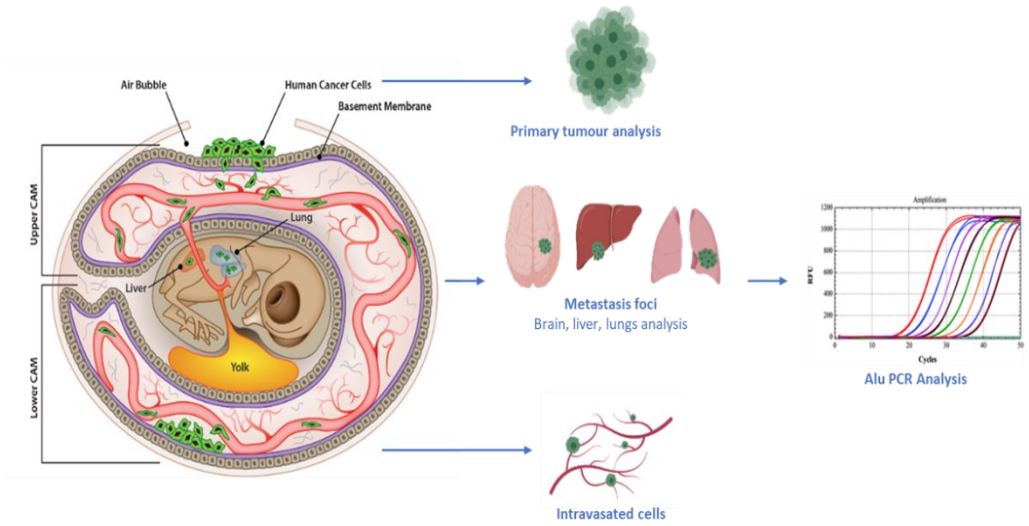

Figure 13. ***Graphic representation of the chick embryo spontaneous metastasis assay****. The CAM sustains the xenografting of mammalian tumour formation after 5 days. The cancer cells invade the epithelium and basement membrane of the upper CAM and move through connective tissue into the vasculature. Cancer cells can metastasize to the lower CAM or organs of the developing chicken. It could be analysed by RT-PCR assay the invasion capability. Adapted from Carcinoma et al., 2013 and Crespo & Casar,*

3.14.1. Real Time-PCR

To detect human cells in the different tissues harvested, we used primers (Sigma) for human Alu sequence (Crespo & Casar, 2016) (Table 13), which are transposable elements, around 300 nucleotides in length, that account for more than 10 % of the human genome and are not present in chicken.

Table 13. ***Primers and sequence used to assess human cells presence in chick tissues*** *(Crespo & Casar, 2016)*

Primer name	Direction	Sequence
Alu	for	ACG CCT GTA ATC CCA GGA CTT
Alu	rev	TCG CCC AGG TGG CTG GGG CA

PCR reaction generally contained 30 ng of genomic DNA as a template in a 20 µL reaction mixture containing 10 µL of 2x PowerUp SYBR Green Master Mix (Thermo Fisher), 100 nM per primer (Alu primers) and DNAase free water.

PCR conditions were the following: 4 minutes at 95 °C followed by 40 cycles of 30 seconds at 95°C to denature DNA, 63°C during 30 seconds for primer annealing and 30 seconds at 72°C to allow DNA polymerase amplification (Table 14).

Table 14. ***RT-PCR conditions for assessing human cells presence in chick tissues***

Step	**1**	**2**	**3**	**4**
Temperature	*95* °C	95 °C	*63* °C	*72* °C
Time	*4 min*	*30 s*	*30 s*	*30 s*
Cycles		*x 40 cycles*		

The number of human cells was determined by the triplicate Ct values against a standard curve generated by DNA extraction of specific non-tumour-cells (100; 1000; and 10000 cells).

3.15. Statistical analysis

Statistical analyses were processed and analysed using GraphPad Prism 7 Software (GraphPad Software, Inc., San Diego, CA).

RESULTS

4. RESULTS

4.1. ERK dimerization under different agonist

RAS-ERK pathway signalling is activated by external factors that regulate multiple biological responses. Since ERK can exert its effects both in monomeric and dimeric form, the main aim of this study is to unravel whether some of ERK functions are specifically undertaken in dimeric or monomeric form, or, alternatively, if ERK oligomerization state is irrelevant.

It was published that active ERK through the receptor tyrosine kinases (TRK) by two different stimuli, NGF (Nerve Growth Factor) and EGF (Epidermal Growth Factor), rise opposite cell responses, differentiation, and proliferation respectively (Santos et al., 2007).

When we stimulated MCF-7 cells with EGF, IGF-1 and insulin, it was found that EGF and IGF-1 stimuli activated ERK phosphorylation after a 3 min treatment but not insulin. However, only EGF stimulation induced ERK dimerization (Figure 14 A).

To ascertain that ERK dimerization upon IGF-1 stimulation did not occur at later stages than that one induced by EGF, we performed analyses of the stimulation time courses followed by either agonist.

Our results revealed that whereas EGF induced ERK dimerization during the first three minutes, ERK dimerization was completely absent throughout the 30 min of IGF-1 stimulation (Figure 14 B). These results demonstrated that ERK dimerization in MCF-7 cells is stimulus-dependent.

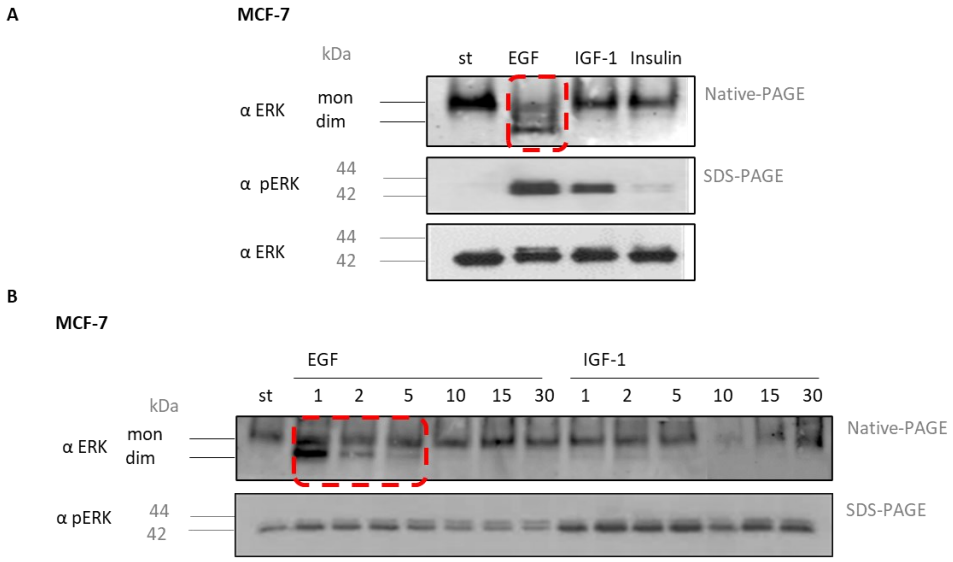

Figure 14. ***ERK dimerization upon EGF and IGF-1 stimulation in MCF-7 cells****. ERK dimers were monitored by Native-PAGE and phosphorylated levels by SDS-PAGE immunoblotting. EGF, 50 ng/mL, and IGF-1, 25 ng/mL, for 3 min in immunoblotting A.*

4.2. ERK dimerization boots differential cell abilities

In light of our results showing that ERK dimerization occurs under specific stimulation conditions, we studied the role of ERK dimerization in the regulation of specific cellular processes, relevant for tumour dissemination. As such, we evaluated chemotaxis and invasive capability, the major drivers of tumour cell dissemination via invasion or metastasis, in response to agonist stimulation.

To assess this, we performed transwell chemotaxis assay, which measures the ability of cells for moving towards the chemo-attractant. To evaluate invasiveness, we performed a transwell invasion assay, which measures the ability of cells for moving through a layer of extracellular matrix.

We observed that EGF but not IGF-1 induced a chemotactic response in MCF-7 cells. In contrast, IGF-1 stimulation but not EGF induced invasiveness (Figure 15).

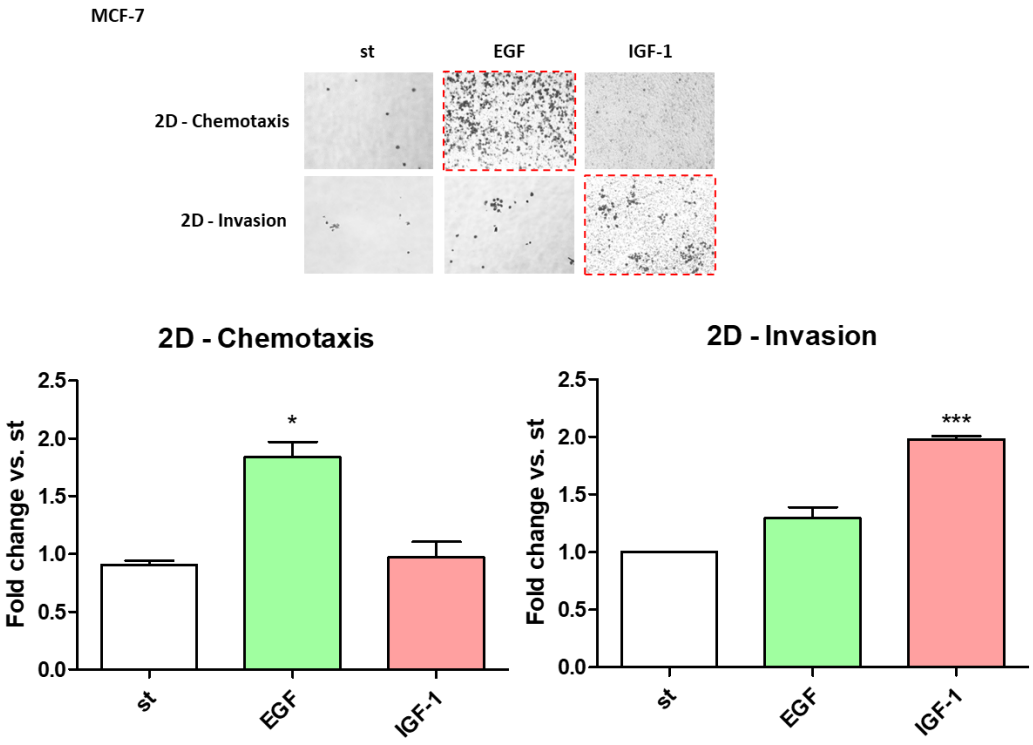

Figure 15. ***Effects of EGF and IGF-1 stimulation on chemotaxis and invasion****. MCF-7 chemotaxis and matrix degradation transwell assay upon different stimulation (EGF, 50 ng/mL, and IGF-1, 25 ng/mL) for 16 h. Cells were incubated, stained with crystal violet, and visualized by optical microscopy. The bottom of the microporous membrane (8 µm) was acquired by quantification of chemotaxis. Cell abilities were determined by measuring the area covered by cells (0.47 µm^2) as relative migration normalized to starved samples (control). The graph represents fold migration changes. Bars indicate mean ± SEM, two replicates of three independent experiments. t-Student, p-value from enrichment test. **

Next, we determined if both chemotaxis and invasiveness as induced by EGF, and IGF-1 respectively were dependent on ERK activation. For this, we treated cells with the MEK inhibitor U0126. It was found that EK inhibition completely impeded EGF-induced

chemotaxis and IGF-stimulated invasiveness (IGF), demonstrating that both processes are ERK-dependent.

Next, we analysed whether ERK dimers were involved in EGF-induced cell chemotaxis. For this, we used the specific ERK dimerization inhibitor DEL-22379 (Herrero et al., 2015). ERK dimerization levels were monitored under EGF and IGF-1 stimulation in MCF-7 cells pre-treated with DEL-22379. U0126 was also included as a positive control of ERK inhibition.

As expected, DEL-22379 treatment blocked EGF-induced ERK dimerization (Figure 16). Similarly, DEL-22379 completely inhibited EGF-stimulated chemotaxis (Figure 17) and, unexpectedly, invasion upon EGF stimulation (Figure 18).

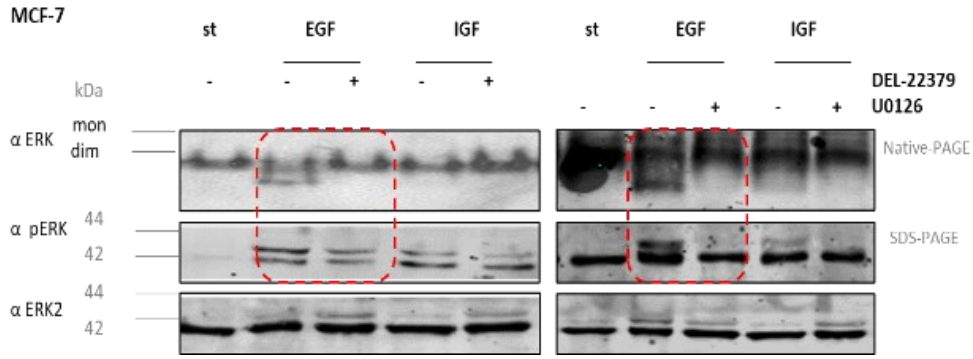

Figure 16. ***ERK dimerization and ERK phosphorylated levels upon DEL-22379 and U0126 treatment.*** *Immunoblotting in MCF-7 cells upon EGF (100 ng/mL) and IGF-1 (50 ng/mL) using ERK-dimer inhibitor and MEK inhibitor (DEL-22379 and U0126, 1h 10 mM)*

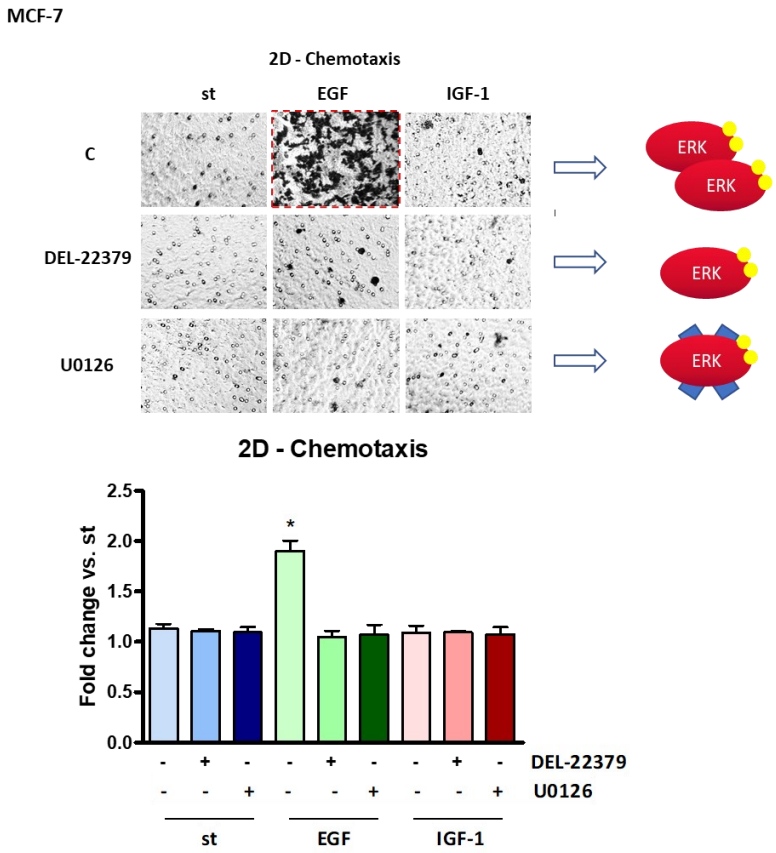

Figure 17. ***Effect of DEL-22379 treatment on cell chemotaxis ability****. Transwell assay of MCF-7 cells into chemotaxis assay upon different stimulation (EGF 50 ng/mL and IGF-1, 25 ng/mL respectively) using ERK-dimer and MEK inhibitors (DEL-22379 and U0126 respectively, 2 µM for 16 h). Cells were incubated in SF 16h, stained with crystal violet and visualised by optical microscopy. The bottom of the microporous membrane (8 µm) was acquired a photo to quantify chemotaxis. Values were expressed as relative chemotaxis normalised to starved samples. Chemotaxis quantification was determined by measuring the area covered by cells (0.47 µm^2). The graph shows fold migration. Bars indicate mean ± SEM (without matrix-gel n=3, two replicates of independent experiments; t-Student; p-value from enrichment test, *, $p < 0.05$).*

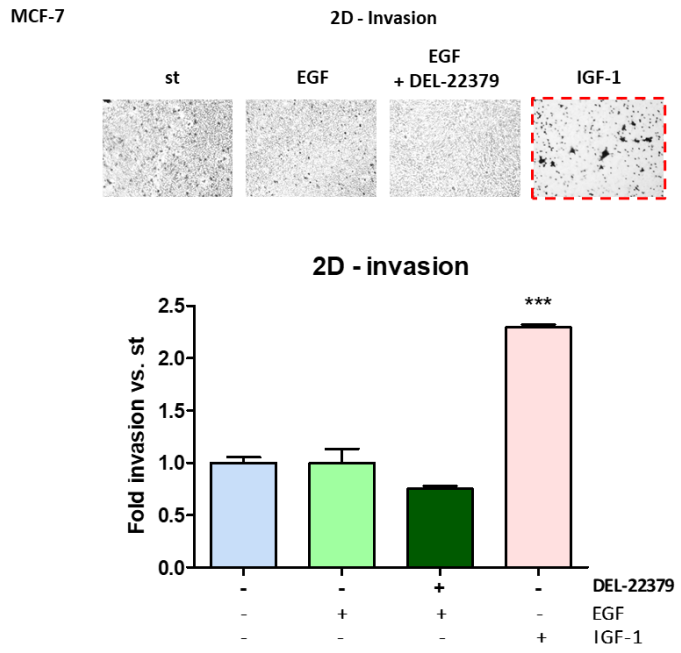

Figure 18. ***Effect of DEL-22379 treatment on cell invasion ability****. Transwell assay of MCF-7 cell into invasion assay upon different stimulation (EGF 50 ng/mL and IGF-1, 25 ng/mL respectively)). Cells were incubated in SF 16h, stained with crystal violet and visualised by optical microscopy. The bottom of the microporous membrane (8 µm) was acquired a photo to quantify chemotaxis. Values were expressed as relative chemotaxis normalised to starved samples. Chemotaxis quantification was determined by measuring the area covered by cells (0.47 µm^2). The graph shows fold migration. Bars indicate mean ± SEM (without matrix-gel n=3, two replicates of independent experiments; t-Student; p-value from enrichment test, *, p < 0.05). DEL-22379 2µM, 16SF*

To further ascertain the role of ERK dimerization on chemotaxis and invasiveness we utilized several ERK mutants. ERK2 H176E, a dimerization-defective mutant, which acts in a dominant inhibitory fashion, preventing endogenous ERK dimerization (Khokhlatchev et al., 1998). We also included ERK2 R65S an intrinsically active mutant (Levin-Salomon et al., 2008) that is also in a constitutively dimerized form, according to the observations in our lab Figure 19. Interestingly, it was found that in MCF-7 cells expressing ERK2 H176E EGF-induced cell chemotaxis was diminished (Figure 20 A). Interestingly, cells expressing

ERK2 R65S displayed increased cell chemotaxis under all conditions tested. These results demonstrated that ERK dimerization is essential for eliciting a chemotactic response irrespective of the stimulus.

On the other hand, in MCF-7 cells the expression of ERK2 H176E invasiveness was promoted under EGF stimulation, while it had no effect on IGF-1 response. Contrarily, invasiveness was largely unaffected by the expression of ERK2 R65S (Figure 20 B). These results suggested that, probably, the invasive response is regulated by ERK in monomeric form not resulting by ERK dimer disrupted by DEL-22379 treatment.

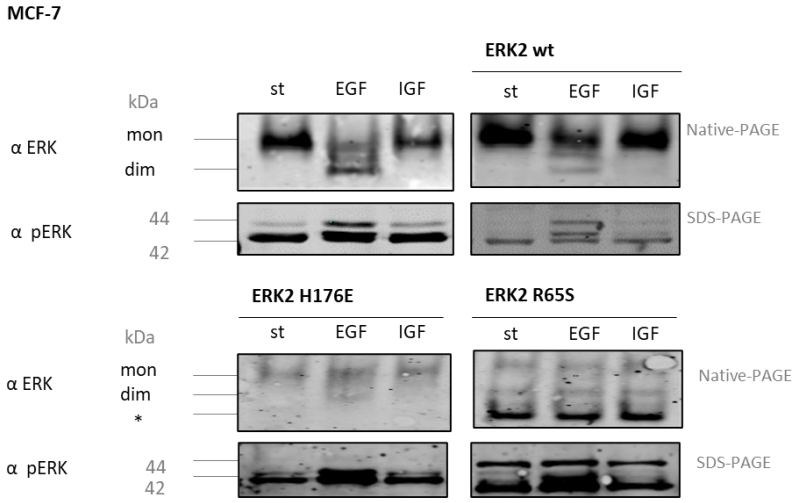

Figure 19. ***Analysis of ERK dimerization and phosphorylated levels of ERK2 wt, ERK2 H176E and ERK2 R65S upon EGF and IGF-1 stimulation****. ERK dimers were monitored by Native-PAGE and phosphorylated levels by SDS-PAGE immunoblotting. EGF 100 ng/mL and IGF-1, 50 ng/mL*

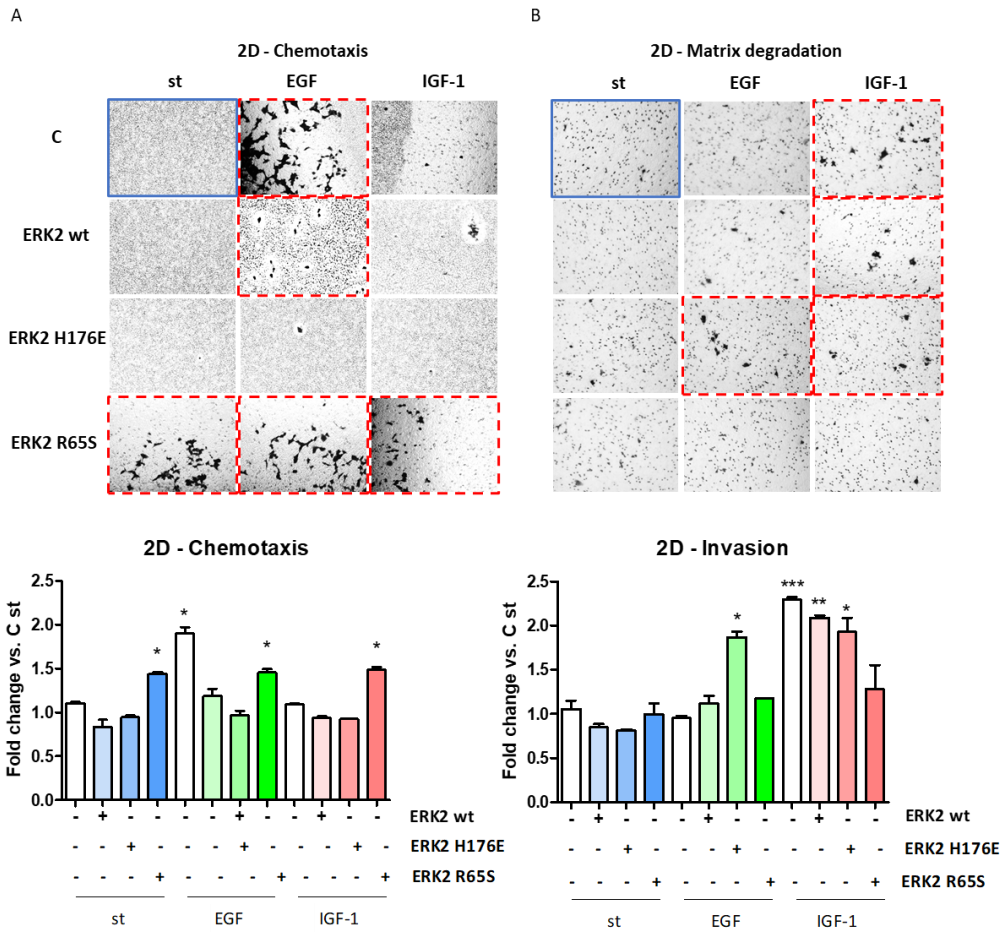

Figure 20. ***Effect of ERK2 H176E and ERK2 R65S overexpression on cell chemotaxis and invasion.*** *Transwell assay of MCF-7 cells transfected with ERK2 mutants into transwell assay upon different stimulation (EGF, 50 ng/mL, and IGF-1, 25 ng/mL). Cells were incubated in SF 16h, stained with crystal violet and visualised by optical microscopy. The bottom of the microporous membrane (8 µm) was acquired a photo to quantify migration, the values were expressed as relative migration normalised to starved samples. Migration was determined by measuring the area covered by cells (0.47 µm2). The graph shows fold migration, bars indicate mean ± SEM (without -and with matrix-gel, chemotaxis and matrix degradation respectively, (n=2 replicates of independent experiments; t-Student; p-value from enrichment test, *, p < 0.05). MG: Matrix gel.*

4.3. Identification of ERK2 interactors upon agonist stimulation

We have previously demonstrated that scaffold proteins function as ERK dimerization platforms and cytoplasm anchors (Casar et al., 2008). Thus, specific agonist stimulation could somehow influence ERK-scaffolds affinity, thereby impact on its dimerization, localization, and substrate specificity and constitutive on its biological effects.

To put this under test, we analysed the ERK2 interactome in HEK 293T cells by mass spectrometry to identify ERK2 specific scaffolds under EGF or IGF-1 stimulation. HEK 293T cells were used as a proper model in experiments ranging from signal transduction and protein interaction studies.

Our mass spect data indicated that EGF stimulation increased KSR1-ERK interactions (Figure 21). To validate the mass spect results, the interaction of the scaffold protein KSR1 with ERK2 was analysed by co-immunoprecipitation assay under EGF and IGF-1 (Figure 22).

In agreement with the mass spect results, upon EGF stimulation, we observed that ERK bound to KSR1 increased under EGF stimulation, but not IGF-1. In consonantly our previous publications (Casar et al., 2008).

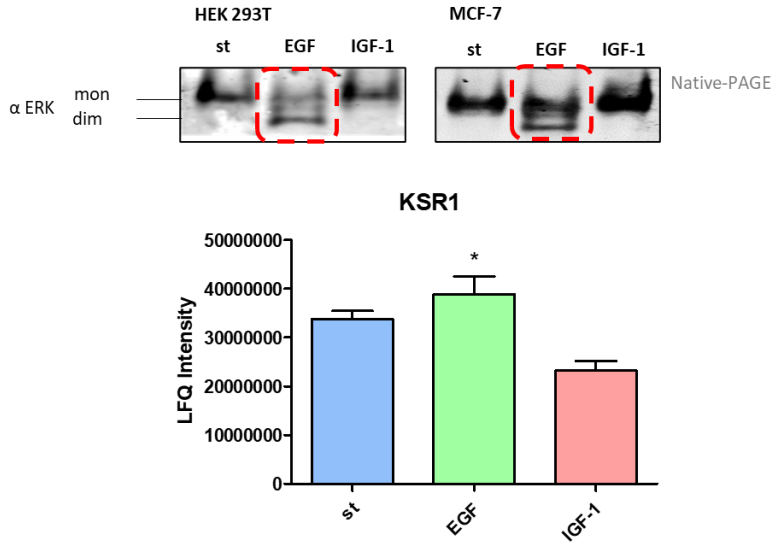

Figure 21. ***ERK2 binding to KSR1 upon EGF stimulation in HEK 293T.*** *On the top, ERK dimerization upon EGF and IGF-1-stimulation in HEK 293T and MCF-7 cell lines. On the bottom, an ERK2 specific interactor upon agonist stimulation. The graph shows the LQF (Label-Free Quantification). Bars indicate mean ± SEM (n=3 replicates of the same experiment; t-Student; p-value from enrichment test, *, p< 0.05). EGF (100 ng/mL) and IGF-1 (50 ng/mL) for 3 min.*

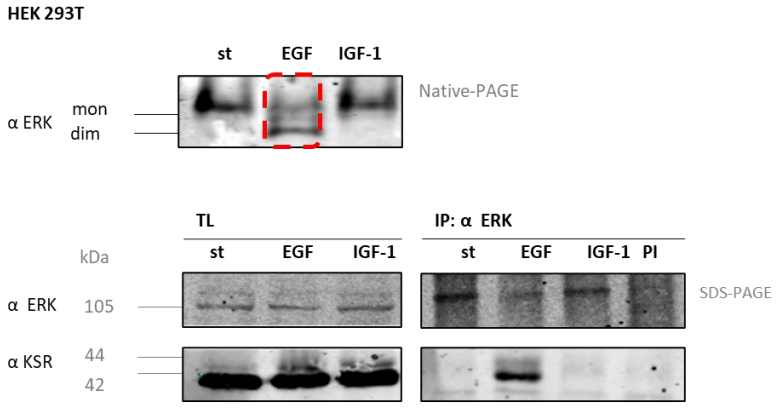

Figure 22. ***Analysis of ERK and KSR1 interaction****. Native-PAGE of ERK dimerization, immunoblotting and co-immunoprecipitation in HEK 293T cell line upon EGF and IGF-1 stimulation (100 and 50 ng/mL, respectively, for 3 min). TL: Total lysate, PI: isogenic antibody*

4.3.1. KSR1 modulates biological outcomes through ERK2 dimers.

Considering our data demonstrating that KSR1 interacts with ERK upon EGF stimulation, we investigated whether KSR1 was implicated in RAS-induced responses. Previously, it was found that KSR1 is involved in promoting cell proliferation in fibroblast cells (Kortum & Lewis, 2004; Razidlo et al., 2004).

We studied the functions of KSR1 in the Biological Process Gene Ontology (GO) database, a tool for computational analysis of large-scale molecular biology and genetics experiments in biomedical research. We found that KSR1 is involved in biological processes like the cellular responses to stimulus and cell communication (Figure 23).

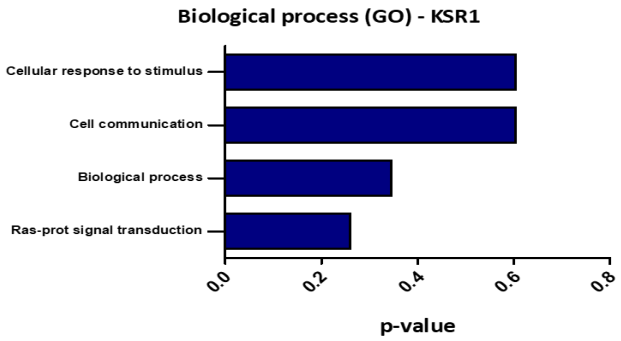

Figure 23. ***Analysis of KSR1 biological responses.*** *The Biological Process Gene Ontology (GO) enrichment over-represented the KSR1 gene functions. Data provided by*

We interested in relating KSR1 role in tumour progression, we investigated cellular responses as such, the participation of KSR1 in chemotaxis and invasiveness transwell assays in MCF-7 cells.

These results suggested that overexpression of KSR1 promoted ERK dimers regulating cell chemotaxis boosted by EGF. In contrast, the downregulation of KSR1 expression induced cell invasiveness in any stimuli condition (basal conditions, EGF and IGF-1) (Figure 24).

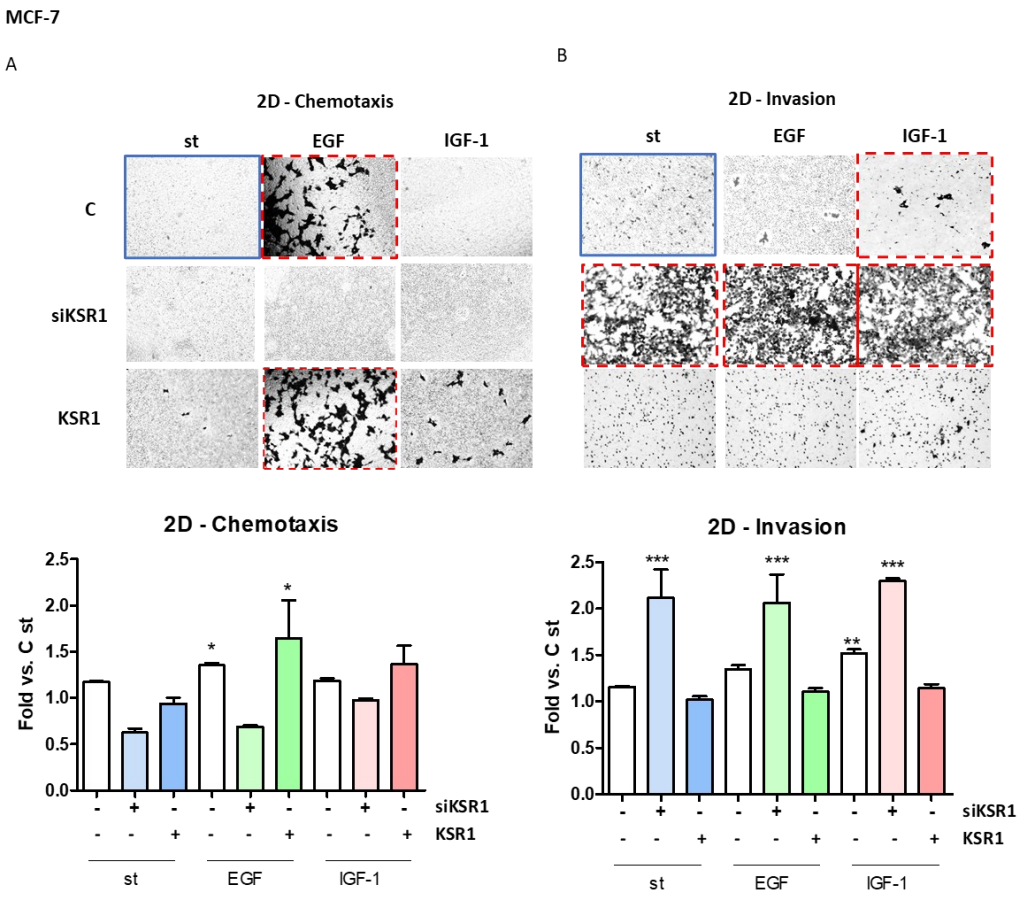

Figure 24. ***Effects of KSR1 on chemotaxis (A) and invasion (B) cell abilities upon agonist stimulation.*** *Transwell assay of MCF-7 transfected cells with KSR1 and siKSR1 plasmid expression into transwell assay upon different stimulation (EGF, 50 ng/mL, and IGF-1, 25 ng/mL). Cells were incubated in SF 16h, stained with crystal violet and visualised by optical microscopy. The bottom of the microporous membrane (8 µm) was acquired a photo to quantify migration, the values were expressed as relative migration normalised to starved samples. Migration was determined by measuring the area covered by cells (0.47 µm^2). The graph shows fold migration. Bars indicate mean ± SEM (without -and with matrix-gel, chemotaxis and matrix degradation respectively, n=3, two replicates of independent*

Since PEA15 is a scaffold that also retains ERK dimers in the cytoplasm (Mace et al., 2013), blocking ERK translocation to the nucleus. It was found of interest to analyse the role of PEA-15 in chemotaxis and matrix degradation upon agonist stimulation.

It was found that PEA-15 downregulation impaired chemotaxis induced by EGF stimulation and promoted matrix degradation upon IGF-1 stimulus (Figure 25).

These results indicated that ERK scaffolds, KSR1 and PEA15, boosted chemotaxis cell capability through cytoplasmic ERK dimerization. Nevertheless, their downregulation expression increased the matrix degradation cell ability.

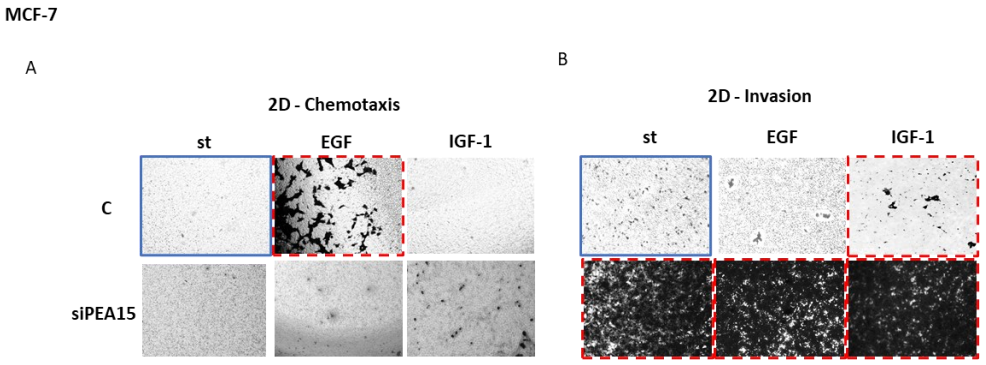

Figure 25. ***Effect of PEA15 on cell chemotaxis and invasion.*** *MCF-7 transfected cells with siPEA15 plasmid expression into transwell assay upon different stimulation (EGF, 50 ng/mL, and IGF-1, 25 ng/mL). Cells were incubated in SF 16h, stained with crystal violet and visualised by optical microscopy. The bottom of the microporous membrane (8 µm) was acquired a photo to quantify migration, the values were expressed as relative migration normalised to starved samples. Migration was determined by measuring the area covered by cells (0.47 µm^2). The graph shows fold migration. Bars indicate mean ± SEM (without -and with matrix-gel, chemotaxis and matrix degradation*

Given that organoid technology allows the analysis of tumoral cell growth and cell invasion, we wished to examine the cellular responses of breast cancer cells upon agonist stimulation in 3D organoids. Interestingly, it was found that KSR1 downregulation induced MCF-7 cell proliferation, whereas KSR1 overexpression decreased it (Figure 26).

Overall, these data suggest that KSR1, as an enabler of ERK dimerization, regulates MCF-7 cell proliferation through ERK dimers.

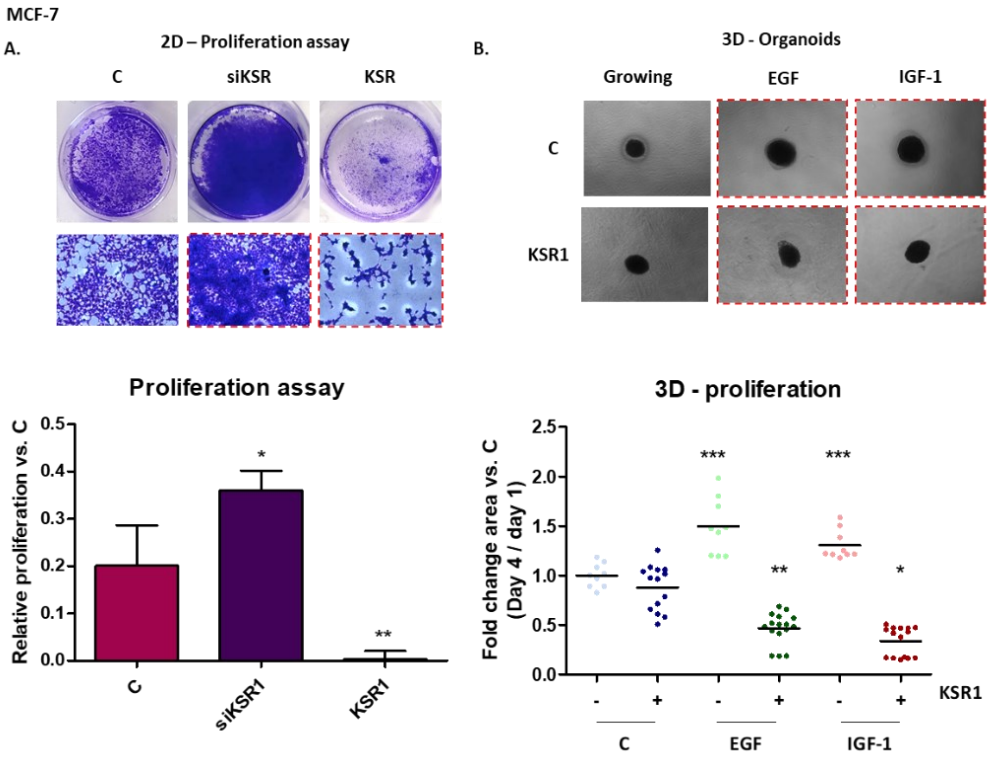

Figure 26. ***Effects of KSR1 expression on MCF-7 cell proliferation****. A. Five hundred cells were seeded in a 0.33 cm^2 dish within a culture medium supplemented with 10 % FBS and transfected with KSR1 and siKSR1. The number of colony formation was counted with Fiji on day 2, 48 h. Representative image of MCF-7 colony formation stained with crystal violet. Images were taken with 4 magnifications. Values were given as mean ± SEM; significant differences of transfected conditions vs. control conditions were analysed by one-way ANOVA/ Bonferroni's post-test and were indicated with non-significative ($p < 0.05$), n = 3, four replicates for the experiment. Error bars were mean ± SEM. B. KSR1 caused a significant reduction of mammosphere numbers related to the number of cells plated: 4*10^4. Results were the mean of 3 independent experiments. The mean diameter of the mammospheres in MCF-7 KSR1 spheroids was significantly less than in control cultures. Values were given as mean ± SEM; significant differences of transfected conditions vs. control conditions in day 1 (not shown) were analysed by one-way ANOVA/ Bonferroni's post-test and were indicated with non-significative (p <*

4.3.2. ERK dimerization promotes cellular morphology changes

During our experiments, we observed cellular shape changes when KSR1 is over-expressed. It was found that the absence of KSR1 boosted less cellular protrusion formation and a roundish morphology, thereby might facilitate amoeboid cell migration ability (Figure 27)

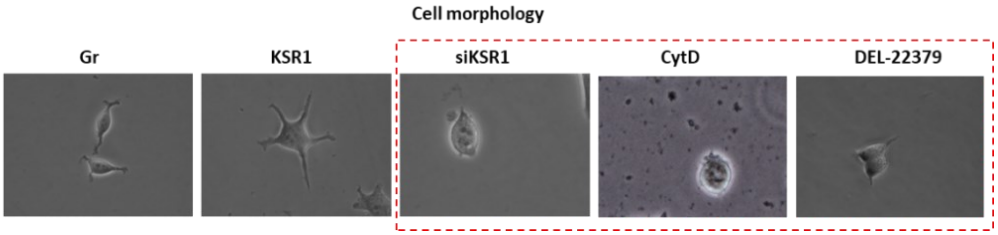

Figure 27. ***KSR1 overexpression modulates the cellular morphology in MCF-7 cells.*** *Cells were transfected with KSR1 plasmid and siKSR1 and seeded in growing conditions for 48 h. Images were taken by optical microscopy at 40 magnification. Gr: Growing conditions, DEL-22379: 2 µM, CytD: cytochalasin D (10 µM).*

Since the dynamic remodelling of the actin cytoskeleton is a critical part of cellular shape and most cellular activities, such as motility and migration, we decided to treat MCF-7 cells cytochalasin D, an actin polymerization inhibitor. To further study ERK dimerization as a determinant of cellular morphology, we blocked ERK dimers formation using DEL-22379 inhibitor.

We have found that cytochalasin D and DEL-22379 promotes roundish morphology.

Overall, these results suggest that KSR1 and actin cytoskeleton regulated cellular shape changes through ERK dimerization.

Considering that actin filaments sustain the cellular cytoskeleton and determine the cellular shape, we wanted to gain an insight into whether differential stimulation and ERK dimerization could regulate cellular morphology through actin. To do so, we firstly performed a confocal immunofluorescence assay.

Our confocal images showed that actin filaments kept the cell shape and took part in lamellipodium formation, upon EGF stimulation especially. In contrast, the actin depolymerization boosted the roundish morphology (Figure 28). These results suggested that EGF stimulation may promote directionally persistent intrinsic cell migration and enhance directed migration during chemotaxis through lamellipodia formation (Petrie et al., 2009).

To compare the effect of ERK dimerization in cell morphology, we studied the role of KSR regulating actin cytoskeleton by immunofluorescence assay.

Our images showed that KSR1 overexpression increased the number of focal adhesions while downregulation of KSR1 boosted roundish morphology (Figure 29).

Altogether these results suggest that KSR regulate cell shape through actin cytoskeleton.

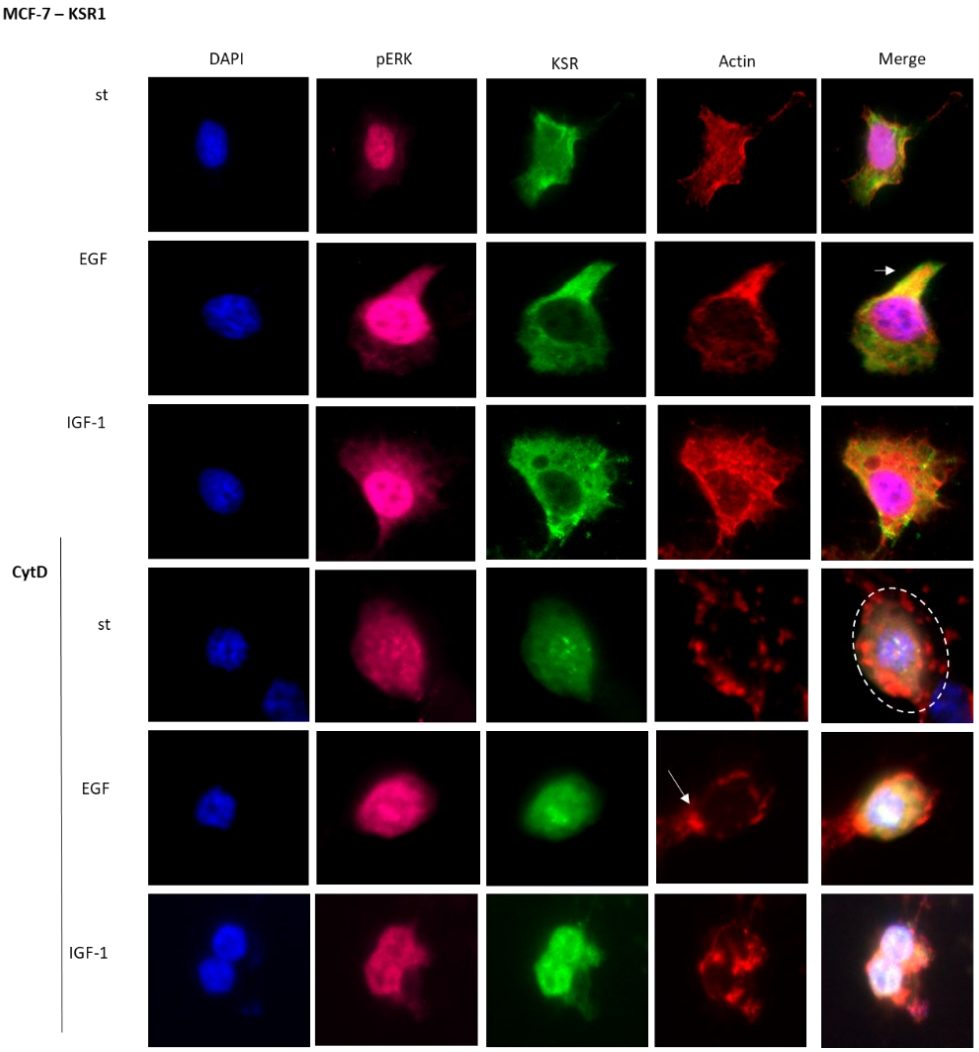

Figure 28. ***Effect of cytochalasin D in MCF-7 cell morphology****. Immunofluorescence microscopy revealed the interaction between ERK and actin proteins upon EGF stimulation and nuclear retention of ERK after cytochalasin D treatment (10 µM for 18 h). Immunofluorescence microscopic images for MCF-7-KSR1 stable cells upon different stimulation (EGF, 100 ng/mL and IGF-1, 50 ng/mL, for 3 min). Left: DAPI (blue) middle: pERK (far red), KSR1 (green) and right: actin (red) and merge. Using the ImageJ program, fluorescence signals which overlap signals are shown in yellow. n = 3. CytD: Cytochalasin D*

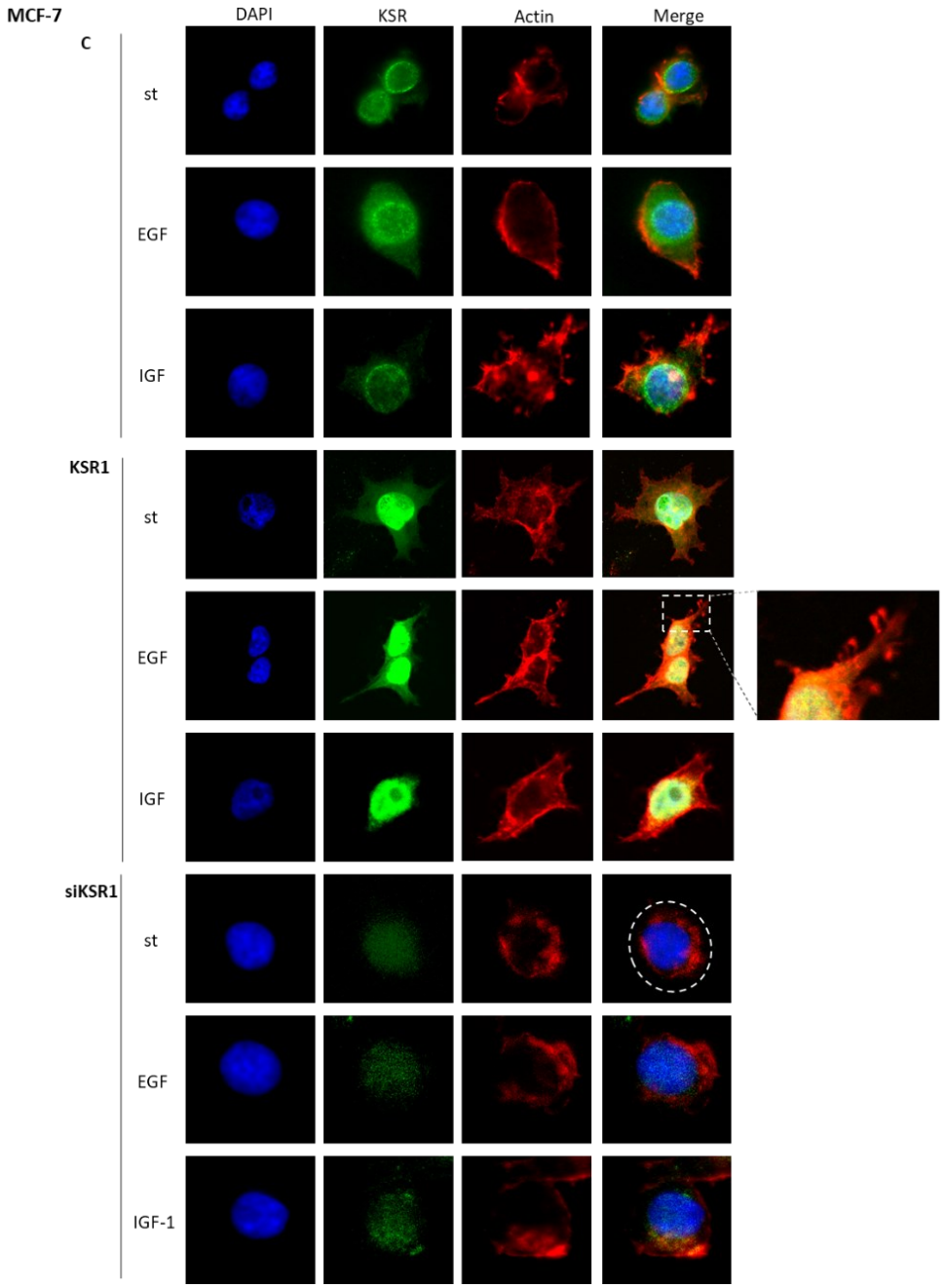

Figure 29. ***Cell morphology analysis of KSR1 expression in MCF-7 cells****. MCF-7 were seeded and transfected with siKSR1 and KSR1 and stimulated (EGF and IGF-1; 100 and 50 ng/mL respectively for 3 min). Left: DAPI (blue) middle: pERK (green), KSR1 (far red) and right: actin (red) and merge (yellow). Using the ImageJ program, fluorescence signals which overlap signals are shown in yellow. n = 3, two replicates for the*

The role of KSR1 and ERK dimerization in cellular chemotaxis ability

Previously results from our lab have demonstrated that ERK dimerization is restricted to mammals (Herrero et al., 2015). To investigate the expression of KSR1 in non-mammal firstly, we did a search using different databases (Table 15).

Next, we demonstrated that KSR1 was expressed in chicken cells (Figure 30 A). To further study the role of KSR-1 in cells in which ERK did not dimerize, we performed co-immunoprecipitation assays (Figure 30 B). We found that KSR1 did not bind to ERK in chicken cells. Although ERK and KSR1 were considered ancestral proteins, the role of KSR1 in non-mammal cells is still unknown.

To further study the function of KSR1 in non-mammal cells, we performed the DF-1 chemotaxis assay (Figure 31). The results revealed that EGF did not induce chemotaxis in DF-1 cells.

Overall, these results indicate that the regulation of ERK dimerization mediated by KSR1 is restricted to mammal cells.

Table 15. Evidence of the KSR1 on vertebrates and invertebrates' animals (Knowledgebases: HGNC, AGR, Monarch, OMIM, GeneCards, MGI, RGD, GEISHA) Whilst, ERK dimerization is exclusive of mammals (in blue) (Herrero et al., 2015)

Human	Mammals	Vertebrates	Invertebrates
Homo sapiens	*Mus musculus* (Mouse)		
	Rattus sp. (Rat)		
		Gallus gallus (Chicken)	
		Danio rerio (Zebrafish)	
		Xenopus sp. (Frog)	
			Drosophila sp. (Fruit fly)

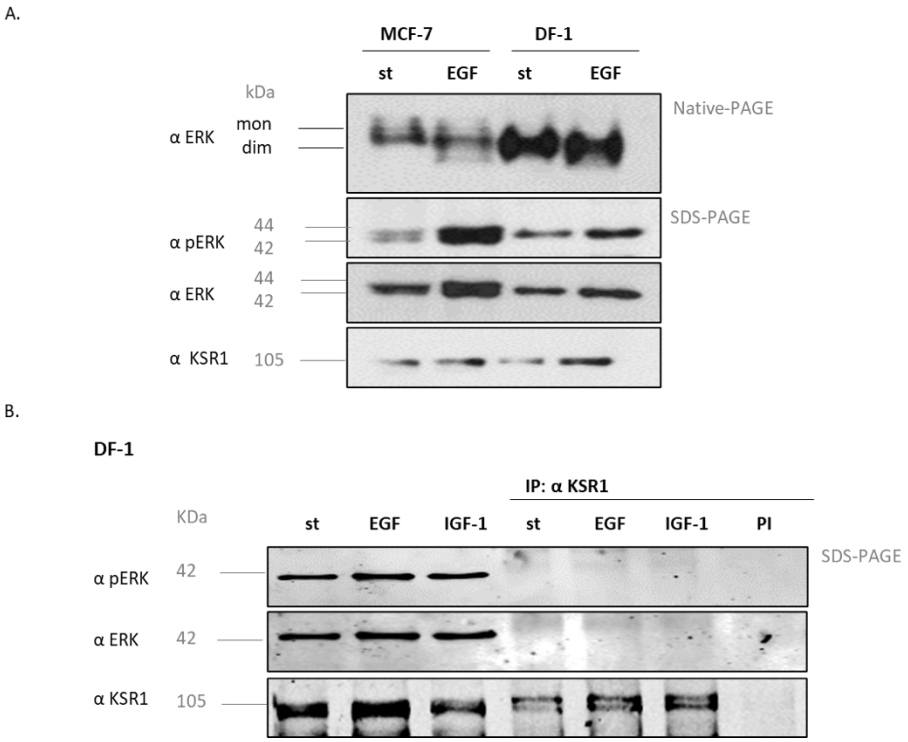

Figure 30. ***KSR1 expression and its binding ERK in non-mammal cells.*** *A. KSR1 is present in Gallus gallus (DF-1 cells) in which ERK does not dimerize, and Homo sapiens (MCF-7 cells) in which ERK dimerizes upon EGF stimulation. B. KSR1 does not bind ERK monomers in co- Immunoprecipitation (IP)/western blot analysis in DF1 cells. An equal number of cellular extracts from DF-1 was subjected to anti-KSR1 IP and Western blots probed with the antibodies indicated. The western blots shown are representative of*

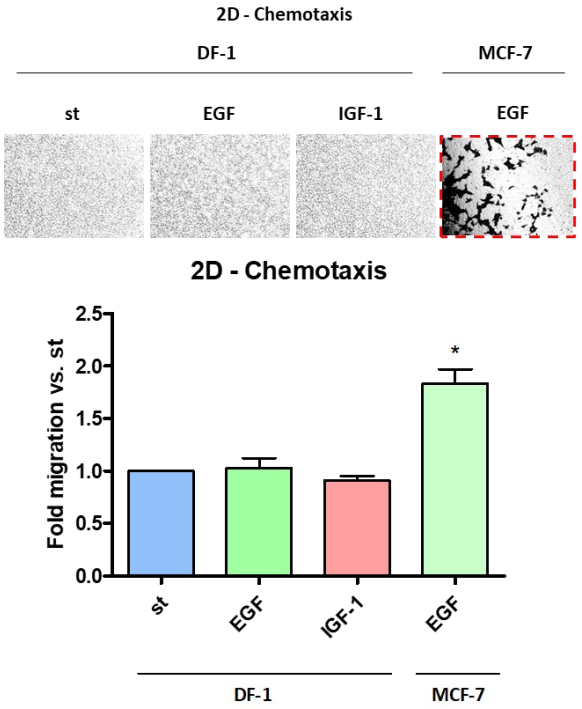

Figure 31. ***Analysis of cell chemotaxis ability of DF-1 cells****. Chemotaxis ability of DF-1 cells treated upon EGF (50 ng/mL) and IGF-1 stimulation (25 ng/mL). Cells were incubated in SF 16 h, stained with crystal violet and visualised by optical microscopy. The bottom of the microporous membrane (8 µm) was acquired a photo to quantify migration, the values were expressed as relative migration normalised to starved samples. Migration was determined by measuring the area covered by cells (0.47 µm^2). The graph shows fold migration. Bars indicate Mean ± SEM (without and with matrix-gel, chemotaxis and matrix degradation respectively, n=2, two replicates of independent experiments; t-Student; p-value from enrichment test, *, p < 0.05). MCF-7 treated with EGF stimulus was used as control.*

4.4. The role of ERK dimerization in epithelial-mesenchymal transition (EMT).

The epithelial-to-mesenchymal transition (EMT) is a highly dynamic process by which epithelial cells can convert into a mesenchymal phenotype. EMT includes enhanced migratory capacity and invasiveness mediated by chemotaxis.

Having established that ERK dimerization regulated chemotaxis and matrix degradation, we decided to characterize migration and EMT gene expression hallmarks upon stimulation. For that, we studied morphology changes and the gene expression at the RNA level during EMT in cancer cell lines.

The cell models used were A549 (lung carcinoma cells) and M38K (mesothelioma cell line) as EMT controls; and MCF-7 and MDA-MB-231, breast cancer cell lines. Besides, to determine the role of ERK dimerization regulating EMT, we used DEL-22379 (ERK dimerization inhibitor).

Firstly, it was determined DEL-22379 concentration to keep the cells alive and decrease ERK dimerization. For that, we performed a cell viability assay for 48 h.

The DEL-22379 concentration standardized was to 2 µM (Figure 32).

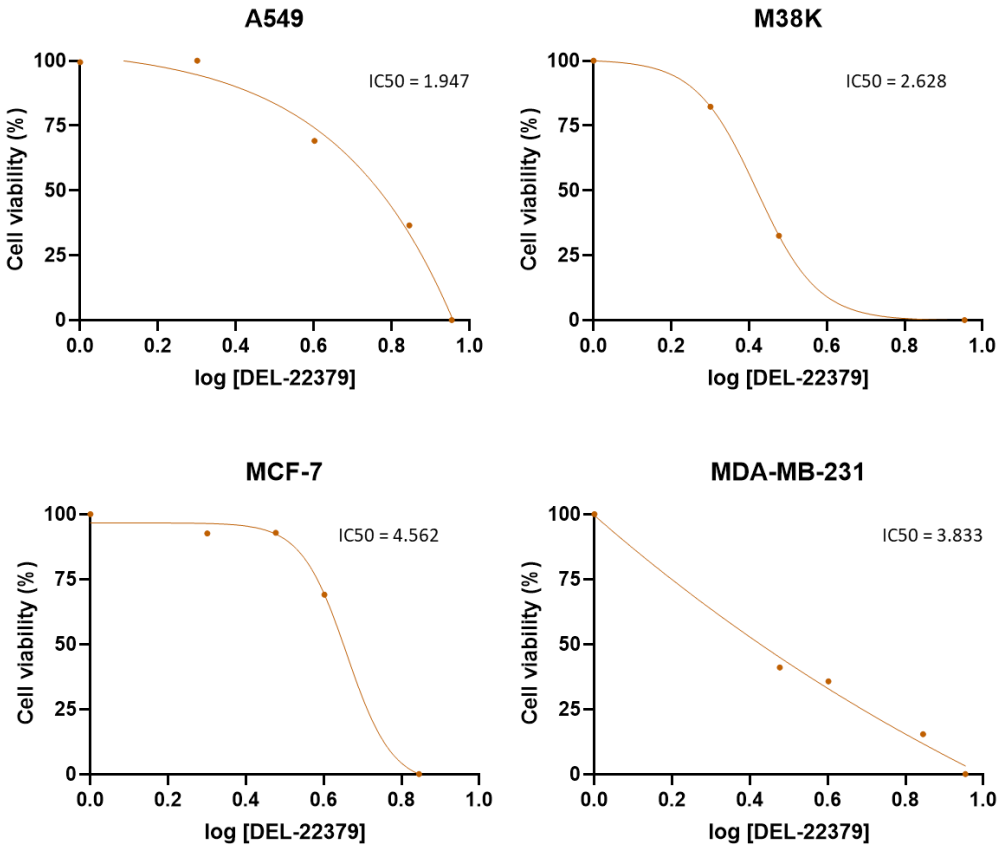

Figure 32. ***Dose-response data after DEL-22379 treatment.*** *Lung (A549), mesothelioma (M38K) and breast (MCF-7, MDA-MB-231) cancer cells were treated with different concentrations of DEL-22379 for 48 h. The charts show the percentage of mean absorbance. IC50 values were normalized as the logarithm of µg/mL.*

The landscape of the role of ERK dimers in EMT

It has already characterised that EMT requires cell morphology and RNA profiles changes upon stimulus, but the mechanism is still unknown.

First, we analysed EMT capability using as a control A549 cells in basal conditions. Gene expression and cell morphology analysis were suitable for EMT definition upon TGFβ stimulation. TGFβ is considered a well-known growth factor that triggers the main signalling pathway involved in EMT (Hao et al., 2019).

It observed that the A549 cellular shape changed upon EGF and TGFβ stimulation. EGF stimulus boosted refringent and fusiform cells while TGFβ stimulus increased flatter cytoplasm (Figure 33). But only TGFβ significantly enhanced N-cadherin, snail, and vimentin RNA expression (Figure 34).

When we treated A549 cells with DEL-22379, we observed that the effect under this treatment promoted refractory cell morphology upon EGF stimulation. Besides, the treatment did not enhance EMT gene expression in comparison with TGFβ stimulation (Figure 34).

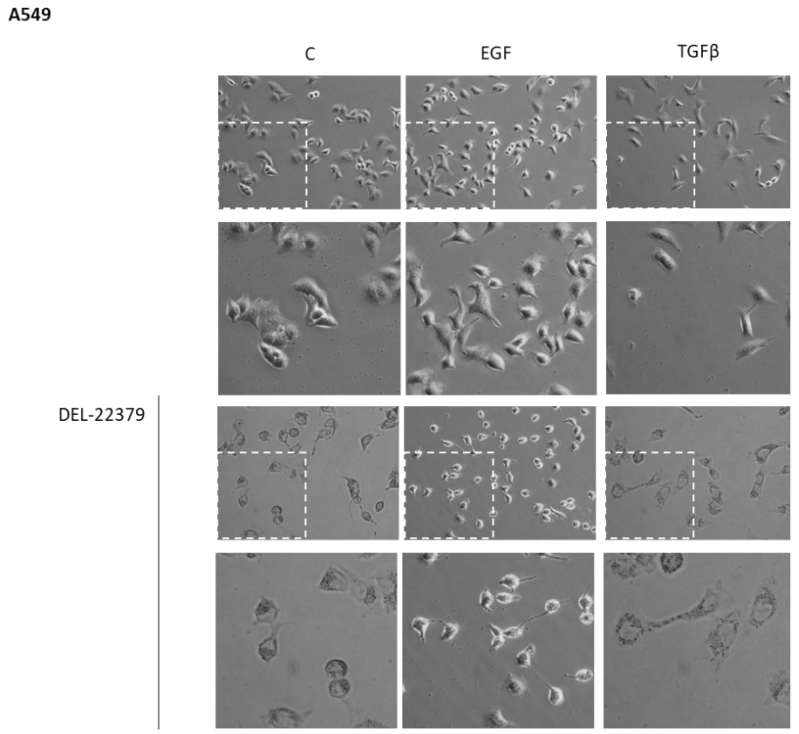

Figure 33. ***Cell morphology analysis of A549 cells after EGF, TGFβ, and DEL-22379 treatment.*** *Representative phase-contrast at a 10 (upper panels) and 20 magnification (lower panels). EGF (50 ng/mL), TGFβ (5 ng/mL) and DEL-22379 (2 μM) treatment for 48 h.*

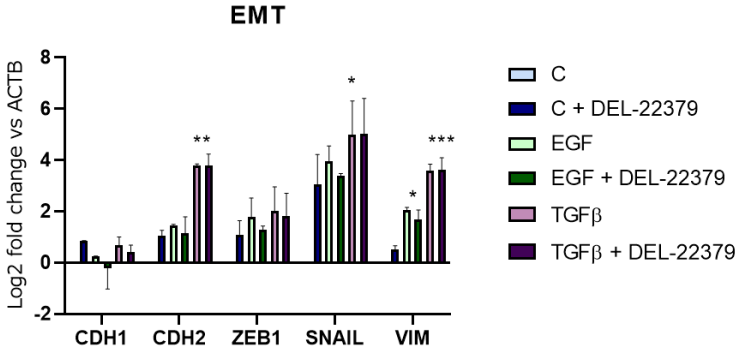

Figure 34. ***Determination of EMT gene expression of A549 cells****. The graph showed the Log2 fold change of gene expression after 48 h of EGF, TGFβ, and DEL-22379 treatment as indicated versus controls of the typical EMT marker genes: E-cadherin (CDH1), N-cadherin (CDH2), Zeb1, and vimentin (VIM). EMT hallmarks were determined by RT-PCR (mean and SEM of three biological repeats performed in duplicates). GAPDH was used as a housekeeping gene for normalization. Data are shown as mean and SEM. ***P < 0.001, **P < 0.01, *P < 0.05 treatment versus control, one-way ANOVA with Sidak's multiple comparisons test. EGF: 50 ng/mL; TGFβ: 5 ng/mL, DEL-22379: 2 µM.*

To further study the role of ERK dimerization during EMT, we used M38K cells.

We found that the cells become fusiform and roundish (circularity tended to 1) after 48 h of EGF stimulation (Figure 35 and Figure 36). Moreover, EGF treatment-induced cell migration (Figure 37 A-B), without differences in speed and straightness between conditions (Figure 37 C-D). Also, EGF enhanced EMT gene expression (N-cadherin, Zeb1, Snail, and Vimentin) (Figure 38).

These results suggest that EGF increased EMT dependent on ERK dimerization. Furthermore, the use of the DEL-22379 small molecule might have an inhibitory effect on migration.

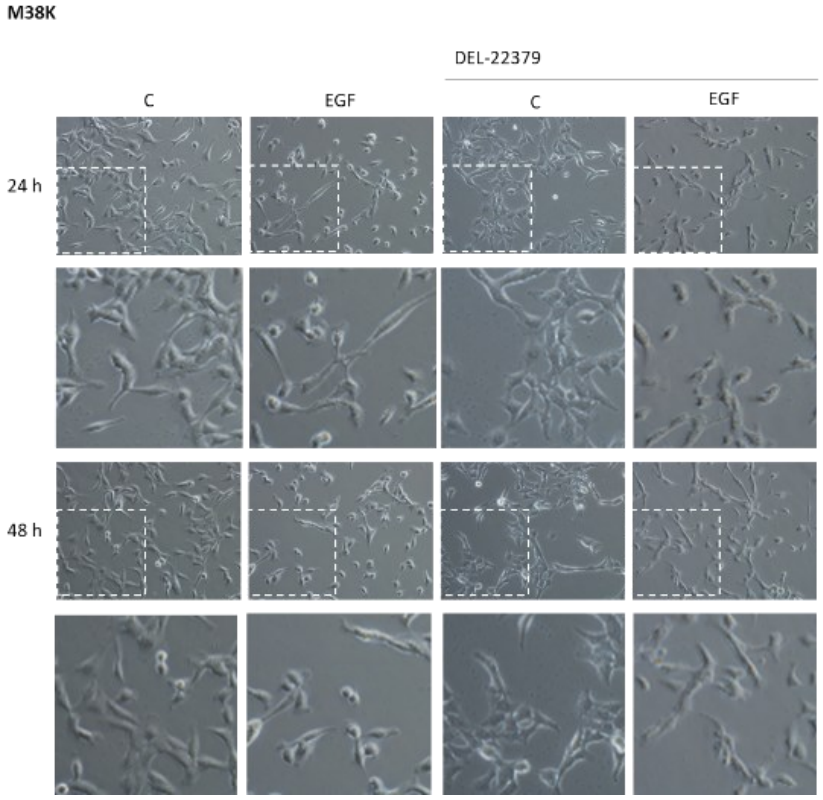

Figure 35. ***Cell morphology analysis of M38K upon EGF stimulation and DEL-22379 treatment.*** *Representative phase-contrast at a 10 (upper panels) and 20 magnification (lower panels). EGF (50 ng/mL) and DEL-22379 treatment (2 µM) for 48 h.*

In addition, it was found that DEL-22379 treatment affected M38K cell migration while it was a more significant EMT gene expression (Figure 39 and Figure 40).

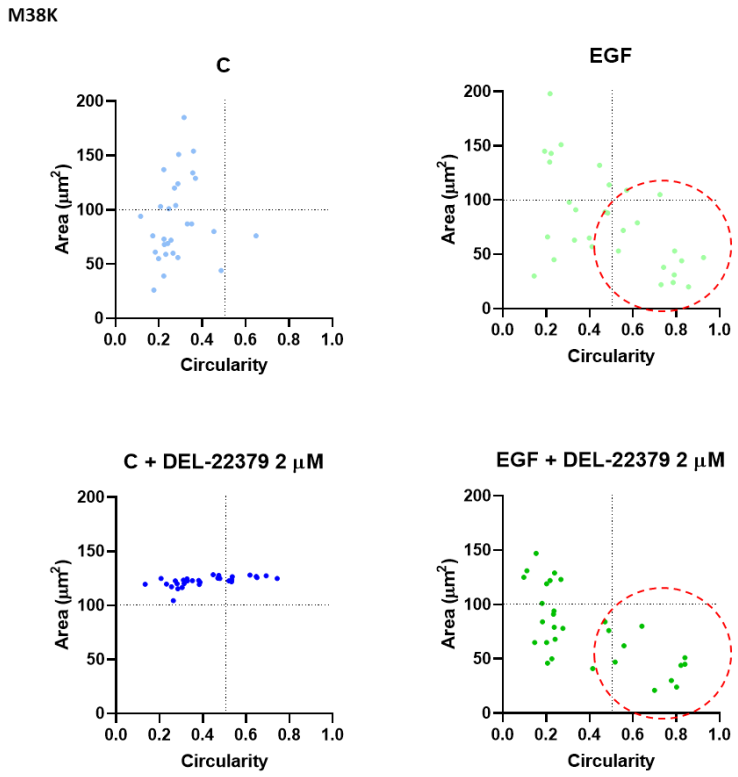

Figure 36. ***Area versus circularity of individual M38K cells*** *upon EGF (50 ng/mL) and DEL-22379 (2 μM) treatment (n=30 per condition).*

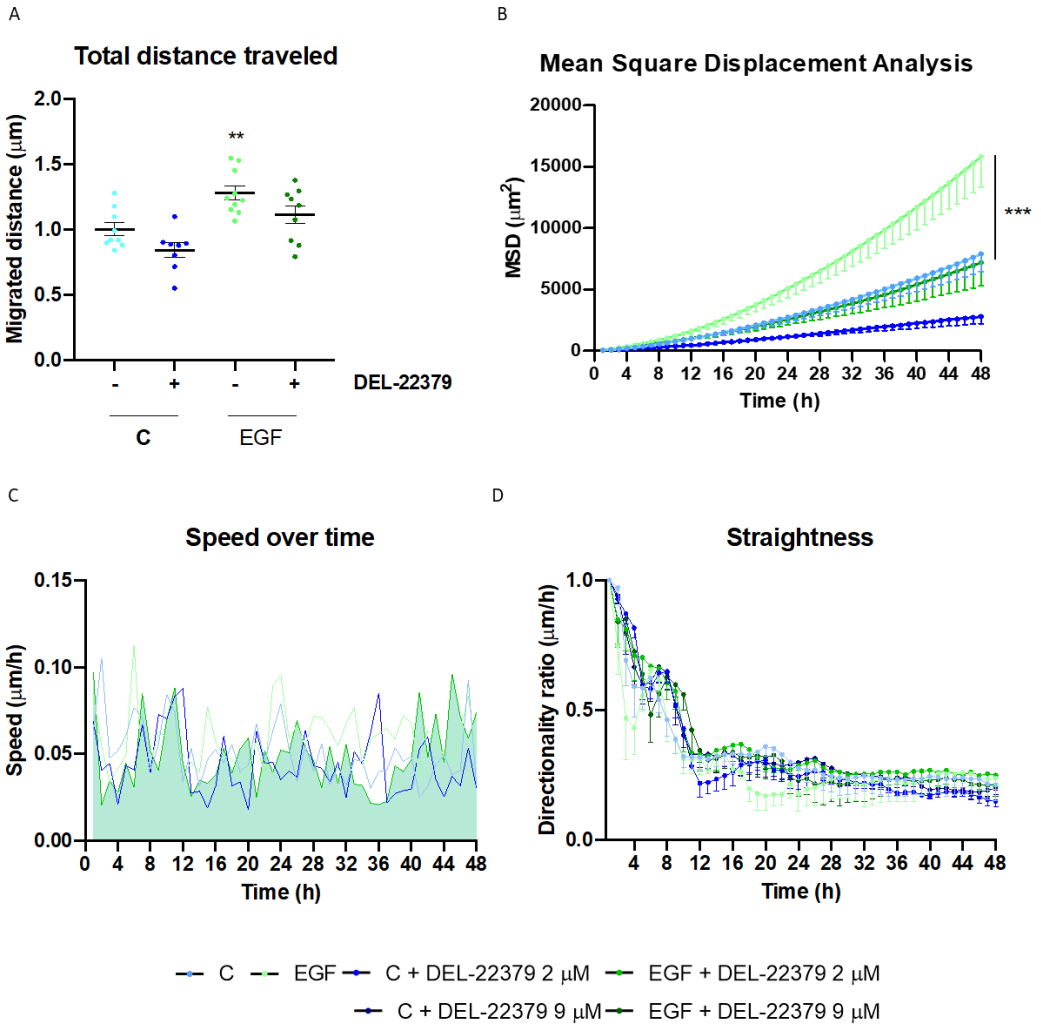

Figure 37. ***EGF-induced cell migration in the M38K cell line.*** *Cells were treated with EGF (50 ng/mL) and DEL-22379 (2 µM), and live-cell video-microscopy was performed over 48 h with pictures taken every 30 min. This experiment was performed two times with three technical replicates. (A) Dots represent the cumulative migrated distance of individual cells (n=10) over 48 h, assessed by manual single-cell tracking using Image J. ****P < 0.001 treatment versus control, One-way ANOVA with Sidak's multiple comparisons test. (B) Mean squared displacement (MSD), (C) average speed, and (D) directionality ratio of representative tracked cells were calculated by DiPer. Lines represent means and SEM in*

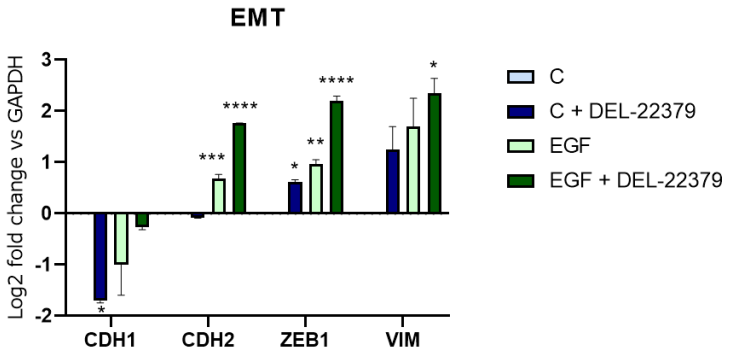

Figure 38. ***Determination of EMT gene expression of M38K cells****. The graph showed the Log2 fold change of gene expression after 48 h of EGF stimulation, and DEL-22379 treatment as indicated versus controls of the typical EMT marker genes: E-cadherin (CDH1), N-cadherin (CDH2), Zeb1, and vimentin (VIM) in M38K cell line. EMT hallmarks were determined by RT-PCR (mean and SEM of three biological repeats performed in duplicates). GAPDH was used as q housekeeping gene for normalization. Data are shown as mean and SEM. ***P < 0.001, **P < 0.01, *P < 0.05 treatment versus control, one-way ANOVA with Sidak's multiple comparisons test. EGF: 50 ng/mL; DEL-22379: 2*

Since we demonstrated that KSR1 expression regulated ERK dimerization and chemotaxis. It was sought to explore the effect of KSR1 overexpression in M38K migratory response.

It was found that KSR1 induced cell migration upon EGF stimulation. Otherwise, the DEL-22379 treatment significantly decreased the migrated distance travelled upon EGF stimulation (Figure 39 and Figure 40).

This data support that KSR-ERK increase cell migration trajectory upon EGF stimulation.

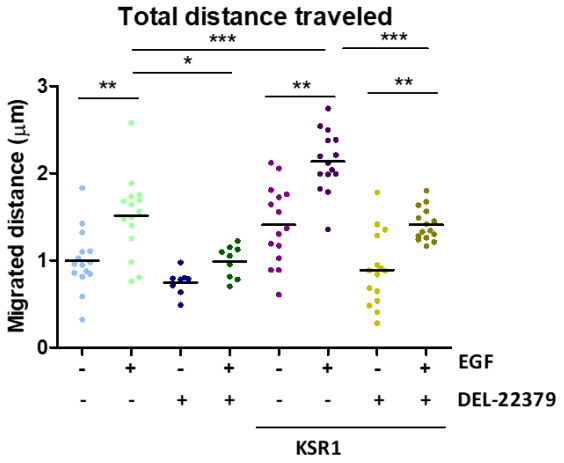

Figure 39. ***Effect of KSR1 overexpression in M38K cell migration****. Cells were transfected and treated with EGF (50 ng/mL), IGF-1 (25 ng/mL), and DEL-22379 (2 µM), and live-cell video-microscopy was performed over 48 h, pictures were taken every 30 min. This experiment was performed two times with three technical replicates. Dots represent the cumulative migrated distance of individual cells (n=30) over 10 h and 48 h, assessed by manual single-cell tracking using Image J. ****P < 0.001 treatment versus control, One-way ANOVA with Sidak's multiple comparisons test.*

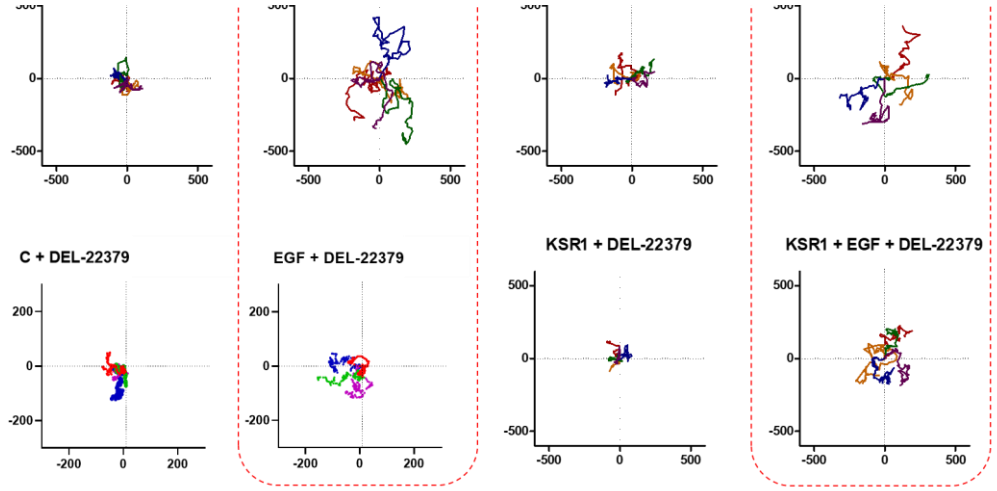

Figure 40. ***Analysis of M38K individual cell migration.*** *Cells were treated with EGF (50 ng/mL), IGF-1 (25 ng/mL), and DEL-22379 (2 µM), and live-cell video microscopy was performed over 48 h with pictures taken every 30 min. This experiment was performed two times with three technical replicates. Origin plots of representative tracked cells were calculated by DiPer.*

In order to determine if EGF and IGF-1 stimulation induce EMT in breast cancer cells, we analysed EMT invasion ability using MCF-7 and MDA-MB-231 cell lines.

At first sight, our breast cell models did not show major morphology changes after 48 h of EGF and IGF-1 stimulation. We found that MCF-7 cells slightly showed flatter than MDA-MB-231 cells, which looked elongated and roundish upon agonist stimulation or DEL-22379 treatment (Figure 41 and Figure 42). In addition, neither EGF nor IGF-1 stimulation induced significant EMT gene expression. Interestingly, we found that DEL-22379 treatment enhanced some EMT gene expression, such as a Twist gene (Figure 43 and Figure 44).

These results revealed that MCF-7 and MDA-MB-231 breast cancer cells were not suited to EMT characteristics.

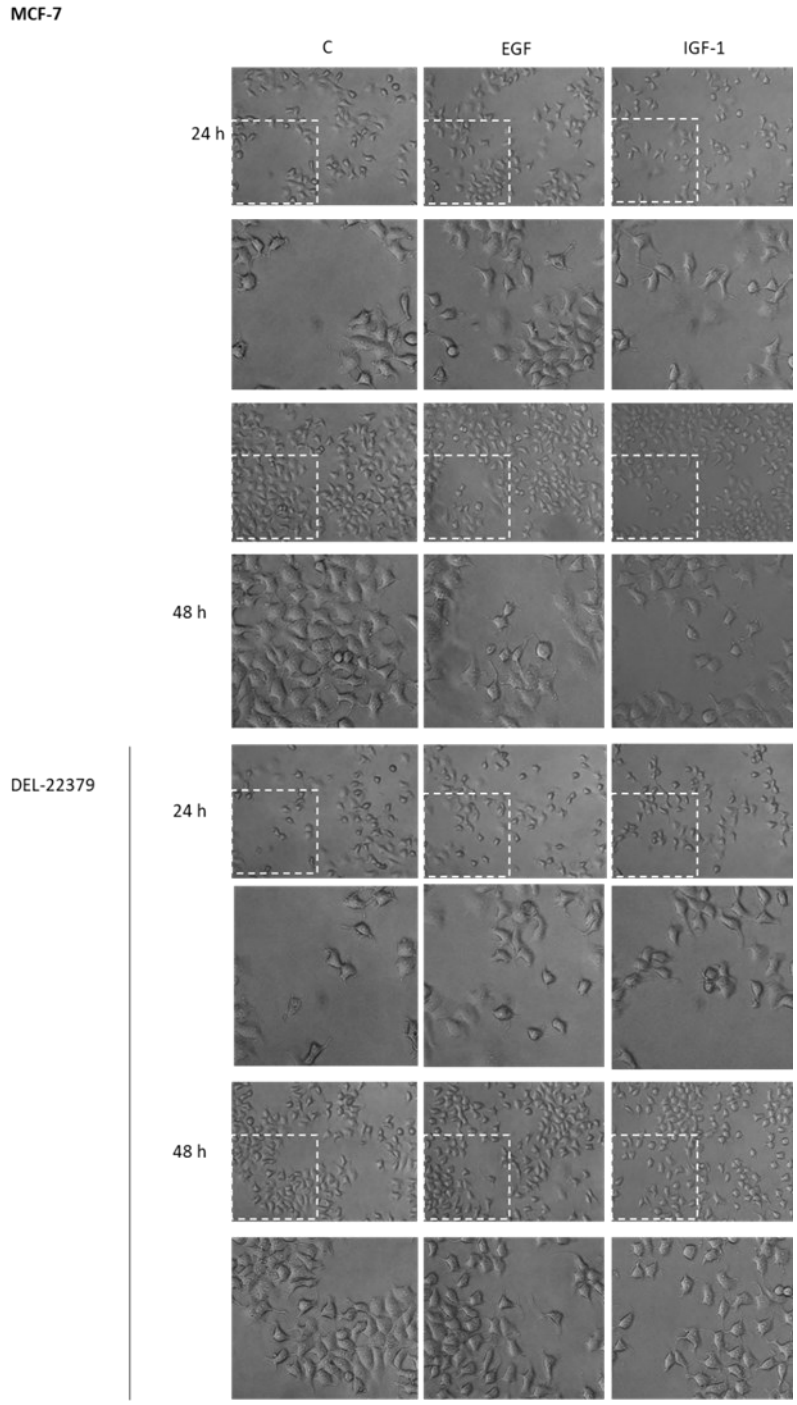

Figure 41. ***Cell morphology analysis of MCF-7 after EGF stimuli and DEL-22379 treatment.*** *Representative phase-contrast at a 10 magnification (upper panels) and 20 magnification (lower panels). EGF (50 ng/mL), IGF-1 (25 ng/mL), DEL-22379: 2 µM*

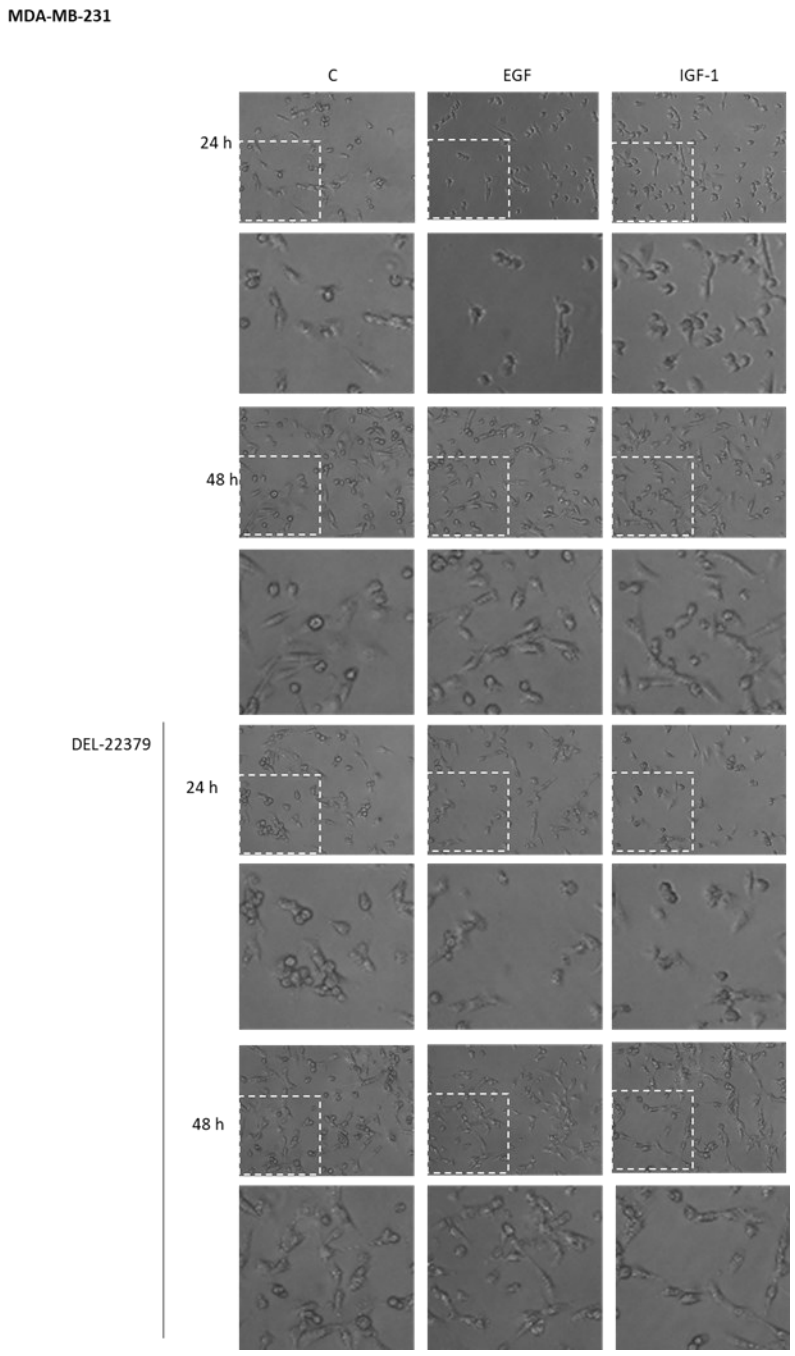

Figure 42. ***Cell morphology analysis of MDA-MB-231 after EGF stimuli and DEL-22379 treatment.*** *Representative phase-contrast at a 10 magnification (upper panels) and 20 magnification (lower panels). EGF (50 ng/mL), IGF-1 (25 ng/mL), DEL-22379: 2 µM treatment for 48 h.*

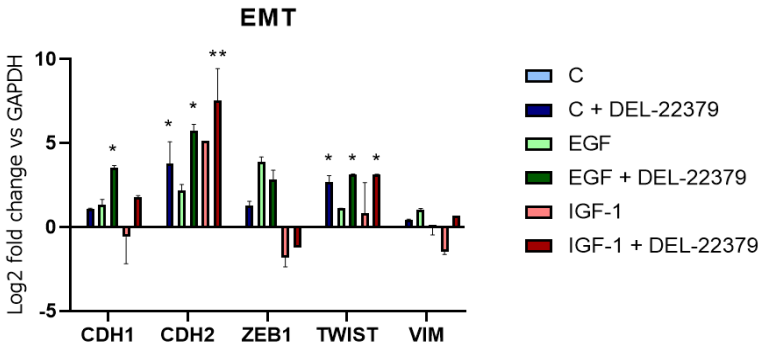

Figure 43. ***Determination of EMT gene expression of MCF-7 cells.*** *Log2 fold change of gene expression after 48 h of treatment as indicated versus controls of the typical EMT marker genes E-cadherin (CDH1), N-cadherin (CDH2), Zeb1, Twist, and Vimentin (VIM) in MCF-7 cells. EGF: 50 ng/mL and IGF-1: 2 5 ng/ mL; DEL-22379: 2 µM*

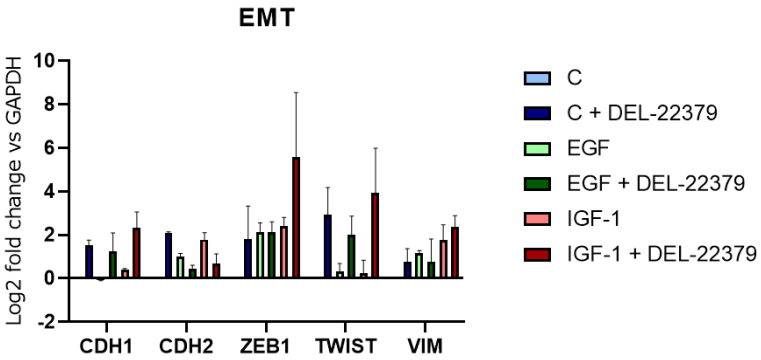

Figure 44. ***Determination of EMT gene expression of MDA-MB-231 cells.*** *Log2 fold change of gene expression after 48 h of treatment as indicated versus controls of the typical EMT marker genes E-cadherin (CDH1), N-cadherin (CDH2), Zeb1, Twist, and Vimentin (VIM) in MDA-MB-231 cells. EGF: 50 ng/mL and IGF-1: 2 5 ng/ mL; DEL-22379: 2 µM.*

Despite that our breast cancer models were poorly EMT invasive, we were interested in assessing their migration ability over time.

We observed that the speed in MCF-7 at first 10 h suffered a peak (Figure 44 C), which correlated with a significant migration upon EGF stimulation (Figure 44 A), then the velocity was maintained over time. However, after 48 h cell migration increased upon IGF-1 stimulation in MCF-7 cells (Figure 44 B). There were not significant differences in directionality ratio (Figure 44 D).

In the case of the MDA-MB-231 cell line, distance migration increased upon EGF stimulation (Figure 45 A), and the speed and the directionality ratio of the cells got kept over time (it tends to 0 value) upon any stimulus (Figure 45 B-C). DEL-22379 treatment increased the straightness upon EGF stimulation in MDA-MB-231 cells (Figure 45 C).

We found that the velocity was ten times more in MDA-MB-231 cells compared to MCF-7 cells (Figure 44 B and Figure 45 B). Moreover, it was found that MDA-MB-231 cells moved faster than MCF-7 cells upon EGF as IGF-1 stimulation. Besides, MDA-MB-231 cells were more sensitive to DEL-22379 (Figure 46).

In parallel, we tested ERK dimerization by immunoblotting with the purpose of relating MDA-MB-231 migration to ERK levels upon agonist stimuli.

It was observed that ERK dimerized upon EGF and IGF-1 stimulation in the MDA-MB-231 cell line (Figure 47)..

Overall, these results indicated that MDA-MB-231 cells had a higher index of migration than MCF-7. Furthermore, the cell migration was reduced by DEL-22379. This suggests that MDA-MB-231 migration ability was ERK dimerization dependent.

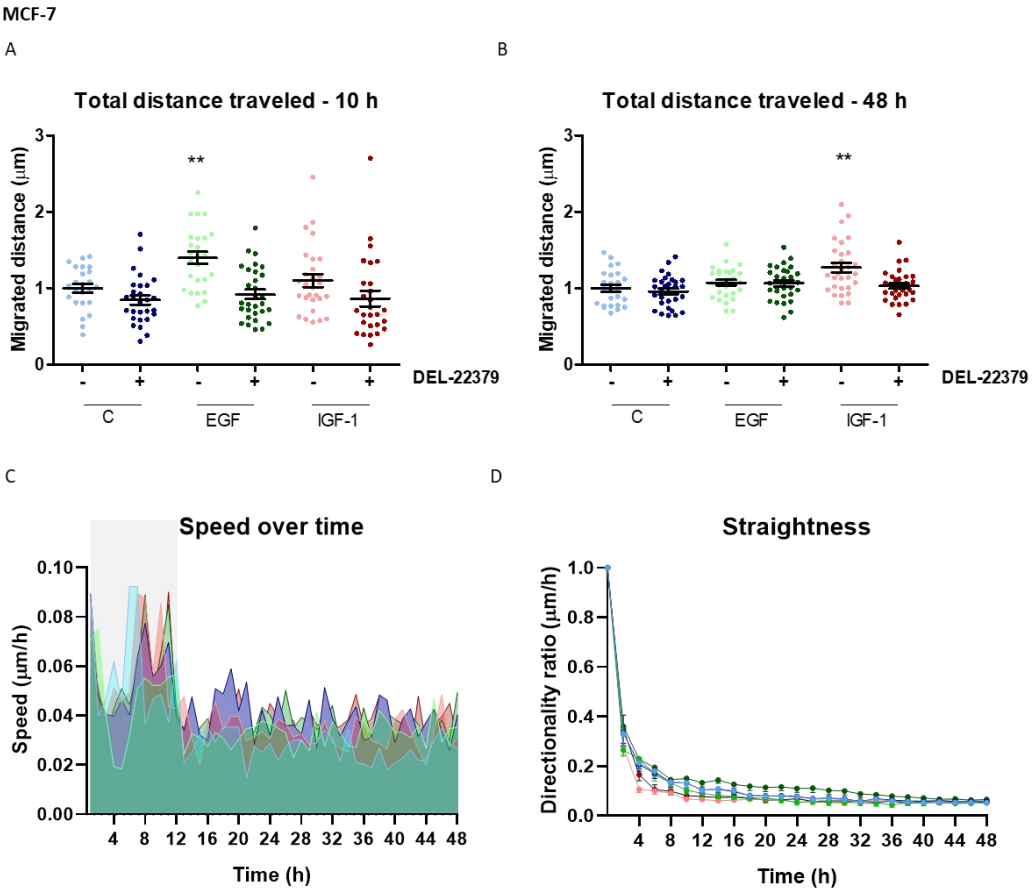

Figure 44. ***Quantification of MCF-7 individual cell migration and speed over time.*** *Cells were treated with EGF (50 ng/mL), IGF-1 (25 ng/mL), and DEL-22379 (2 µM), and live-cell video-microscopy was performed over 48 h, pictures were taken every 30 min. This experiment was performed two times with three technical replicates. On the top, dots represent the cumulative migrated distance of individual cells (n=30) over 10 and 48 h, assessed by manual single-cell tracking using Image J. ****P < 0.001 treatment versus control, One-way ANOVA with Sidak's multiple comparisons test. On the bottom, graph lines represent mean tracked cells calculated by DiPer in average speed. This experiment*

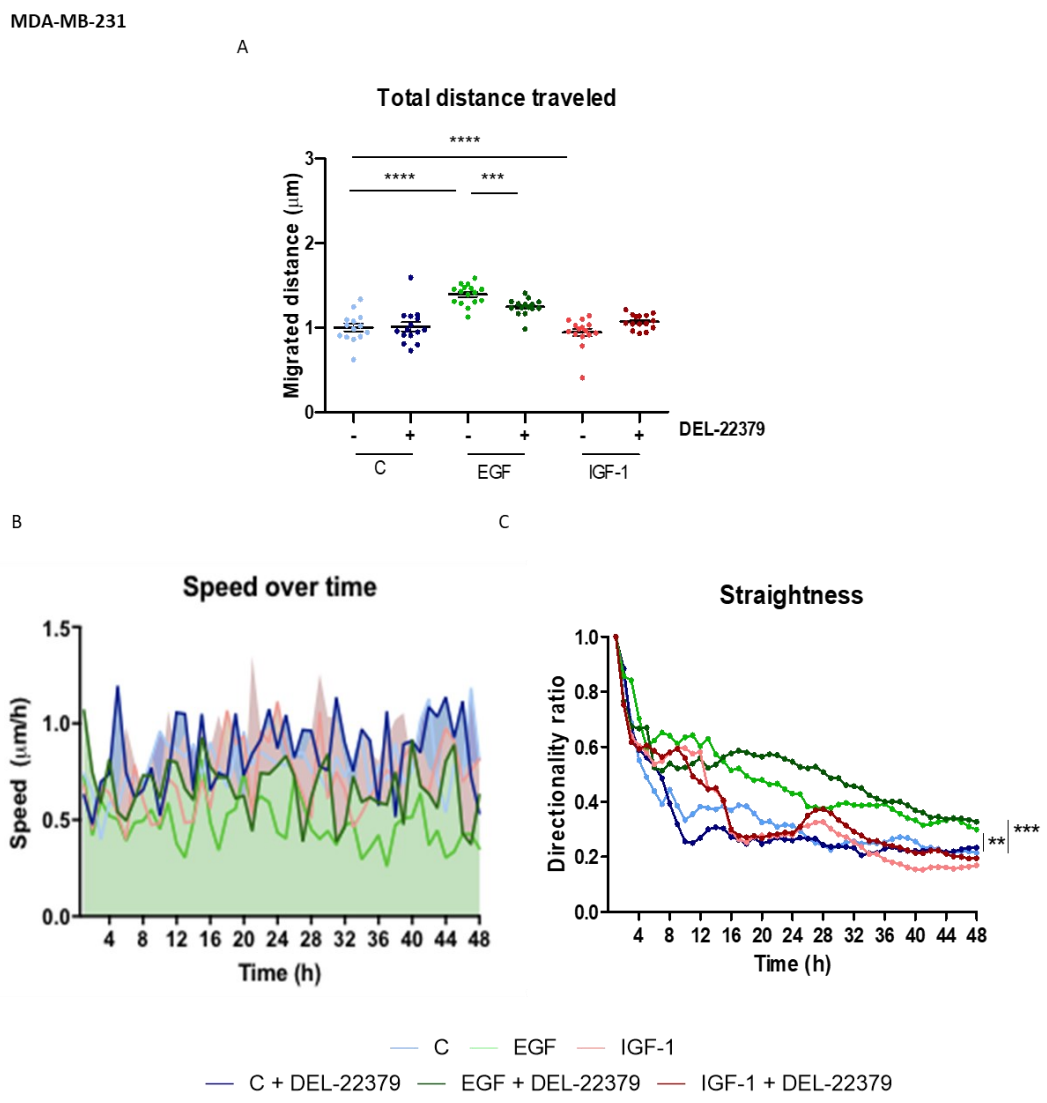

Figure 45. ***Study of migration over time in MDA-MB-231 cells****. Cells were treated with EGF (50 ng/mL), IGF-1 (25 ng/mL), and DEL-22379 (2 µM), and live-cell video microscopy was performed over 48 h, pictures were taken every 30 min. On the top, dots represent the cumulative migrated distance of individual cells (n=30) over 48 h, assessed by manual single-cell tracking using Image J. ****P < 0.001 treatment versus control, One-way ANOVA with Sidak's multiple comparisons test. On the bottom, graph lines represent mean tracked cells calculated by DiPer in average speed. This experiment was performed two times with three technical replicates.*

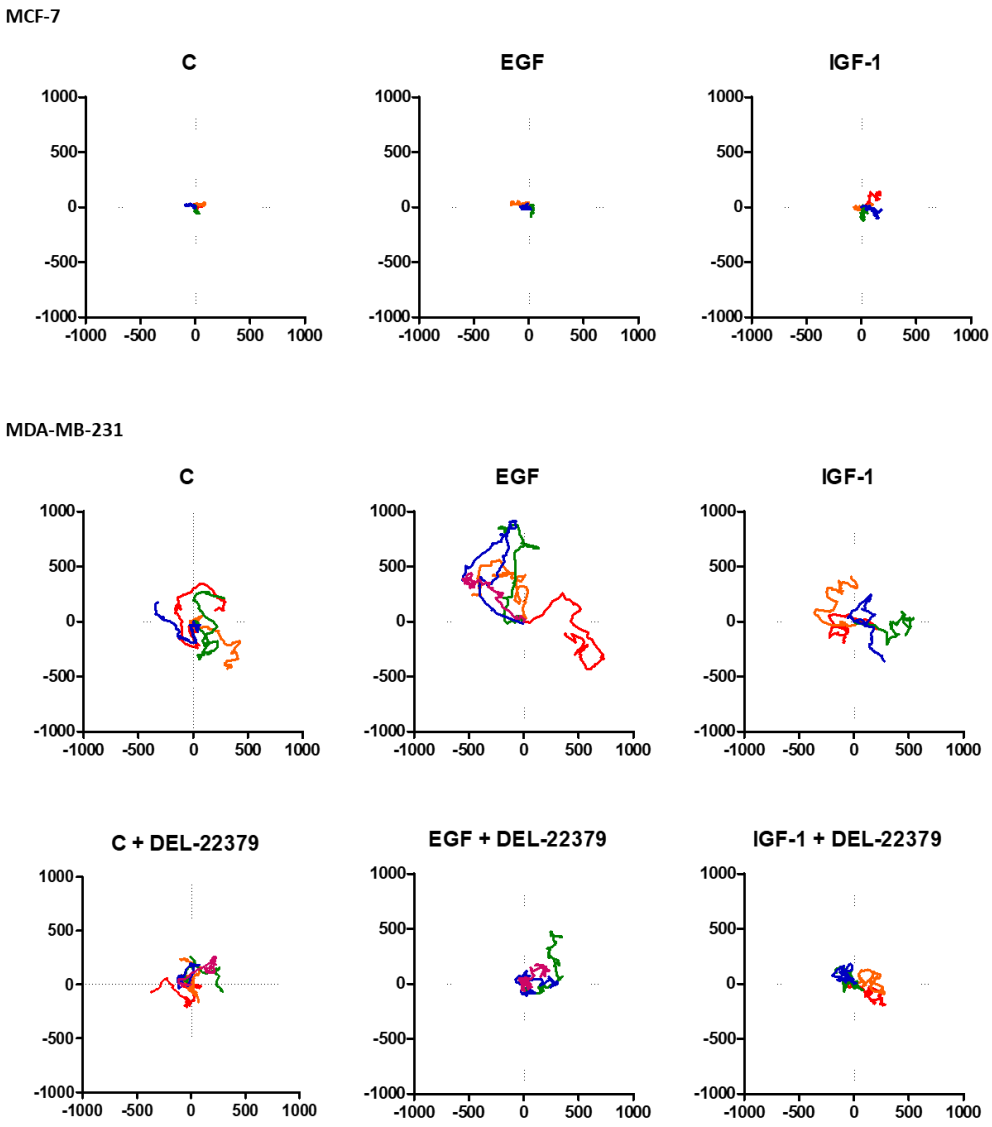

Figure 46. ***Individual cell migration after agonist stimulation and DEL-22379 treatment.*** *MCF-7 and MDA-MB-231 cells were treated with EGF (50 ng/mL), IGF-1 (25 ng/mL), and MDA-MB-231 cells, which have a higher rate of migration, were treated with DEL-22379 (2 µM), and live-cell videomicroscopy was performed over 48 h, pictures were taken every 30 min. This experiment was performed two times with three technical replicates. Origin plots of representative tracked cells were calculated by*

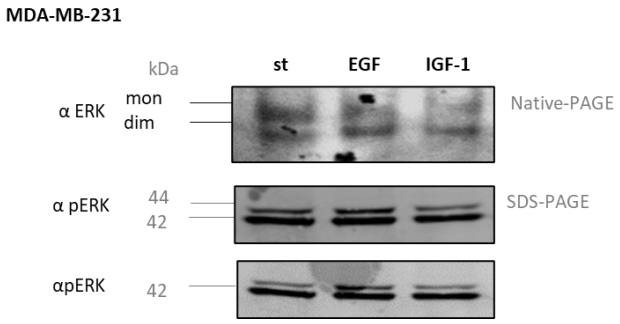

Figure 47. ***Analysis of ERK dimerization and phosphorylated levels upon EGF and IGF-1 stimulation in MDA-MB-231 cells****. ERK dimers were monitored by Native-PAGE and phosphorylated levels by SDS-PAGE immunoblotting. EGF 100 ng/mL and IGF-1, 50 ng/mL*

4.5. ERK dimers increase organoid invasion

To further substantiate the above findings, we analysed the effect of DEL-22379 in MDA-MB-231 cells. Considering that ERK dimerization and subcellular distribution are mechanistically linked and knowing that ERK dimers are restricted to the cytoplasm and ERK monomers to the nucleus (Casar et al., 20008), we wanted to investigate ERK localization in MDA-MB-231 cells.

For this purpose, we performed nucleus-cytoplasm fractionation. It was found that DEL-22379 treatment-induced ERK nuclear translocation (Figure 48) after disrupting ERK dimers (Figure 49). In addition, we performed an immunofluorescence assay to determine ERK subcellular distribution after ERK dimerization inhibitors treatment (Figure 49).

We observed that ERK monomers were localized at the nucleus after DEL-22379 treatment in MDA-MB-231 cells. Moreover, we have found that DEL-22379 treatment-induced actin relocalization around the nuclear membrane (Figure 50).

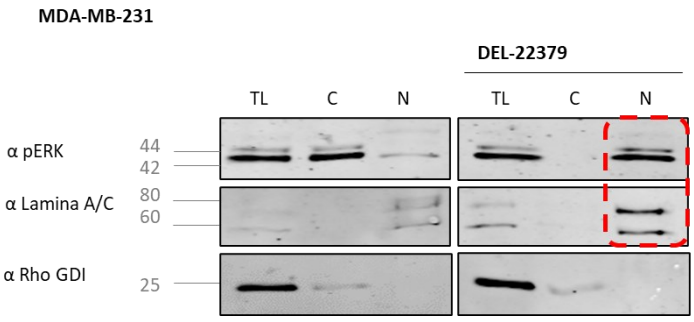

Figure 48. ***Effect of DEL-22379 treatment on ERK cell localization in MDA-MB-231 cells****. Cells were treated with DEL-22379 (10 µM, 1 h).*

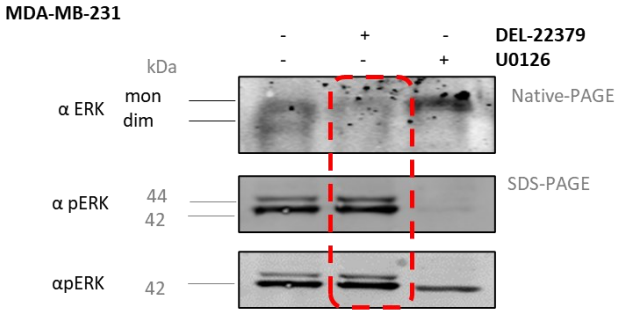

Figure 49. ***Effect of DEL-22379 treatment on ERK dimerization in MDA-MB-231 cells.*** *ERK dimers were monitored by Native-PAGE and phosphorylated levels by SDS-PAGE immunoblotting. Cells were treated with DEL-22379 (10 µM, 1 h).*

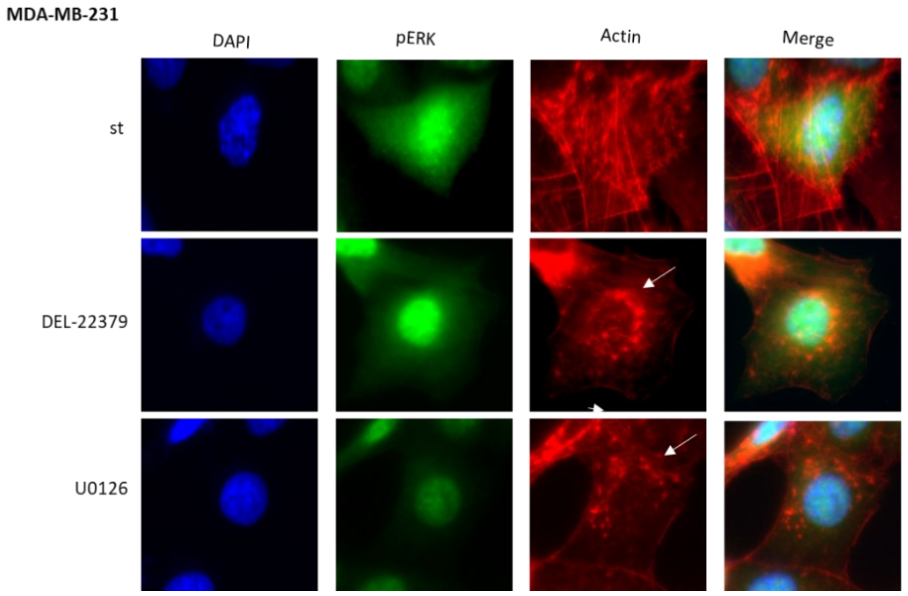

Figure 50. ***Identification of ERK dimerization after ERK inhibitor treatment in MDA-MB-231 cells****. Immunofluorescence microscopy revealed an interaction between ERK and actin proteins, and nuclear retention of ERK after DEL-22379 and U0126 treatment, whereas actin was observed around the nucleus. Immunofluorescence microscopic images for MDA-MB-231 cells after treating with DEL-22379 and U0126. Left: DAPI (blue) middle: ERK2 (green) and right: actin (red) and merge. Using the ImageJ program, fluorescence signals which overlap were shown in yellow. n = 2, starved cells were stimulated with EGF, IGF-1 (100 and 50 ng/mL respectively for 3 min) and treated with DEL-22379 and U0126 (10 uM, 1 h).*

In light of our results showing that MDA-MB-231 cell migration is due to ERK dimerization through actin cytoskeleton, we studied the role of ERK dimers in invasiveness.

For this purpose, we performed the chemotaxis transwell assay and 3D invasion in MDA-MB-231 cells after ERK dimer inhibitor (DEL-22379).

Expectedly, ERK dimers were involved in chemotaxis. As well, ERK dimers promote organoid invasion experiment showed (Figure 51).

To further study, we stained the MDA-MB-231 spheroids to relate ERK dimers with actin filaments.

The stained mammospheres showed that ERK dimers were responsible for cell-single and collective invasion together with actin cytoskeleton structure. The colocalization coefficient between ERK dimers and actin proteins was significant (Figure 52 and Figure 53).

After studying a single migratory cell, we found that ERK and actin antibody signals colocalize in the plasma membrane (Figure 53).

It suggests that ERK dimers together with the actin cytoskeleton were related to the plasma membrane,

According to Cellular Components (GO) analysis (Figure 54), ERK was related to focal adhesions and cell-substrate junctions. It suggests that ERK dimers through actin cytoskeleton might be involved in cell invasion.

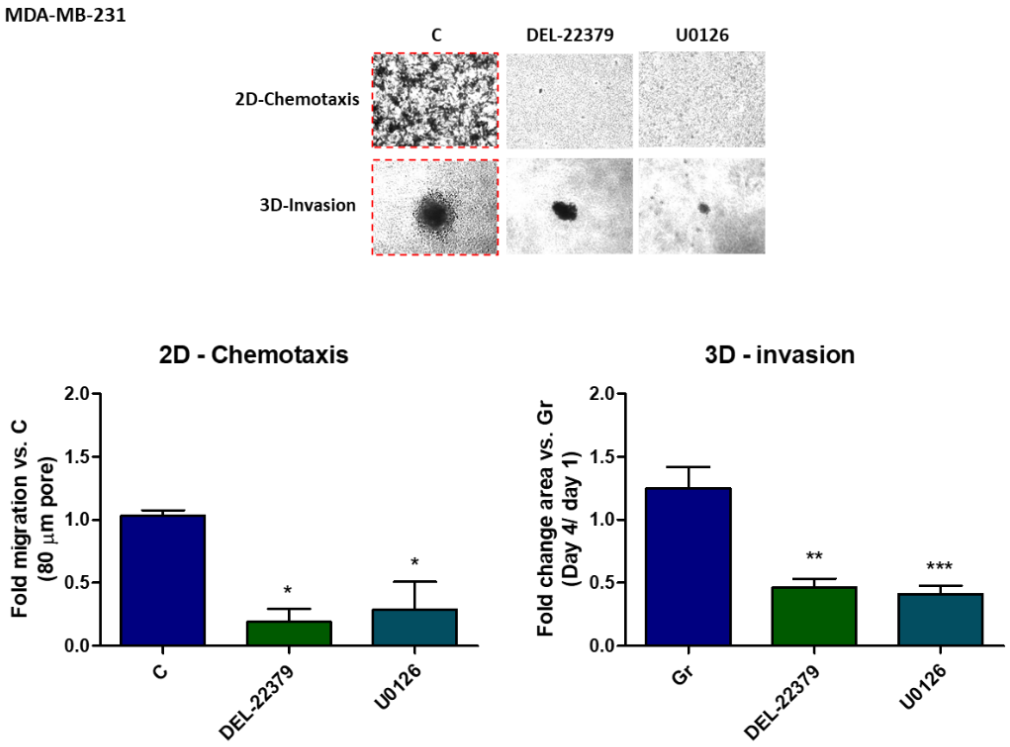

Figure 51. ***Analysis of chemotaxis and invasion in MDA-MB-231 cells.*** *Cell chemotaxis assay of MDA-MB-231 cells into transwell assay after DEL-22379 and U0126 treatment (2 µM for 16 h). Cells were incubated for 16 h, stained with crystal violet, and visualised by optical microscopy. The bottom of the microporous membrane (8 µm) photo was acquired by quantification of migration. Values were expressed as relative migration normalised to starved samples. Chemotaxis was determined by measuring the area covered by cells (0.47 µm2). The graph shows fold migration. Bars indicate mean ± SEM (n=3, five replicates of independent experiments; t-Student; p-value from enrichment test, *, p < 0.05). Representative control and treated MDA-MB-231 3D-invasion at day 4 (DEL-22379 and U0126, 2 µM the last 2 days). Fold of total size spheroid after four days. Error bars display the standard deviation of independent measurements. Images were acquired quantification of invasion values were expressed as relative migration*

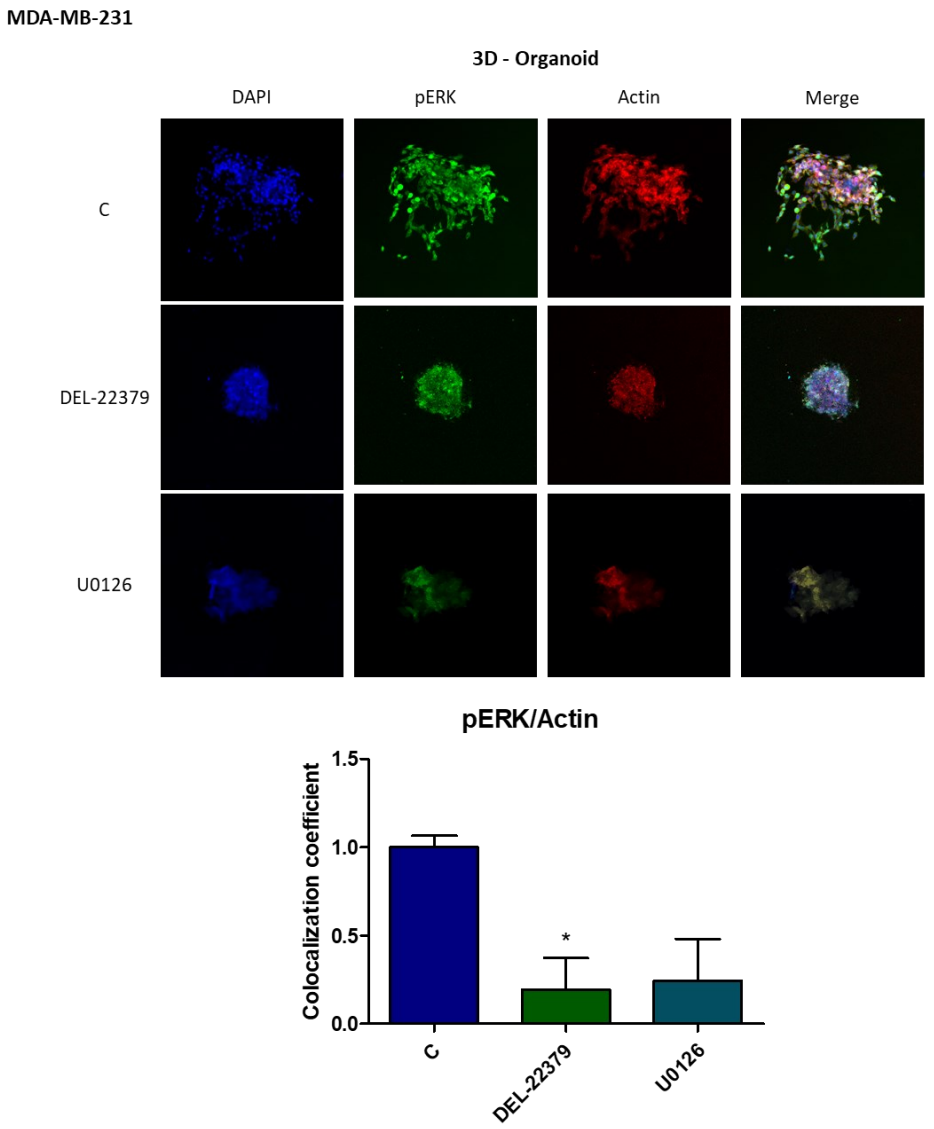

Figure 52. ***Immunofluorescence confocal microscopic images for breast cell line after DEL-22379 treatment****. (DEL-22379 and U0126, 2 µM). Left: DAPI (blue) middle: pERK (green), actin(red) and right: merge. Using the ImageJ program, the fluorescence signal overlapped were shown in yellow. The ratio of fluorescence intensity per unit area relative to the control conditions. Bars indicate mean ± SEM (n=3, five replicates of independent experiments; t-Student; p-value from enrichment test, *, p < 0.05).*

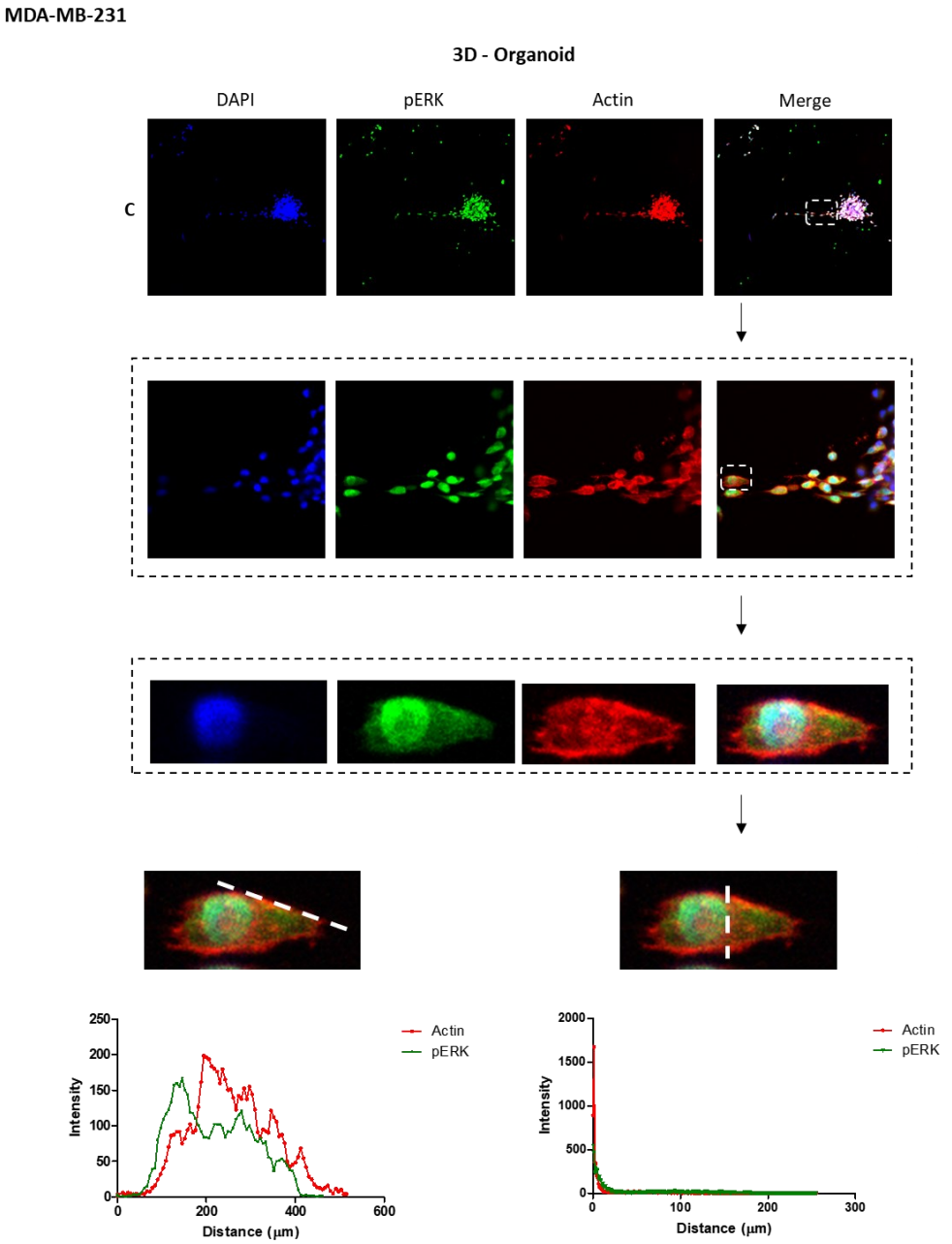

Figure 53. ***MDA-MB-231 cell collective migration in a collagen network matrix.*** *5 magnification images of the control organoids (C) showed the invasive collective cells from the core of the tumour. On the bottom, analysis of the ERK and actin colocalization in the individual invasive cell. The colour histogram of the longitudinal and transversal sections of the individual invasive cell shows the overlap between ERK and actin.*

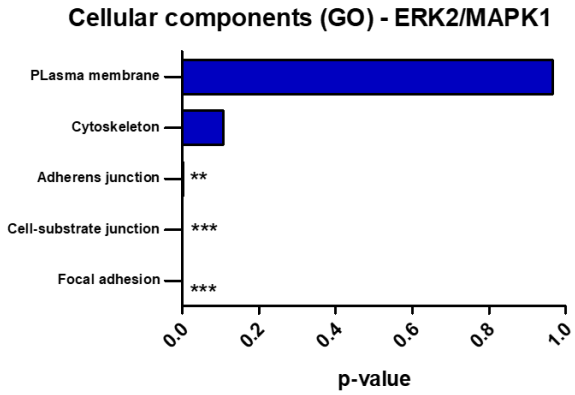

Figure 54. ***Analysis of ERK2 cellular components.*** *The Biological Process Gene Ontology (GO) enrichment over-represented the ERK2 gene functions. Data provided by Cancertool.*

4.6. ERK dimers involve in spontaneous metastasis

The chick spontaneous metastasis model has been widely used to study tumour growth, intravasation and metastasis of tumoural human cells.

To investigate the role of ERK dimerization in breast tumour progression and metastasis, we used a chick embryo metastasis model. This model allowed analyzing whether MDA-MB-231 cells were grafted onto the distal CAM, which means intravasation into the CAM vasculature, or colonized distant organs such as the liver and brain. We treated the primary tumour with ERK inhibitor, DEL-22379, to monitor ERK dimerization in tumour progression.

It was found that DEL-22379 reduced primary tumour size (Figure 55). Moreover, blocking ERK dimerization significantly reduced CAM intravasation, as well as liver and brain colonization (Figure 56).

Overall, these results demonstrate that ERK dimerization regulates breast tumour progression and metastasis.

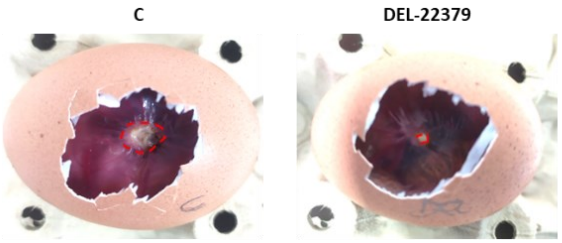

Figure 55. ***Effect of DEL-22379 over primary chick embryo tumours after five days of MDA-MB-231 cell inoculation.***

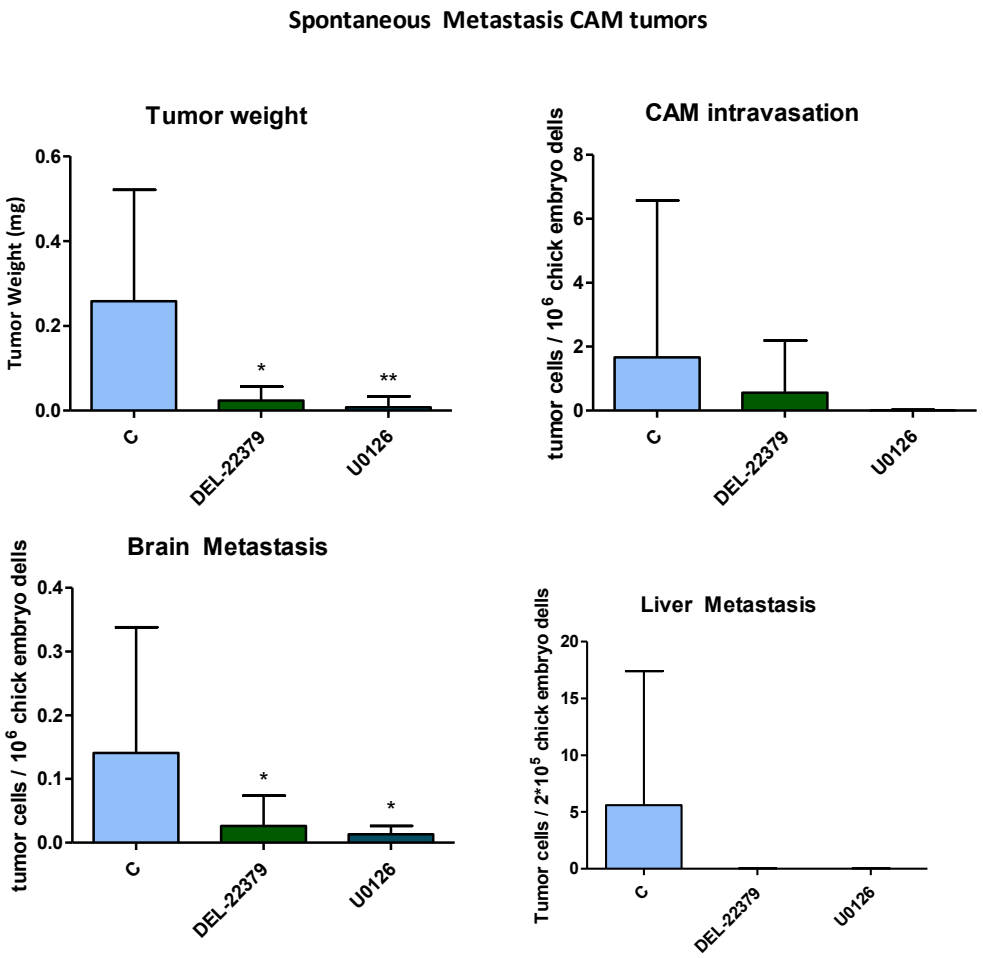

Figure 56. ***Effects of ERK inhibitors (DEL-22379 and U0126) in MDA-MB-231-chick embryo xenografts.*** *2*105 MDA-MB-231 cells were grafted on 10-days chick embryos. Five days after, the primary tumours were collected and weighed (mg), and distal portions of the CAM were analyzed by qPCR showing the % of embryos that underwent spontaneous intravasation (distal CAM colonization), liver and lung colonization, allowing us to determine the relative numbers of human cells per 2*105 chicken cells in CAM, liver or lungs. Error bars show (MEAN ± SEM). Data is from three independent experiments employing from 7 to 12 embryos per cell variant. Statistical significance was determined using a double-tailed unpaired student t-test. *p<0.0001*

DISCUSSION

6. DISCUSSION

In our research into understanding mechanisms of action to be exploited as new therapeutic targets of tumorigenesis and tumour progression, we have focused on ERK dimerization. Over the last few decades, there has been an imperative search for effective drugs to block the MAPK signalling pathway to diminish tumorigenesis and tumour progression. We have previously described that ERK dimerization promotes tumour growth, regulating the activation of cytoplasmic substrates (Casar et al., 2008). As mentioned in the introduction, the cellular redistribution that ERK experiments upon stimulation enables it to reach and phosphorylate over 200 substrates, about half of which are extranuclear. Indeed, upon activation, a substantial proportion of the ERK pool remains at the cytoplasm regulating proliferation, cell death, migration, and invasion. However, little is known about how ERK dimerization is responsible for triggering tumour progression in response to different stimuli.

We, therefore, hypothesized that the different response to the specific stimulus is related to ERK dimerization and its differential sublocalization in the cell, where it can modulate a wide range of proteins and genetic programs. In consequence, the global aim of this thesis was to study how ERK dimerization under agonist stimulation can modulate tumour progression factors.

Firstly, to analyse ERK dimerization upon different stimuli, we used MCF-7 cells treated with EGF, IGF-1 and insulin. We have demonstrated that only EGF stimulation triggers ERK dimerization in MCF-7. Though, ERK was activated in response to EGF and IGF-1 stimuli. According to our previous results, we found that EGF and IGF-1 stimulation activate ERK phosphorylation but only EGF induces ERK dimerization.

Since ERK dimerization regulated tumour growth and tumour progression factors, next we investigated chemotaxis, analyzing the chemotactic capability of cells toward a chemoattractant; and invasion, the directed movement of cells through an extracellular matrix in response to a chemical stimulus in a process that involves ECM degradation and

proteolysis. The extracellular matrix is a reservoir of stimuli that activates the RAS-ERK pathway activation that triggers different tumoral characteristics depending on the duration and intensity of the stimuli (Herrero et al., 2016). In this work has been determined that growth factors trigger differential ERK activation promoting different cellular responses. Using breast carcinoma cells lines, we performed chemotaxis and invasion transwell assays. A number of important observations were noticed: i) EGF promotes chemotaxis through ERK dimerization, ii) Blocking ERK dimerization reduces chemotaxis, iii) IGF-1 induces invasion through ERK monomers.

Therefore, we posit the ERK dimerization regulates breast cancer cells' chemotaxis in response to EGF. It could be due to ERK dimers activate specific ERK substrates at the cytoplasm to increase the ability of the tumours cells to migrate through the pore membrane toward the chemoattractant. We also found that IGF-induced invasion of breast cancer cells is not dependent on ERK dimerization. It could be due to IGF stimulation promotes ERK monomers translocation to the nucleus and therefore modulate the expression of different proteins and genetic programs related to ECM degradation. Therefore, further work is needed to unravel how ERK activated as a monomer regulates tumour cells invasion. We have previously unveiled that ERKs cytoplasmic component mechanistically is linked to ERKs dimerization. We showed that scaffold proteins present solely at the cytoplasm and serve as ERK dimerization platforms. In such a way, ERK dimers would be stably bound to the scaffold complex. Importantly, this process is essential for ERK cytoplasmic activation, but not nuclear substrates (Casar et al., 2008).

In the same vein, we have demonstrated that downregulating KSR levels, using siRNAs, induces invasion of breast cancer cells.

Besides, KSR1 boots these cellular abilities triggering membrane protrusions. These focal adhesions, kept thanks to the actin cytoskeleton, allowing the cell to migrate and establish cell-substrate interactions. On the other hand, we have found that ERK2 H176E mutant, enable to dimerize (Khokhlatchev et al., 1998), increase invasion. It suggests that

IGF-1 stimulation increases ERK monomers that might interact with nuclear substrates related to the expression of proteins involved in matrix degradation. It makes us think that external stimuli activate intracellular signalling involved in a dendritic network of actin filaments. The cells undergo a morphological change that allows them to migrate and invade by cell-ECM interactions. It might be favoured by ameboid morphology.

In light of these data, it might determine that KSR through ERK dimers is involved in generating morphological changes dropping anchor the cell to the substrate, like focal adhesion formation or cell-substrate adhesion. These cellular components could be stronger by a possible transphosphorylation between scaffolds such as KSR1-GIT1 at the post-traduction level. GIT1 was previously described as a scaffold in the focal adhesions through ERK signal (Chen et al., 2015). The transphosphorylation could boost the ERK signal exercising control over the actin cytoskeleton.

The question remains as to why KSR1 downregulation in spite of stopping tumour progression, as some therapeutical drugs has been designed for that, increase matrix degradation. Nevertheless, the final result may explain the controversial results about developing the scaffold-specific drug or the appearance of drug resistance. Set example, APS-2-3-79 described as a druggable regulator of oncogenic Ras (Dhawan et al., 2016). Our results that KSR1 targeting is not enough to avoid tumorigenesis, which does not keep an extra control to invasion ability. It could explain that previous studies saw that the loss of KSR1 in mice showed resistance to RAS-dependent tumour formation (Hansen et al., 1997; Lozano et al., 2003; Nguyen et al., 2002). So, to continue searching for other complementary targets, some candidates could be purposed like nucleoporin or HDAC inhibitors to prevent ERK monomers translocation and avoid gene expression related to proteolytic ECM reorganization.

This work might have evidence that KSR1 influences cell tumour abilities. So that, studying the role of KSR1 in non-mammal cells could explain whether this pseudokinase has any intrinsic role in keeping cell shape independent of serving as an ERK dimerization platform. KSR1 is also present in a non-mammal organism like *Gallus gallus*

(E1C7R3_CHICK) with an 83 % homology with the human gene (J3QSG8_HUMAN), according to Blast tool. Nevertheless, ERK dimers were described as exclusive of mammal features, as has been mentioned before (Herrero et al., 2015). The previous experiments of this work reveal that KSR1 does not serve as a platform of chick ERK monomers, nor chemotaxis ability is trigged as was expected. The role of KSR1 could cover a wide range of possibilities apart from cellular morphology changes and facilitating ERK dimerization not known until now.

The cellular morphology observed in this work reveals that KSR1-ERK dimers and the actin cytoskeleton have a narrow relationship in cellular outcomes. Both maintain the cell shape, suiting cells to different terrains during the plasticity of cancer migration and invasion modes.

More than ERK dimers are responsible for the migration ability, the results have shown that the cells become migrating mesenchymal cells during 3D-invasion (organoids formation) (Wu et al., 2021). Cell migration can be further partitioned based on the specific cell-substrate junctions, the contractility of the cytoskeleton, and the turnover of cell attachments to the extracellular matrix (ECM) (Friedl & Alexander, 2011; Masi et al., 2020; Pandya, Orgaz, & Sanz-moreno, 2017; Pandya, Orgaz, & Sanz-Moreno, 2017; Wu et al., 2021). It suggests that ERK dimers can mediate the collagen I matrix degradation through specific metalloproteases like MMP1. However, the effect of matrix degradation is significant when cells adopt morphological spherical shapes. That is referred to here as amoeboid migration, morphology that we found when KSR1 expression was downregulated. In this case, it is supposed that ERK monomer substrates enhance the proteolytic mechanism involved in matrix degradation and, ERK dimerization might have control over the plasticity of morphological cell changes crucial to migrate and invade. It is worth not forgetting that the high levels of ERK dimers do not exclude the presence of ERK monomers that could enhance the invasive gene expression in parallel.

Thus, studying EMT we observed that EGF stimulation and DEL-22379 treatment enhanced EMT gene expression. We have realized that does DEL-22379 inhibit ERK dimer

but also migration mechanism. DEL-22379 migration inhibition could be due to this drug interacts with another intracellular signalling like the ROCK pathway or integrin-mediated ECM adhesion. Undoubtedly, whether it is demonstrated that DEL-22379 treatment blocks ROCK signalling, this drug might be used to abolish cytoskeleton remodelling through ERK dimerization. The first bits of knowledge that support this hypothesis are the following. First, RHOC is involved in actin contraction for cell migration through MAP Kinase signalling (Leicht et al., 2007; Wu et al., 2021). Secondly, upon any EGF and TGFβ, as EMT-invasive stimulus, ROCK inhibitors decrease migration (Schelch et al., 2021). And third, Orgaz and colleagues' publications showed that the cytoskeletal remodelling and changes in expression of the ROCK-myosin II pathway are involved in MAPK inhibitor resistance in melanoma (Orgaz et al., 2020).

Referring to EMT invasion ability, previous publications confirm that MCF-7 and MDA-MB-231 cell lines can suffer EMT, a mode of invasion, upon EGF and IGF-1 stimulation (Kim et al., 2016; Walsh & Damjanovski, 2011). Certainly, some genes related to EMT are expressed, like N-cadherin upon IGF-1 stimulation, but not with high significance. It might be due to experimental conditions like growth factor concentrations used in these breast cancer models. On the other hand, we have found that upon DEL-223789 treatment, EMT gene expressions are significant, like Twist. It suggests that ERK dimer inhibition increases EMT gene expression. So, ERK nuclear signal through its specific substrates could enhance an EMT invasion mode, as previous studies showed (Olea-Flores et al., 2019). Even though MAPK is not the only signalling pathway that triggers EMT, TGFβ is a potential growth factor involved in this biological process independent of active ERK (Gui et al., 2012; Schelch et al., 2021).

To further study the role of ERK nuclear targets upon IGF-1 stimulation, the mass spect results could identify them. First clues point to STK40, a serine-threonine kinase 40 induced by IGF-1 might be a good candidate, but no conclusive results have been obtained until now.

Under-discussing in vitro methods to evaluate the morphology changes and the cell scattering, in this work, EMT-invasion has been studied under this premise without matrix gel. The cellular changes suffered upon different stimulations help understand the outputs of active cellular signalling; however, the feedback response to the matrix barrier impact on the cell is omitted. Another drawback is the mode of use of the novel drugs. In the EMT study, we have found that the use of DEL-22379 inhibitor following the protocol provided by previous studies (Herrero et al., 2015) was struggling. The adjustment of the drug concentration has been crucial to keep the survival stage and study the role of ERK dimerization after 48 h.

On the other hand, the results obtained by 2D chemotaxis with 2D migration assays suggest that EGF stimulus increases cell movement towards the chemoattractant, creating pseudopods by actin network in MCF-7 cells through early ERK dimerization. Nevertheless, during 48 h, the intracellular signalling is reorganized, the IGF-1 mainly stimulation keeps the cell movement. The reason is likely that the mutation cell profiles become stronger, IGF-1 stimulus boosts the PI3K-AKT mutant signalling beyond EGF stimuli. Despite this, the MCF-7 cell line is a suitable model to study the power of early ERK dimers upon acute stimuli. Study the role of ERK dimerization in a natural microenvironment would be the next step. In this case, to omit de aberrant PI3K signalling, another cell line should be used. To investigate how different paracrine factors of the extracellular matrix (ECM) would affect the model proposed through the MAPK signalling in the present work. To determine how growth factors are associated with the medium and matrix to allow storage of large quantities of signalling molecules to proceed to slow down diffusion in the absence of new protein synthesis (Taipale & Jorma Keski-oja, 1997), and the cellular memory after stimulation is involved in switching on the autocrine or paracrine loops (Eckley et al., 2019; Schulze et al., 2001).

Moreover, new evidence has already related ERK scaffolds with invasion abilities simulating a tumour microenvironment. Rao and colleagues suggest that KSR1 promotes EMT-like phenotype in colorectal cancer through EPST11 reducing the number of colony formations. Rao confirms that EMT requires EPSTI1 in colorectal cancer (Rao et al., 2021).

This protein highly expresses in breast cancer upon the interaction between tumour cells and stromal cells in vitro (Nielsen et al., 2002). Our results predict that KSR-ERK dimers increase migration through ERK dimers in the absence of the surrounding stroma. It would suggest that EPSTI1 could modulate cellular morphology towards a stem mesenchymal cell through KSR1 and ERK dimerization in the presence of fibroblast. The intracellular signalling reorganization could be involved in the reservoir of growth factors in the natural microenvironment. These are some open perspectives to explore.

To sum up, our results suggest that ERK dimerization is involved in tumour progression factors in response to different stimuli. Besides, the external stimuli sustain the cellular mechanism to modulate diverse biological responses through ERK dimerization. Thus, ERK dimerization inhibitors could be an effective antitumor agent for breast cancer patients. Based on our findings, we propose a model to explain how ERK dimerization regulates tumour progression factors upon specific stimulation (Figure 57).

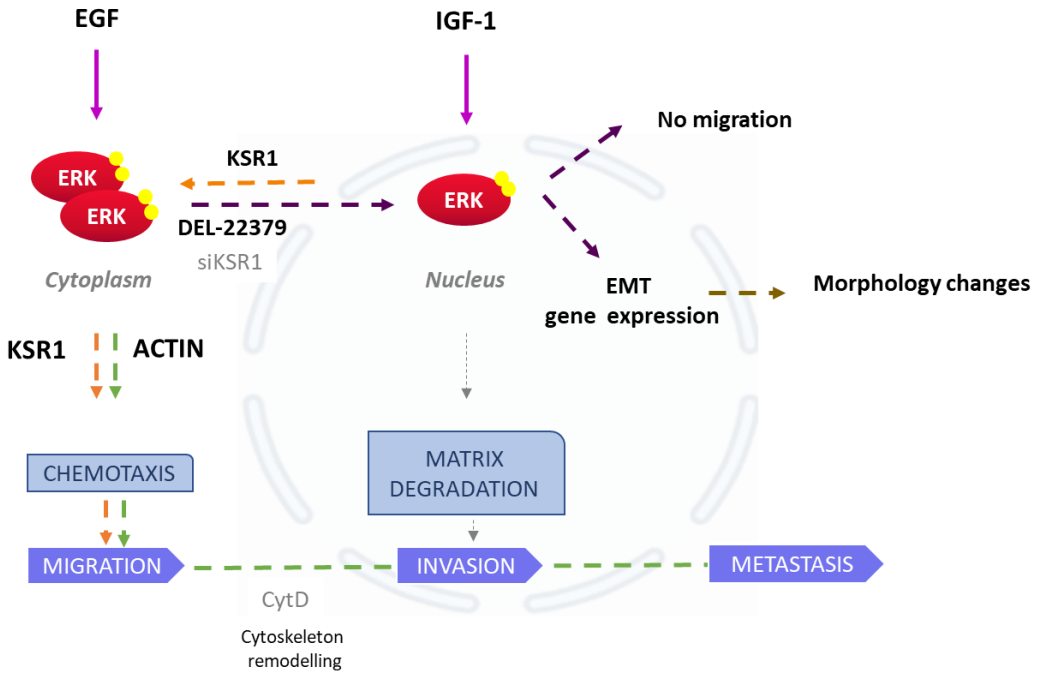

Figure 57. ***Model of tumour progression regulated by ERK dimerization in response to EGF and IGF-1 stimuli.***

CONCLUSIONS

6. CONCLUSIONS

1. Regulation of ERK signalling depends on its dimerization in response to external stimuli. The growth factor EGF triggers ERK dimerization, but IGF-1 does not.
2. ERK dimerization promotes distinct cellular responses. Dimeric ERK increases cell chemotaxis, and monomeric ERK increases extracellular matrix degradation.
3. The EGF stimulus-specific scaffold protein KSR1 increases cell chemotaxis, while the use of siKSR1 increases extracellular matrix degradation. These cellular effects are related to a change in cell morphology, epithelial-ameboid transition.
4. Treatment with DEL-22379 inhibits ERK dimerization. Under its effect, it activates the expression of EMT-related genes while arresting cell migration.
5. ERK dimerization and actin filaments at the plasma membrane are involved in collective cell invasion in 3D organoids.
6. ERK dimers are associated with tumour growth in 3D organoids and spontaneous metastasis chick embryo models.

REFERENCES

7. REFERENCES

Ahearn, I., Zhou, M., & Philips, M. (2018). Post-Translational Modifications of RAS Proteins. *Cold Spring Harb Perspect Med.*, *8*(11), 1–22. https://doi.org/10.1101/cshperspect.a031484

Ahn, N. G., Seger, R., Bratlien, R. L., Diltz, C. D., Tonks, N. K., & Krebs, E. G. (1991). Multiple components in an epidermal growth factor-stimulated protein kinase cascade: In vitro activation of a myelin basic protein/microtubule-associated protein 2 kinase. *Journal of Biological Chemistry*, *266*(7), 4220–4227.

Aronov, A. M., Qing, T., Martinez-Botella, G., Bemis, G. W., Cao, J., Chen, G., Ewing, N. P., Ford, P. J., Germann, U. A., Green, J., Hale, M. R., Jacobs, M., Janetka, J. W., Maltais, F., Markland, W., Namchuk, M. N., Nanthakumar, S., Poondru, S., Straub, J., … Xiaoling, X. (2009). Structure-guided design of potent and selective pyrimidylpyrrole inhibitors of extracellular signal-regulated kinase (ERK) using conformational control. *Journal of Medicinal Chemistry*, *52*(20), 6362–6368. https://doi.org/10.1021/jm900630q

Arozarena, I., Calvo, F., & Crespo, P. (2011). Ras , an Actor on Many Stages : Posttranslational Modifications , Localization , and Site-Specified Events. *Genes and Cancer*, *2*(3), 182–194. https://doi.org/10.1177/1947601911409213

Bissel, M. J., & Radisky, D. (2001). Putting tumours in context. *Nature Reviews Cancer*, *1*(1), 46–54. https://doi.org/10.1038/35094059.PUTTING

Boga, S. B., Deng, Y., Zhu, L., Nan, Y., Cooper, A. B., Shipps, G. W., Doll, R., Shih, N. Y., Zhu, H., Sun, R., Wang, T., Paliwal, S., Tsui, H. C., Gao, X., Yao, X., Desai, J., Wang, J., Alhassan, A. B., Kelly, J., … Samatar, A. A. (2018). MK-8353: Discovery of an Orally Bioavailable Dual Mechanism ERK Inhibitor for Oncology. *ACS Medicinal Chemistry Letters*, *9*(7), 761–767. https://doi.org/10.1021/acsmedchemlett.8b00220

Bogoyevitch, M. A., Ngoei, K. R. W., Zhao, T. T., Yeap, Y. Y. C., & Ng, D. C. H. (2010). c-Jun

N-terminal kinase (JNK) signaling: Recent advances and challenges. *Biochimica et Biophysica Acta - Proteins and Proteomics*, *1804*(3), 463–475. https://doi.org/10.1016/j.bbapap.2009.11.002

Bollag, G., Tsai, J., Zhang, J., Zhang, C., Ibrahim, P., Nolop, K., & Hirth, P. (2012). Vemurafenib: The first drug approved for BRAF-mutant cancer. *Nature Reviews Drug Discovery*, *11*(11), 873–886. https://doi.org/10.1038/nrd3847

Boudeau, J., Miranda-Saavedra, D., Barton, G. J., & Alessi, D. R. (2006). Emerging roles of pseudokinases. *Trends in Cell Biology*, *16*(9), 443–452. https://doi.org/10.1016/j.tcb.2006.07.003

Boulton, T. G., Nye, S. H., Robbins, D. J., Ip, N. Y., Radzlejewska, E., Morgenbesser, S. D., DePinho, R. A., Panayotatos, N., Cobb, M. H., & Yancopoulos, G. D. (1991). ERKs: A family of protein-serine/threonine kinases that are activated and tyrosine phosphorylated in response to insulin and NGF. *Cell*, *65*(4), 663–675. https://doi.org/10.1016/0092-8674(91)90098-J

Boulton, T. G., Yancopoulos, G. D., Gregory, J. S., Slaughter, C., Moomaw, C., Hsu, J., & Cobb, M. H. (1990). An insulin-stimulated protein kinase similar to yeast kinases involved in cell cycle control. *Science*, *249*(4964), 64–67. https://doi.org/10.1126/science.2164259

Bredin, C. G., Liu, Z., Hauzenberger, D., & Klominek, J. (1999). Growth-factor-dependent migration of human lung-cancer cells. *International Journal of Cancer*, *82*(3), 338–345. https://doi.org/10.1002/(sici)1097-0215(19990730)82:3<338::aid-ijc6>3.0.co;2-y

Brennan, D. F., Dar, A. C., Hertz, N. T., Chao, W. C. H., Burlingame, A. L., Shokat, K. M., & Barford, D. (2011). A Raf-induced allosteric transition of KSR stimulates phosphorylation of MEK. *Nature*, *472*(7343), 366–369. https://doi.org/10.1038/nature09860

Brennan, J. A., Volle, D. J., Chaika, O. V., & Lewis, R. E. (2002). Phosphorylation regulates

the nucleocytoplasmic distribution of kinase suppressor of Ras. *Journal of Biological Chemistry*, *277*(7), 5369–5377. https://doi.org/10.1074/jbc.M109875200

Brown, M. D., & Sacks, D. B. (2006). IQGAP1 in cellular signaling : bridging the GAP. *Trends in Cell Biology*, *16*(5), 5–7. https://doi.org/10.1016/j.tcb.2006.03.002

Cacace, A. M., Michaud, N. R., Therrien, M., Mathes, K., Copeland, T., Rubin, G. M., & Morrison, D. K. (1999). Identification of Constitutive and Ras-Inducible Phosphorylation Sites of KSR: Implications for 14-3-3 Binding, Mitogen-Activated Protein Kinase Binding, and KSR Overexpression. *Molecular and Cellular Biology*, *19*(1), 229–240. https://doi.org/10.1128/mcb.19.1.229

Cargnello, M., & Roux, P. P. (2011). Activation and Function of the MAPKs and Their Substrates, the MAPK-Activated Protein Kinases. *Microbiology and Molecular Biology Reviews*, *75*(1), 50–83. https://doi.org/10.1128/mmbr.00031-10

Casar, B., Arozarena, I., Sanz-Moreno, V., Pinto, A., Agudo-Ibanez, L., Marais, R., Lewis, R. E., Berciano, M. T., & Crespo, P. (2009). Ras Subcellular Localization Defines Extracellular Signal-Regulated Kinase 1 and 2 Substrate Specificity through Distinct Utilization of Scaffold Proteins. *Molecular and Cellular Biology*. https://doi.org/10.1128/MCB.01359-08

Casar, Berta, & Crespo, P. (2016). ERK Signals: Scaffolding Scaffolds? *Frontiers in Cell and Developmental Biology*. https://doi.org/10.3389/fcell.2016.00049

Casar, Berta, Pinto, A., & Crespo, P. (2008). Essential Role of ERK Dimers in the Activation of Cytoplasmic but Not Nuclear Substrates by ERK-Scaffold Complexes. *Molecular Cell*. https://doi.org/10.1016/j.molcel.2008.07.024

Casar, Berta, Pinto, A., & Crespo, P. (2009). ERK dimers and scaffold proteins: Unexpected partners for a forgotten (cytoplasmic) task. In *Cell Cycle*. https://doi.org/10.4161/cc.8.7.8078

Celià-Terrassa, T., Bastian, C., Liu, D., Ell, B., Aiello, N. M., Wei, Y., Zamalloa, J., Blanco, A.

M., Hang, X., Kunisky, D., Li, W., Williams, E. D., Rabitz, H., & Kang, Y. (2018). Hysteresis control of epithelial-mesenchymal transition dynamics conveys a distinct program with enhanced metastatic ability. *Nature Communications*, *9*(1). https://doi.org/10.1038/s41467-018-07538-7

Channavajhala, P. L., Wu, L., Cuozzo, J. W., Hall, J. P., Liu, W., Lin, L. L., & Zhang, Y. (2003). Identification of a Novel Human Kinase Supporter of Ras (hKSR-2) That Functions as a Negative Regulator of Cot (Tp12) Signaling. *Journal of Biological Chemistry*, *278*(47), 47089–47097. https://doi.org/10.1074/jbc.M306002200

Charalambous, M., Smith, F. M., Bennett, W. R., Crew, T. E., Mackenzie, F., & Ward, A. (2003). Disruption of the imprinted Grb10 gene leads to disproportionate overgrowth by an Igf2-independent mechanism. *Proceedings of the National Academy of Sciences of the United States of America*, *100*(14), 8292–8297. https://doi.org/10.1073/pnas.1532175100

Clapéron, A., & Therrien, M. (2007). KSR and CNK: Two scaffolds regulating RAS-mediated RAF activation. *Oncogene*, *26*(22), 3143–3158. https://doi.org/10.1038/sj.onc.1210408

Costa, E. C., Moreira, A. F., de Melo-Diogo, D., Gaspar, V. M., Carvalho, M. P., & Correia, I. J. (2016). 3D tumor spheroids: an overview on the tools and techniques used for their analysis. *Biotechnology Advances*, *34*(8), 1427–1441. https://doi.org/10.1016/j.biotechadv.2016.11.002

Cox, A. D., & Der, C. J. (2010). Ras history: The saga continues. *Small GTPases*, *1*(1), 2–27. https://doi.org/10.4161/sgtp.1.1.12178

Cox, A. D., Fesik, S. W., Kimmelman, A. C., Luo, J., & Der, C. J. (2014). Drugging the undruggable RAs: mission possible? *Nat Rev Drug Discov*, *13*(11), 828–851. https://doi.org/10.1038/nrd4389.Drugging

Cox, J., & Mann, M. (2008). MaxQuant enables high peptide identification rates, individualized p.p.b.-range mass accuracies and proteome-wide protein

quantification. *Nature Biotechnology*, *26*(12), 1367–1372. https://doi.org/10.1038/nbt.1511

Crespo, P., & Casar, B. (2016). The Chick Embryo Chorioallantoic Membrane as an in vivo Model to Study Metastasis. *BIO-PROTOCOL*, *6*(20). https://doi.org/10.21769/BioProtoc.1962

Crews, C. M., Alessandrini, A., & Erikson, R. L. (1990). *The Primary Structure of MEK , a Protein Kinase That Phosphorylates the ERK Gene Product*. *1*(10).

Cuadrado, A., & Nebreda, A. R. (2010). Mechanisms and functions of p38 MAPK signalling. *Biochemical Journal*, *429*(3), 403–417. https://doi.org/10.1042/BJ20100323

Deakin, N. O., Pignatelli, J., & Turner, C. E. (2012). Diverse Roles for the Paxillin Family of Proteins in Cancer. *Genes and Cancer*, *3*, 362–370. https://doi.org/10.1177/1947601912458582

DeFea, K. A., Zalevsky, J., Thoma, M. S., Dery, O., Mullins, R. D., & Bunnett, N. W. (2000). β-Arrestin-dependent endocytosis of proteinase-activated receptor 2 is required for intracellular targeting of activated ERK1/2. *Journal of Cell Biology*, *148*(6), 1267–1281. https://doi.org/10.1083/jcb.148.6.1267

Deng, Y., Zhang, M., & Riedel, H. (2008). Mitogenic roles of Gab1 and Grb10 as direct cellular partners in the regulation of MAP kinase signaling. *Journal of Cellular Biochemistry*, *105*(5), 1172–1182. https://doi.org/10.1002/jcb.21829

Dewire, S. M., Ahn, S., Lefkowitz, R. J., & Shenoy, S. K. (2007). β -Arrestins and Cell Signaling. *Annu. Rev. Physiol.*, *69*, 483–510. https://doi.org/10.1146/annurev.physiol.69.022405.154749

Dhillon, A. S., Meikle, S., Yazici, Z., Eulitz, M., & Kolch, W. (2002). Regulation of Raf-1 activation and signalling by dephosphorylation. *EMBO Journal*, *21*(1–2), 64–71. https://doi.org/10.1093/emboj/21.1.64

Dohlman, H. G., & Campbell, S. L. (2019). Regulation of large and small G proteins by

ubiquitination. *Journal of Biological Chemistry*, *294*(49), 18613–18623. https://doi.org/10.1074/jbc.REV119.011068

Dongre, A., & Weinberg, R. A. (2019). New insights into the mechanisms of epithelial–mesenchymal transition and implications for cancer. *Nature Reviews Molecular Cell Biology*, *20*(2), 69–84. https://doi.org/10.1038/s41580-018-0080-4

Driedger, P. E., & Blumberg, P. M. (1980). Specific binding of phorbol ester tumor promoters to mouse skin. *Proc. Natl. Acad. Sci. USA*, *77*(1), 567–571. https://doi.org/10.1016/0092-8674(80)90093-8

Du, Z., & Lovly, C. M. (2018). *Mechanisms of receptor tyrosine kinase activation in cancer*. 1–13.

Dudley, D. T., Pang, L., Decker, S. J., Bridges, A. J., & Saltiel, A. R. (1995). A synthetic inhibitor of the mitogen-activated protein kinase cascade. *Proceedings of the National Academy of Sciences of the United States of America*, *92*(17), 7686–7689. https://doi.org/10.1073/pnas.92.17.7686

Eyers, P. A., & Murphy, J. M. (2013). Exploring Kinomes: Pseudokinases and beyond: Dawn of the dead: Protein pseudokinases signal new adventures in cell biology. *Biochemical Society Transactions*, *41*(4), 969–974. https://doi.org/10.1042/BST20130115

Fernández-Medarde, A., & Santos, E. (2011). Ras in cancer and developmental diseases. *Genes and Cancer*, *2*(3), 344–358. https://doi.org/10.1177/1947601911411084

Fife, C. M., McCarroll, J. A., & Kavallaris, M. (2014). Movers and shakers: Cell cytoskeleton in cancer metastasis. In *British Journal of Pharmacology*. https://doi.org/10.1111/bph.12704

Frémin, C., & Meloche, S. (2010). From basic research to clinical development of MEK1/2 inhibitors for cancer therapy. *Journal of Hematology and Oncology*, *3*, 1–11. https://doi.org/10.1186/1756-8722-3-8

Fürthauer, M., Lin, W., Ang, S., Thisse, B., & Thisse, C. (2002). *Sef is a feedback-induced antagonist of Ras / MAPK-mediated FGF signalling*. *4*(February). https://doi.org/10.1038/ncb750

Gangopadhyay, S. S., Kengni, E., Appel, S., Gallant, C., Kim, H. R., Leavis, P., DeGnore, J., & Morgan, K. G. (2009). Smooth muscle archvillin is an ERK scaffolding protein. *The Journal of Biological Chemistry*, *284*(26), 17607–17615. https://doi.org/10.1074/jbc.M109.002386

Germann, U. A., Furey, B. F., Markland, W., Hoover, R. R., Aronov, A. M., Roix, J. J., Hale, M., Boucher, D. M., Sorrell, D. A., Martinez-Botella, G., Fitzgibbon, M., Shapiro, P., Wick, M. J., Samadani, R., Meshaw, K., Groover, A., DeCrescenzo, G., Namchuk, M., Emery, C. M., … Welsch, D. J. (2017). Targeting the MAPK signaling pathway in cancer: Promising preclinical activity with the novel selective ERK1/2 inhibitor BVD-523 (ulixertinib). *Molecular Cancer Therapeutics*, *16*(11), 2351–2363. https://doi.org/10.1158/1535-7163.MCT-17-0456

Giblett, S. M., Lloyd, D. J., Light, Y., Marais, R., & Pritchard, C. A. (2002). Expression of kinase suppressor of Ras in the normal adult and embryonic mouse. *Cell Growth and Differentiation*, *13*(7), 307–313.

Glenney, J. R., & Zokas, L. (1989). *Novel Tyrosine Kinase Substrates from Rous Sarcoma Virus- transformed Cells Are Present in the Membrane Skeleton*. *108*(June), 2401–2408.

Goettel, J. A., Liangb, D., Hilliarda, V. C., Edelbluma, K. L., R., M. B., Hanksa, S. K., & Polka, D. B. (2011). KSR1 is a functional protein kinase capable of serine autophosphorylation and direct phosphorylation of MEK1. *Exp Cell Res.*, *317*(4), 452–463. https://doi.org/10.1016/j.yexcr.2010.11.018

Gorelik, R., & Gautreau, A. (2014). Quantitative and unbiased analysis of directional persistence in cell migration. *Nature Protocols*, *9*(8), 1931–1943. https://doi.org/10.1038/nprot.2014.131

Guo, Y., Pan, W., Liu, S., Shen, Z., Xu, Y., & Hu, L. (2020). ERK/MAPK signalling pathway and tumorigenesis (Review). *Experimental and Therapeutic Medicine*, 1997–2007. https://doi.org/10.3892/etm.2020.8454

Hansen, L. A., Alexander, N., Hogan, M. E., Sundberg, J. P., Dlugosz, A., Threadgill, D. W., Magnuson, T., & Yuspa, S. H. (1997). Genetically null mice reveal a central role for epidermal growth factor receptor in the differentiation of the hair follicle and normal hair development. *American Journal of Pathology*, *150*(6), 1959–1975.

Hao, Y., Baker, D., & Dijke, P. Ten. (2019). TGF-β-mediated epithelial-mesenchymal transition and cancer metastasis. *International Journal of Molecular Sciences*, *20*(11). https://doi.org/10.3390/ijms20112767

Henry, M. D., Costanzo-Garvey, D. L., Klutho, P. J., & Lewis, R. E. (2014). Obesity-dependent dysregulation of glucose homeostasis in kinase suppressor of ras 2-/- mice. *Physiological Reports*, *2*(7), 1–12. https://doi.org/10.14814/phy2.12053

Herrero, A., Pinto, A., Colón-Bolea, P., Casar, B., Jones, M., Agudo-Ibáñez, L., Vidal, R., Tenbaum, S. P., Nuciforo, P., Valdizán, E. M., Horvath, Z., Orfi, L., Pineda-Lucena, A., Bony, E., Keri, G., Rivas, G., Pazos, A., Gozalbes, R., Palmer, H. G., … Crespo, P. (2015). Small Molecule Inhibition of ERK Dimerization Prevents Tumorigenesis by RAS-ERK Pathway Oncogenes. *Cancer Cell*. https://doi.org/10.1016/j.ccell.2015.07.001

Hong, D. S., Fakih, M. G., Strickler, J. H., Desai, J., Durm, G. A., Shapiro, G. I., Falchook, G. S., Price, T. J., Sacher, A., Denlinger, C. S., Bang, Y.-J., Dy, G. K., Krauss, J. C., Kuboki, Y., Kuo, J. C., Coveler, A. L., Park, K., Kim, T. W., Barlesi, F., … Li, B. T. (2020). KRAS G12C Inhibition with Sotorasib in Advanced Solid Tumors . *New England Journal of Medicine*, *383*(13), 1207–1217. https://doi.org/10.1056/nejmoa1917239

Horwitz, A. R., & Parsons, J. T. (1999). Cell migration - Movin' on. *Science*, *286*(5442), 1102–1103. https://doi.org/10.1126/science.286.5442.1102

Hu, J., Yu, H., Kornev, A. P., Zhao, J., Filbert, E. L., Taylor, S. S., & Shaw, A. S. (2011). Mutation that blocks ATP binding creates a pseudokinase stabilizing the scaffolding

function of kinase suppressor of Ras, CRAF and BRAF. *Proceedings of the National Academy of Sciences of the United States of America*, *108*(15), 6067–6072. https://doi.org/10.1073/pnas.1102554108

Imai, K., & Takaoka, A. (2006). Comparing antibody and small-molecule therapies for cancer. *Nature Reviews Cancer*, *6*(9), 714–727. https://doi.org/10.1038/nrc1913

Ishibe, S., Joly, D., Liu, Z., Cantley, L. G., & Haven, N. (2004). Paxillin Serves as an ERK-Regulated Scaffold for Coordinating FAK and Rac Activation in Epithelial Morphogenesis. *Molecular Cell*, *16*, 257–267. https://doi.org/10.1016/j.molcel.2004.10.006

Jadeski, L., Mataraza, J. M., Jeong, H., Li, Z., & Sacks, D. B. (2008). IQGAP1 Stimulates Proliferation and Enhances Tumorigenesis of Human Breast Epithelial Cells *. *The Journal of Biological Chemistry*, *283*(2), 1008–1017. https://doi.org/10.1074/jbc.M708466200

Jameson, K. L., Mazur, P. K., Zehnder, A. M., Zhang, J., Zarnegar, B., Sage, J., & Khavari, P. A. (2013). IQGAP1 scaffold-kinase interaction blockade selectively targets RAS-MAP kinase–driven tumors. *Nat Med*, *19*(5), 626–630. https://doi.org/10.1038/nm.3165.IQGAP1

Khojasteh Poor, F., Keivan, M., Ramazii, M., Ghaedrahmati, F., Anbiyaiee, A., Panahandeh, S., Khoshnam, S. E., & Farzaneh, M. (2021). Mini review: The FDA-approved prescription drugs that target the MAPK signaling pathway in women with breast cancer. *Breast Disease*, *40*, 51–62. https://doi.org/10.3233/BD-201063

Khokhlatchev, A. V, Canagarajah, B., Wilsbacher, J., Robinson, M., Atkinson, M., Goldsmith, E., & Cobb, M. H. (1998). Phosphorylation of the MAP Kinase ERK2 Promotes Its Homodimerization and Nuclear Translocation complex. In *Cell* (Vol. 93). Treisman. https://ac.els-cdn.com/S0092867400811897/1-s2.0-S0092867400811897-main.pdf?_tid=465e4db3-16fd-4797-8b87-3291df7ca260&acdnat=1537869674_bb000de12db9acf77f29531712f4f05b

Kim, S., Choi, J. H., Lim, H. I., Lee, S.-K., Kim, W. W., Cho, S., Kim, J. S., Kim, J.-H., Choe, J.-H., Nam, S. J., Lee, J. E., & Yang, J.-H. (2009). EGF-induced MMP-9 expression is mediated by the JAK3/ERK pathway, but not by the JAK3/STAT-3 pathway in a SKBR3 breast cancer cell line. *Cellular Signalling*, *21*(6), 892–898. https://doi.org/10.1016/j.cellsig.2009.01.034

Kohno, M., & Pouyssegur, J. (1986). *a-Thrombin-induced tyrosine phosphorylation of 43000- and 41 000AMr proteins is independent of cytoplasmic alkalimization in quiescent fibroblasts*. *238*.

Kolch, W., Calder, M., & Gilbert, D. (2005). When kinases meet mathematics : the systems biology of MAPK signalling. *FEBS Letters*, *579*, 1891–1895. https://doi.org/10.1016/j.febslet.2005.02.002

Kornfeld, K., Hom, D. B., & Horvitz, H. R. (1995). The ksr-1 gene encodes a novel protein kinase involved in Ras-mediated signaling in C. elegans. *Cell*, *83*(6), 903–913. https://doi.org/10.1016/0092-8674(95)90206-6

Kumar, D., Patel, S. A., Hassan, M. K., Mohapatra, N., Pattanaik, N., & Dixit, M. (2021). Reduced IQGAP2 expression promotes EMT and inhibits apoptosis by modulating the MEK-ERK and p38 signaling in breast cancer irrespective of ER status. *Cell Death and Disease*, *12*(4). https://doi.org/10.1038/s41419-021-03673-0

Kunimoto, K., Nojima, H., Yamazaki, Y., Yoshikawa, T., Okanoue, T., & Tsukita, S. (2009). Involvement of IQGAP3, a regulator of Ras/ERK-related cascade, in hepatocyte proliferation in mouse liver regeneration and development. *Journal of Cellular Physiology*, *220*(3), 621–631. https://doi.org/10.1002/jcp.21798

Lamouille, S., Xu, J., & Derynck, R. (2014). Molecular mechanisms of epithelial–mesenchymal transition Samy. *Nature Reviews Molecular Cell Biology*, *15*(3), 178–196. https://doi.org/10.1038/nrm3758

Langlais, P., Dong, L. Q., Ramos, F. J., Hu, D., Li, Y., Quon, M. J., & Liu, F. (2004). Negative regulation of insulin-stimulated mitogen-activated protein kinase signaling by

Grb10. *Molecular Endocrinology (Baltimore, Md.)*, *18*(2), 350–358. https://doi.org/10.1210/me.2003-0117

Lavoie, H., & Therrien, M. (2015). Regulation of RAF protein kinases in ERK signalling. *Nature Reviews Molecular Cell Biology*, *16*(5), 281–298. https://doi.org/10.1038/nrm3979

Leicht, D. T., Balan, V., Kaplun, A., Singh-Gupta, V., Kaplun, L., Dobson, M., & Tzivion, G. (2007). Raf kinases: Function, regulation and role in human cancer. *Biochimica et Biophysica Acta - Molecular Cell Research*, *1773*(8), 1196–1212. https://doi.org/10.1016/j.bbamcr.2007.05.001

Levchenko, A., Bruck, J., & Sternberg, P. W. (2000). Scaffold proteins may biphasically affect the levels of mitogen-activated protein kinase signaling and reduce its threshold properties. *PNAS*, *97*, 5818–5823.

Levin-Salomon, V., Kogan, K., Ahn, N. G., Livnah, O., & Engelberg, D. (2008). Isolation of intrinsically active (MEK-independent) variants of the ERK family of mitogen-activated protein (MAP) kinases. *The Journal of Biological Chemistry*, *283*(50), 34500–34510. https://doi.org/10.1074/jbc.M806443200

Li, C., Scott, D. A., Hatch, E., Tian, X., & Mansour, S. L. (2007). Dusp6(Mkp3) is a negative feedback regulator of FGF stimulated ERK signaling during mouse development. Developtment, 134(1), 1667–196. https://doi.org/10.1242/dev.02701

Li, J., Guo, Y., Duan, L., Hu, X., Zhang, X., Hu, J., Huang, L., He, R., Hu, Z., Luo, W., Tan, T., Huang, R., Liao, D., Zhu, Y.-S., & Luo, D.-X. (2017). AKR1B10 promotes breast cancer cell migration and invasion via activation of ERK signaling. *Oncotarget*, *8*(20). https://doi.org/10.18632/oncotarget.16624

Liao, G., Wang, M., Ou, Y., & Zhao, Y. (2014). IGF-1-induced epithelial-mesenchymal transition in MCF-7 cells is mediated by MUC1. *Cellular Signalling*, *26*(10), 2131–2137. https://doi.org/10.1016/j.cellsig.2014.06.004

Locasale, J. W., Shaw, A. S., & Chakraborty, A. K. (2007). Scaffold proteins confer diverse regulatory properties to protein kinase cascades. *Proc Natl Acad Sci U S A.*, *104*(33), 13307–13312. https://doi.org/10.1073/pnas.0706311104

Lozano, J., Xing, R., Cai, Z., Jensen, H. L., Trempus, C., Mark, W., Cannon, R., & Kolesnick, R. (2003). Deficiency of kinase suppressor of Ras1 prevents oncogenic Ras signaling in mice. *Cancer Research*, *63*(14), 4232–4238.

Luttrell, L. M., & Lefkowitz, R. J. (2002). The role of beta-arrestins in the termination and transduction of G-protein-coupled receptor signals. *Journal of Cell Science*, *115*(Pt 3), 455–465.

Mace, P. D., Wallez, Y., Egger, M. F., Dobaczewska, M. K., Robinson, H., Pasquale, E. B., & Riedl, S. J. (2013). Structure of ERK2 bound to PEA-15 reveals a mechanism for rapid release of activated MAPK. *Nat Commun.*, *4*, 1681. https://doi.org/10.1038/ncomms2687.Structure

Mackinnon, A. C., Tretiakova, M., Henderson, L., Mehta, R. G., Yan, B. C., Joseph, L., Krausz, T., Husain, A. N., Reid, M. E., & Salgia, R. (2011). Paxillin expression and amplification in early lung lesions of high-risk patients , lung adenocarcinoma and metastatic disease. *J Clin Pathol*, 16–24. https://doi.org/10.1136/jcp.2010.075853

Maillet, M., Purcell, N. H., Sargent, M. A., York, A. J., Bueno, O. F., & Molkentin, J. D. (2008). DUSP6 (MKP3) null mice show enhanced ERK1/2 phosphorylation at baseline and increased myocyte proliferation in the heart affecting disease susceptibility. *Journal of Biological Chemistry*, *283*(45), 31246–31255. https://doi.org/10.1074/jbc.M806085200

Manning, G., Whyte, D. B., Martinez, R., Hunter, T., & Sudarsanam, S. (2002). The protein kinase complement of the human genome. *Science*, *298*(5600), 1912–1934. https://doi.org/10.1126/science.1075762

Masi, I., Caprara, V., Bagnato, A., & Rosanò, L. (2020). Tumor Cellular and Microenvironmental Cues Controlling Invadopodia Formation. *Frontiers in Cell and*

Developmental Biology, *8*(October). https://doi.org/10.3389/fcell.2020.584181

Matheny, S. A., Chen, C., Kortum, R. L., Razidlo, G. L., Lewis, R. E., & White, M. A. (2004). Ras regulates assembly of mitogenic signalling complexes through the effector protein IMP. *Nature*, *427*(January). https://doi.org/10.1038/nature02240.1.

Matheny, S. A., & White, M. A. (2009). Signaling threshold regulation by the Ras effector IMP. *Journal of Biological Chemistry*, *284*(17), 11007–11011. https://doi.org/10.1074/jbc.R800082200

McKay, M. M., Ritt, D. A., & Morrison, D. K. (2009). Signaling dynamics of the KSR1 scaffold complex. *Proceedings of the National Academy of Sciences*, *106*(27), 11022–11027. https://doi.org/10.1073/pnas.0901590106

Michaud, N. R., Therrien, M., Cacace, A., Edsall, L. C., Spiegel, S., Rubin, G. M., & Morrison, D. K. (1997). KSR stimulates Raf-1 activity in a kinase-independent manner. *Proceedings of the National Academy of Sciences of the United States of America*, *94*(24), 12792–12796. https://doi.org/10.1073/pnas.94.24.12792

Moelling, K., Heimann, B., Beimling, P., Rapp, U. R., & Sander, T. (1984). Serine- and threonine-specific protein kinase activities of purified gag-mil and gag-raf proteins. *Nature*, *312*(5994), 558–561. https://doi.org/10.1038/312558a0

Mörchen, M., Zambrano, O., Alexander, P., Salgado, P., Penniecook, J., Lindau, A. B. Von, & Lewis, D. (2019). Disability-Disaggregated Data Collection : Hospital-Based Application of the Washington Group Questions in an Eye Hospital in Paraguay. *International Journal of Environmental Research and Public Health*.

Morel, A. P., Lièvre, M., Thomas, C., Hinkal, G., Ansieau, S., & Puisieux, A. (2008). Generation of breast cancer stem cells through epithelial-mesenchymal transition. *PLoS ONE*, *3*(8), 1–7. https://doi.org/10.1371/journal.pone.0002888

Morgillo, F., Maria, C., Corte, D., Fasano, M., Ciardiello, F., Magrassi, " F, & Lanzara, A. (2016). Mechanisms of resistance to EGFR-targeted drugs: lung cancer. *ESMO Open*,

1, 1–9. https://doi.org/10.1136/esmoopen-2016-000060

Morrison, D. K., & Davis, R. J. (2003). REGULATION OF MAP K INASE S IGNALING M ODULES BY S CAFFOLD P ROTEINS IN M AMMALS ∗. *Annual Review of Cell and Developmental Biology*, *19*, 91–118. https://doi.org/10.1146/annurev.cellbio.19.111401.091942

Müller, J., Ory, S., Copeland, T., Piwnica-Worms, H., & Morrison, D. K. (2001). C-TAK1 Regulates Ras Signaling by Phosphorylating the MAPK Scaffold, KSR1. *Molecular Cell*, *8*(5), 983–993. https://doi.org/10.1016/S1097-2765(01)00383-5

Murphy, L. O., Cluck, M. W., Lovas, S., Ötvös, F., Murphy, R. F., Schally, A. V., Permert, J., Larsson, J., Knezetic, J. A., & Adrian, T. E. (2001). Pancreatic cancer cells require an EGF receptor-mediated autocrine pathway for proliferation in serum-free conditions. *British Journal of Cancer*. https://doi.org/10.1054/bjoc.2001.1698

Nakielny, S., Cohen, P., Wu, J., & Sturgill, T. (1992). *MAP kinase activator from insulin-stimulated skeletal muscle is a protein threonine / tyrosine kinase*. *1*(6), 2123–2129.

Nassef, M. Z., Kopp, S., Wehland, M., Melnik, D., Sahana, J., Krüger, M., Corydon, T. J., Oltmann, H., Schmitz, B., Schütte, A., Bauer, T. J., Infanger, M., & Grimm, D. (2019). Real microgravity influences the cytoskeleton and focal adhesions in human breast cancer cells. *International Journal of Molecular Sciences*, *20*(13), 1–25. https://doi.org/10.3390/ijms20133156

Nguyen, A., Burack, W. R., Stock, J. L., Kortum, R., Chaika, O. V., Afkarian, M., Muller, W. J., Murphy, K. M., Morrison, D. K., Lewis, R. E., McNeish, J., & Shaw, A. S. (2002). Kinase Suppressor of Ras (KSR) Is a Scaffold Which Facilitates Mitogen-Activated Protein Kinase Activation In Vivo. *Molecular and Cellular Biology*, *22*(9), 3035–3045. https://doi.org/10.1128/mcb.22.9.3035-3045.2002

Nguyen, T., Wang, J., & Schulz, R. A. (2002). Mutations within the conserved MADS box of the D-MEF2 muscle differentiation factor result in a loss of DNA binding ability and lethality in Drosophila. *Differentiation*, *70*(8), 438–446. https://doi.org/10.1046/j.1432-0436.2002.700806.x

Nojima, H., Adachi, M., Matsui, T., Okawa, K., Tsukita, S., & Tsukita, S. (2008). IQGAP3 regulates cell proliferation through the Ras/ERK signalling cascade. *Nature Cell Biology*, *10*(8), 971–978. https://doi.org/10.1038/ncb1757

Nussinov, R., Tsai, C., & Jang, H. (2019). *Does Ras Activate Raf and PI3K Allosterically ? 9*, 1–10. https://doi.org/10.3389/fonc.2019.01231

Obenauf, A. C., & Massagué, J. (2015). Surviving at a Distance: Organ-Specific Metastasis. *Trends in Cancer*, *1*(1), 76–91. https://doi.org/10.1016/j.trecan.2015.07.009

Ohori, M., Kinoshita, T., Okubo, M., Sato, K., Yamazaki, A., Arakawa, H., Nishimura, S., Inamura, N., Nakajima, H., Neya, M., Miyake, H., & Fujii, T. (2005). Identification of a selective ERK inhibitor and structural determination of the inhibitor-ERK2 complex. *Biochemical and Biophysical Research Communications*, *336*(1), 357–363. https://doi.org/10.1016/j.bbrc.2005.08.082

Olson, H. M., & Nechiporuk, A. V. (2021). Lamellipodia-like protrusions and focal adhesions contribute to collective cell migration in zebrafish. *Developmental Biology*, *469*, 125–134. https://doi.org/10.1016/j.ydbio.2020.10.007

Orgaz, J. L., Crosas-Molist, E., Sadok, A., Perdrix-Rosell, A., Maiques, O., Rodriguez-Hernandez, I., Monger, J., Mele, S., Georgouli, M., Bridgeman, V., Karagiannis, P., Lee, R., Pandya, P., Boehme, L., Wallberg, F., Tape, C., Karagiannis, S. N., Malanchi, I., & Sanz-Moreno, V. (2020). Myosin II Reactivation and Cytoskeletal Remodeling as a Hallmark and a Vulnerability in Melanoma Therapy Resistance. *Cancer Cell*, *37*(1), 85-103.e9. https://doi.org/10.1016/j.ccell.2019.12.003

Ostrem, J. M. L., & Shokat, K. M. (2016). Direct small-molecule inhibitors of KRAS: From structural insights to mechanism-based design. *Nature Reviews Drug Discovery*, *15*(11), 771–785. https://doi.org/10.1038/nrd.2016.139

Pandya, P., Orgaz, J. L., & Sanz-moreno, V. (2017). *Modes of invasion during tumour dissemination*. *11*, 5–27. https://doi.org/10.1002/1878-0261.12019

Pandya, P., Orgaz, J. L., & Sanz-Moreno, V. (2017). Actomyosin contractility and collective migration: may the force be with you. *Current Opinion in Cell Biology*, *48*, 87–96. https://doi.org/10.1016/j.ceb.2017.06.006

Park, Sarah, Jung, H. H., Park, Y. H., Ahn, J. S., & Im, Y. H. (2011). ERK/MAPK pathways play critical roles in EGFR ligands-induced MMP1 expression. *Biochemical and Biophysical Research Communications*, *407*(4), 680–686. https://doi.org/10.1016/j.bbrc.2011.03.075

Park, Sungdae, Yeung, M. L., Beach, S., Shields, J. M., & Yeung, K. C. (2005). RKIP downregulates B-Raf kinase activity in melanoma cancer cells. *Oncogene*, *24*(21), 3535–3540. https://doi.org/10.1038/sj.onc.1208435

Pasquier, J., Abu-Kaoud, N., Al Thani, H., & Rafii, A. (2015). Epithelial to Mesenchymal Transition in a Clinical Perspective. *Journal of Oncology*, *2015*, 19–21. https://doi.org/10.1155/2015/792182

Pearce, L. R., Atanassova, N., Banton, M. C., Bottomley, B., Van Der Klaauw, A. A., Revelli, J. P., Hendricks, A., Keogh, J. M., Henning, E., Doree, D., Jeter-Jones, S., Garg, S., Bochukova, E. G., Bounds, R., Ashford, S., Gayton, E., Hindmarsh, P. C., Shield, J. P. H., Crowne, E., … Farooqi, I. S. (2013). XKSR2 mutations are associated with obesity, insulin resistance, and impaired cellular fuel oxidation. *Cell*, *155*(4), 765. https://doi.org/10.1016/j.cell.2013.09.058

Pearson, G., Robinson, F., Gibson, T. B., Xu, B. E., Karandikar, M., Berman, K., & Cobb, M. H. (2001). Mitogen-activated protein (MAP) kinase pathways: Regulation and physiological functions. *Endocrine Reviews*, *22*(2), 153–183. https://doi.org/10.1210/er.22.2.153

Petrie, R. J., Doyle, A. D., & Yamada, K. M. (2009). Random versus directionally persistent cell migration. *Nat Rev Mol Cell Biol*, *10*(8), 538–549. https://doi.org/10.1038/nrm2729.Random

Philipova, R., & Whitaker, M. (2005). Active ERK1 is dimerized in vivo: bisphosphodimers

generate peak kinase activity and monophosphodimers maintain basal ERK1 activity. *Journal of Cell Science*, *118*(Pt 24), 5767–5776. https://doi.org/10.1242/jcs.02683

Philips MR. (2004). Sef : A MEK / ERK Catcher. *Molecular Cell*, *15*(2), 168–169. https://doi.org/10.1016/j.molcel.2004.07.003

Pijuan, J., Barceló, C., Moreno, D. F., Maiques, O., Sisó, P., Marti, R. M., Macià, A., & Panosa, A. (2019). In vitro cell migration, invasion, and adhesion assays: From cell imaging to data analysis. *Frontiers in Cell and Developmental Biology*, *7*(JUN), 1–16. https://doi.org/10.3389/fcell.2019.00107

Pinto, A., & Crespo, P. (2010). *Analysis of ERKs' Dimerization by Electrophoresis* (pp. 335–342). Humana Press, Totowa, NJ. https://doi.org/10.1007/978-1-60761-795-2_20

Prior A., I., & Hancock, J. F. (2012). Ras trafficking, localization and compartmentalized signalling Ian. *Semin Cell Dev Biol*, *32*(2), 145–153. https://doi.org/10.1016/j.semcdb.2011.09.002

Pullikuth, A., Mckinnon, E., Schaeffer, H., & Catling, A. D. (2005). The MEK1 Scaffolding Protein MP1 Regulates Cell Spreading by Integrating PAK1 and Rho Signals. *Molecular and Cellular Biology*, *25*(12), 5119–5133. https://doi.org/10.1128/MCB.25.12.5119

Putz, T., Culig, Z., Eder, I. E., Nessler-Menardi, C., Bartsch, G., Grunicke, H., Überall, F., & Klocker, H. (1999). Epidermal growth factor (EGF) receptor blockade inhibits the action of EGF, insulin-like growth factor I, and a protein kinase a activator on the mitogen-activated protein kinase pathway in prostate cancer cell lines. *Cancer Research*, *59*(1), 227–233.

Rajakulendran, T., Sahmi, M., Lefrançois, M., Sicheri, F., & Therrien, M. (2009). A dimerization-dependent mechanism drives RAF catalytic activation. *Nature*, *461*(7263), 542–545. https://doi.org/10.1038/nature08314

Raman, M., Chen, W., & Cobb, M. H. (2007a). Differential regulation and properties of

MAPKs. *Oncogene*, *26*(22), 3100–3112. https://doi.org/10.1038/sj.onc.1210392

Rapp, U. R., Goldsborough, M. D., Mark, G. E., Bonner, T. I., Groffen, J., Reynolds, F. H., & Stephenson, J. R. (1983). Structure and biological activity of v-raf, a unique oncogene transduced by a retrovirus. *Proceedings of the National Academy of Sciences of the United States of America*, *80*(14 I), 4218–4222. https://doi.org/10.1073/pnas.80.14.4218

Revelli, J. P., Smith, D., Allen, J., Jeter-Jones, S., Shadoan, M. K., Desai, U., Schneider, M., Van Sligtenhorst, I., Kirkpatrick, L., Platt, K. A., Suwanichkul, A., Savelieva, K., Gerhardt, B., Mitchell, J., Syrewicz, J., Zambrowicz, B., Hamman, B. D., Vogel, P., & Powell, D. R. (2011). Profound obesity secondary to hyperphagia in mice lacking kinase suppressor of ras 2. *Obesity*, *19*(5), 1010–1018. https://doi.org/10.1038/oby.2010.282

Rheault, T. R., Stellwagen, J. C., Adjabeng, G. M., Hornberger, K. R., Petrov, K. G., Waterson, A. G., Dickerson, S. H., Mook, R. A., Laquerre, S. G., King, A. J., Rossanese, O. W., Arnone, M. R., Smitheman, K. N., Kane-carson, L. S., Han, C., Moorthy, G. S., Moss, K. G., & Uehling, D. E. (2013). Discovery of Dabrafenib: A Selective Inhibitor of Raf Kinases with Antitumor Activity against B - Raf-Driven Tumors. *ACS Medical Chemistry Letters*, *4*, 358–362. https://doi.org/10.1021/ml4000063

Ritterhoff, S., Farah, C. M., Grabitzki, J., Lochnit, G., Skurat, A. V, & Schmitz, M. L. (2010). The WD40-repeat protein Han11 functions as a scaffold protein to control HIPK2 and MEKK1 kinase functions. *The EMBO Journal*, *29*(22), 3750–3761. https://doi.org/10.1038/emboj.2010.251

Roskoski R. (2012). ERK1 / 2 MAP kinases : Structure , function , and regulation. *Pharmacological Research*, *66*(2), 105–143. https://doi.org/10.1016/j.phrs.2012.04.005

Rotblat, B., Ehrlich, M., Haklai, R., & Kloog, Y. (2008). The Ras Inhibitor Farnesylthiosalicylic Acid (Salirasib) Disrupts The Spatiotemporal Localization Of Active Ras: A Potential

Treatment For Cancer. *Methods in Enzymology*, *439*(07), 467–489. https://doi.org/10.1016/S0076-6879(07)00432-6

Roy, F., & Therrien, M. (2002). MAP Kinase Module : The Ksr Connection Ksr has been genetically defined as a component of. *Current Biology*, *12*(02), 325–327. https://doi.org/10.1016/s0960-9822(02)00831-x

Roy, M., Li, Z., & Sacks, D. B. (2005). IQGAP1 Is a Scaffold for Mitogen-Activated Protein Kinase Signaling. *Molecular and Cellular Biology*, *25*(18), 7940–7952. https://doi.org/10.1128/MCB.25.18.7940

Samatar, A. A., & Poulikakos, P. I. (2014). Targeting RAS-ERK signalling in cancer: Promises and challenges. *Nature Reviews Drug Discovery*, *13*(12), 928–942. https://doi.org/10.1038/nrd4281

Samson, S. C., Elliott, A., Mueller, B. D., Kim, X. Y., Carney, K. R., Bergman, J. P., Blenis, J., & Mendoza, X. M. C. (2019). p90 ribosomal S6 kinase (RSK) phosphorylates myosin phosphatase and thereby controls edge dynamics during cell. *JBC*, *294*, 10846–10862. https://doi.org/10.1074/jbc.RA119.007431

Santos, S. D. M., Verveer, P. J., & Bastiaens, P. I. H. (2007). *Growth factor-induced MAPK network topology shapes Erk response determining PC-12 cell fate*. *9*(3). https://doi.org/10.1038/ncb1543

Saw, T. B., Jain, S., Ladoux, B., & Lim, C. T. (2014). Mechanobiology of Collective Cell Migration. *Cellular and Molecular Bioengineering*, *8*(1), 3–13. https://doi.org/10.1007/s12195-014-0366-3

Schaeffer, H. J., Catling, A. D., Eblen, S. T., Collier, L. S., Weber, M. J., Schaeffer, H. J., Catling, A. D., & Eblen, S. T. (2016). *MP1 : A MEK Binding Partner That Enhances Enzymatic Activation of the MAP Kinase Cascade Published by : American Association for the Advancement of Science Stable URL : http://www.jstor.org/stable/2896379 Linked references are available on JSTOR for this* . *281*(5383), 1668–1671.

Schelch, K., Vogel, L., Schneller, A., Brankovic, J., Mohr, T., Mayer, R. L., Slany, A., Gerner, C., & Grusch, M. (2021). EGF Induces Migration Independent of EMT or Invasion in A549 Lung Adenocarcinoma Cells. *Frontiers in Cell and Developmental Biology*, *9*(March), 1–16. https://doi.org/10.3389/fcell.2021.634371

Seger, R., Ahnl, N. G., Posadall, J., Munarb, S., Jensens, A. M., Cooper, J. A., Cobb, M. H., & Krebssllss, G. (1992). *Purification and Characterization of Mitogen-activated Protein Kinase Activator (s) from Epidermal Growth Factor-stimulated*. *267*(20), 14373–14381.

Shenoy, S. K., & Lefkowitz, R. J. (2011). β-arrestin-mediated receptor trafficking and signal transduction. *Trends Pharmacol Sci.*, *32*(9), 521–533. https://doi.org/10.1016/j.tips.2011.05.002.

Singh, M., Yelle, N., Venugopal, C., & Singh, S. K. (2018). EMT: Mechanisms and therapeutic implications. *Pharmacology and Therapeutics*, *182*(August 2017), 80–94. https://doi.org/10.1016/j.pharmthera.2017.08.009

Sluss, H. K., Barrett, T., Dérijard, B., & Davis, R. J. (1994). Signal transduction by tumor necrosis factor mediated by JNK protein kinases. *Molecular and Cellular Biology*, *14*(12), 8376–8384. https://doi.org/10.1128/mcb.14.12.8376

Sobolesky, P. M., & Moussa, O. (2013). The role of β-arrestins in cancer. *Progress in Molecular Biology and Translational Science*, *118*, 395–411. https://doi.org/10.1016/B978-0-12-394440-5.00015-2

Stephen, A. G., Esposito, D., Bagni, R. K., & Mccormick, F. (2014). Dragging Ras Back in the Ring. *Cancer Cell*, *25*(3), 272–281. https://doi.org/10.1016/j.ccr.2014.02.017

Stewart, S., Sundaram, M., Zhang, Y., Lee, J., Han, M., & Guan, K.-L. (1999). Kinase Suppressor of Ras Forms a Multiprotein Signaling Complex and Modulates MEK Localization. *Molecular and Cellular Biology*, *19*(8), 5523–5534. https://doi.org/10.1128/mcb.19.8.5523

Subauste, M. C., Kupriyanova, T. A., Conn, E. M., Ardi, V. C., James, P., & Deryugina, E. I. (2009). Evaluation of metastatic and angiogenic potentials of human colon carcinoma cells in chick embryo model systems M. *Clin Exp Metastasis*, *26*(8), 1033–1047. https://doi.org/10.1007/s10585-009-9293-4.Evaluation

Sundaram, M., & Han, M. (1995). The C. elegans ksr-1 gene encodes a novel Raf-related kinase involved in Ras-mediated signal transduction. *Cell*, *83*(6), 889–901. https://doi.org/10.1016/0092-8674(95)90205-8

Sutrave, P., Bonner, T. I., U.R., R., H.W., J., T., P., & K., B. (1984). Nucleotide sequence of avian retroviral oncogen v-mil: homologue of murine retroviral oncogene v-raf. *Nature*, *3–9*(309(5963)), 85–88. https://doi.org/10.1038/309085a0

Strugill, T. W., Ray, L. B., Erikson, E., & Maller, J. L. (1988). Insulin-stimulated MAP-2 kinase phosphorylates and ativates ribosomal protein S6 kinase II. Nature, 334(25), 715. https://doi.org/10.1038/334715a0

Takekawa, M., Tatebayashi, K., & Saito, H. (2005). *for Activation of Mammalian MAP Kinase Kinases by Specific MAP Kinase Kinase Kinases*. *18*, 295–306. https://doi.org/10.1016/j.molcel.2005.04.001

Teis, D., Taub, N., Kurzbauer, R., Hilber, D., Araujo, M. E. De, Erlacher, M., Offterdinger, M., Villunger, A., Geley, S., Bohn, G., Klein, C., Hess, M. W., & Huber, L. A. (2006). p14–MP1-MEK1 signaling regulates endosomal traffi c and cellular proliferation during tissue homeostasis. *The Journal of Cell Biology*, *175*(6), 861–868. https://doi.org/10.1083/jcb.200607025

Teis, D., Wunderlich, W., & Huber, L. A. (2002). Localization of the MP1-MAPK Scaffold Complex to Endosomes Is Mediated by p14 and Required for Signal Transduction. *Developmental Cell*, *3*, 803–814. https://doi.org/10.1016/s1534-5807(02)00364-7

Therrien, M., Chang, H. C., Solomon, N. M., Karim, F. D., Wassarman, D. A., & Rubin, G. M. (1995). KSR, a novel protein kinase required for RAS signal transduction. *Cell*, *83*(6), 879–888. https://doi.org/10.1016/0092-8674(95)90204-X

Torii, S., Kusakabe, M., Yamamoto, T., Maekawa, M., & Nishida, E. (2004). Sef Is a Spatial Regulator for Ras / MAP Kinase Signaling. *Developmental Cell*, *7*, 33–44. https://doi.org/10.1016/j.devcel.2004.05.019

Tsang, M., Friesel, R., Kudoh, T., & Dawid, I. B. (2003). *Identification of Sef , a novel modulator of FGF signalling*. *4*(February 2002), 165–170. https://doi.org/10.1038/ncb749

Turner, C. E., Glenney, J. R., & Burridge, K. (1990). Paxillin : A New Vinculin-binding Protein Present in Focal Adhesions. *J Cell Biol*, *111*(3), 1059–1068.

Turriziani, B., Garcia-Munoz, A., Pilkington, R., Raso, C., Kolch, W., & Von Kriegsheim, A. (2014). On-Beads Digestion in Conjunction with Data-Dependent Mass Spectrometry: A Shortcut to Quantitative and Dynamic Interaction Proteomics. *Biology*, *3*, 320–332. https://doi.org/10.3390/biology3020320

Ünal, E. B., Uhlitz, F., & Blüthgen, N. (2017). A compendium of ERK targets. *FEBS Letters*, *591*(17), 2607–2615. https://doi.org/10.1002/1873-3468.12740

Verlande, A., Krafčíková, M., Potěšil, D., Trantírek, L., Zdráhal, Z., Elkalaf, M., Trnka, J., Souček, K., Rauch, N., Rauch, J., Kolch, W., & Uldrijan, S. (2018). Metabolic stress regulates ERK activity by controlling KSR-RAF heterodimerization. *EMBO Reports*, *19*(2), 320–336. https://doi.org/10.15252/embr.201744524

Vicente-Manzanares, M., & Horwitz, A. R. (2011). Cell migration: An Overview. In *Comprehensive Biotechnology*. https://doi.org/10.1007/978-1-61779-207-6_1

Volle, D. J., Fulton, J. A., Chaika, O. V., McDermott, K., Huang, H., Steinke, L. A., & Lewis, R. E. (1999). Phosphorylation of the kinase suppressor of Ras by associated kinases. *Biochemistry*, *38*(16), 5130–5137. https://doi.org/10.1021/bi983050d

Vomastek, T., Schaeffer, H.-J., Tarcsafalvi, A., Smolkin, M. E., Bissonette, E. A., & Weber, M. J. (2004). Modular construction of a signaling scaffold: MORG1 interacts with components of the ERK cascade and links ERK signaling to specific agonists.

Proceedings of the National Academy of Sciences of the United States of America, *101*(18), 6981–6986. https://doi.org/10.1073/pnas.0305894101

Walsh, J. H. (1991). *Conferences and Reviews Autocrine Growth Factors and Solid Tumor Malignancy*. *562*, 152–163.

Wang, D., Boerner, S. A., Winkler, J. D., & LoRusso, P. M. (2007). Clinical experience of MEK inhibitors in cancer therapy. *Biochimica et Biophysica Acta - Molecular Cell Research*, *1773*(8), 1248–1255. https://doi.org/10.1016/j.bbamcr.2006.11.009

Wang, P.-Y., Weng, J., & Anderson, R. G. W. (2005). OSBP is a cholesterol-regulated scaffolding protein in control of ERK 1/2 activation. *Science (New York, N.Y.)*, *307*(5714), 1472–1476. https://doi.org/10.1126/science.1107710

Wang, X., & Tournier, C. (2006). Regulation of cellular functions by the ERK5 signalling pathway. *Cellular Signalling*, *18*(6), 753–760. https://doi.org/10.1016/j.cellsig.2005.11.003

Weir, M. L., & Muschler, J. (2003). Dystroglycan: emerging roles in mammary gland function. *Journal of Mammary Gland Biology and Neoplasia*, *8*(4), 409–419. https://doi.org/10.1023/B:JOMG.0000017428.38034.a7

Weissbach, L., Settleman, J., Kalady, M. F., Snijders, A. J., Murthy, A. E., Yan, Y. X., & Bernards, A. (1994). Identification of a human rasGAP-related protein containing calmodulin-binding motifs. *The Journal of Biological Chemistry*, *269*(32), 20517–20521.

Wellbrock, C., Karasarides, M., & Marais, R. (2004). The RAF proteins take centre stage. *Nature Reviews Molecular Cell Biology*, *5*(11), 875–885. https://doi.org/10.1038/nrm1498

Wen, L., Zhang, X., Zhang, J., Chen, S., Ma, Y., Hu, J., Yue, T., Wang, J., Zhu, J., Wu, T., & Wang, X. (2020). Paxillin knockdown suppresses metastasis and epithelial-mesenchymal transition in colorectal cancer via the ERK signalling pathway.

Oncology Reports, *44*(3), 1105–1115. https://doi.org/10.3892/or.2020.7687

White, C. D., Brown, M. D., & Sacks, D. B. (2009). IQGAPs in cancer: A family of scaffold proteins underlying tumorigenesis. *FEBS Letters*, *583*(12), 1817–1824. https://doi.org/10.1016/j.febslet.2009.05.007

Wilhelm, S. M., Carter, C., Tang, L., Wilkie, D., Mcnabola, A., Rong, H., Chen, C., Zhang, X., Vincent, P., Mchugh, M., Cao, Y., Shujath, J., Gawlak, S., Eveleigh, D., Rowley, B., Liu, L., Adnane, L., Lynch, M., Auclair, D., … Trail, P. A. (2004). BAY 43-9006 Exhibits Broad Spectrum Oral Antitumor Activity and Targets the RAF / MEK / ERK Pathway and Receptor Tyrosine Kinases Involved in Tumor Progression and Angiogenesis. *Cancer Research*, *64*, 7099–7109.

Willard, M. D., Willard, F. S., Li, X., Cappell, S. D., Snider, W. D., & Siderovski, D. P. (2007). Selective role for RGS12 as a Ras/Raf/MEK scaffold in nerve growth factor-mediated differentiation. *The EMBO Journal*, *26*(8), 2029–2040. https://doi.org/10.1038/sj.emboj.7601659

Wong, D. J. L., Robert, L., Atefi, M. S., Lassen, A., Avarappatt, G., Cerniglia, M., Avramis, E., Tsoi, J., Foulad, D., Graeber, T. G., Comin-Anduix, B., Samatar, A., Lo, R. S., & Ribas, A. (2014). Antitumor activity of the ERK inhibitor SCH722984 against BRAF mutant, NRAS mutant and wild-type melanoma. *Molecular Cancer*, *13*(1), 1–15. https://doi.org/10.1186/1476-4598-13-194

Wu, J. shun, Jiang, J., Chen, B. jun, Wang, K., Tang, Y. ling, & Liang, X. hua. (2021). Plasticity of cancer cell invasion: Patterns and mechanisms. *Translational Oncology*, *14*(1), 100899. https://doi.org/10.1016/j.tranon.2020.100899

Yaeger, R., & Corcoran, R. B. (2019). Targeting alterations in the RAF–MEK pathway. *Cancer Discovery*, *9*(3), 329–341. https://doi.org/10.1158/2159-8290.CD-18-1321

Ye, X., Tam, W. L., Shibue, T., Kaygusuz, Y., Reinhardt, F., Eaton, E., & Weinberg, R. A. (2015). Distinct EMT programs control normal mammary stem cells and tumour-initiating cells. *Nature*, *525*(7568), 256–260. https://doi.org/10.1038/nature14897

Yin, G., Haendeler, J., Yan, C., & Berk, B. C. (2004). GIT1 functions as a scaffold for MEK1-extracellular signal-regulated kinase 1 and 2 activation by angiotensin II and epidermal growth factor. *Molecular and Cellular Biology*, *24*(2), 875–885. https://doi.org/10.1128/MCB.24.2.875-885.2004

Yin, G., Zheng, Q., Yan, C., & Berk, B. C. (2005). GIT1 is a scaffold for ERK1/2 activation in focal adhesions. *The Journal of Biological Chemistry*, *280*(30), 27705–27712. https://doi.org/10.1074/jbc.M502271200

Zaballos, M. A., Acuña-ruiz, A., Morante, M., Crespo, P., & Santisteban, P. (2019). Regulators of the RAS-ERK pathway as therapeutic targets in thyroid cancer. *Endocrine-Related Cancer*, *26*(6), 319–344. https://doi.org/10.1530/ERC-19-0098

Zhang, H., Koo, C. Y., Stebbing, J., & Giamas, G. (2013). The dual function of KSR1: A pseudokinase and beyond. *Biochemical Society Transactions*, *41*(4), 1078–1082. https://doi.org/10.1042/BST20130042

Zhang, Y., Bei, Y., Delikat, S., Bayoumy, S., Xin-Hua, L., Basu, S., McGinley, M., Chan-Hui, P. Y., Lichenstein, H., & Kolesnick, R. (1997). Kinase suppressor of Ras is ceramide-activated protein kinase. *Cell*, *89*(1), 63–72. https://doi.org/10.1016/S0092-8674(00)80183-X

Zhou, G., Bao, Z. Q., & Dixon, J. E. (1995). Components of a new human protein kinase signal transduction pathway. In *Journal of Biological Chemistry* (Vol. 270, Issue 21, pp. 12665–12669). https://doi.org/10.1074/jbc.270.21.12665

Zhou, M., Horita, D. A., Waugh, D. S., Byrd, R. A., & Morrison, D. K. (2002). Solution structure and functional analysis of the cysteine-rich C1 domain of kinase suppressor of Ras (KSR). *Journal of Molecular Biology*, *315*(3), 435–446. https://doi.org/10.1006/jmbi.2001.5263